Fate and Transport Modeling of Cohesive Sediment and Sediment-bound HCB in the Middle Elbe River Basin

Modellierung des Transports kohäsiver Sedimente und des Verbleibs sedimentgebundenen Hexachlorbenzols (HCB) im Einzugsgebiet der mittleren Elbe

Vom Promotionsausschuss der
Technischen Universität Hamburg-Harburg
zur Erlangung des akademischen Grades
Doktorin der Naturwissenschaften
genehmigte Dissertation

Kari Moshenberg
aus
New York, USA

2013

1. Gutachter:	Prof. Dr.-Ing. Wolfgang Calmano
	Institut für Umwelttechnik und Energiewirtschaft
	Eißendorfer Str. 40
	21073 Hamburg
2. Gutachterin:	Prof. Dr. rer. nat. Susanne Heise
	Hochschule für Angewandte Wissenschaften Hamburg
	Gefahrenstoffe und Umwelttoxikologie
	Lohbrügger Kirchstr. 65
	21033 Hamburg

Tag der mündlichen Prüfung: 30. October 2013

Acknowledgements

I am tremendously grateful to Prof. Dr. Susanne Heise for her steadfast support, insight, and patience. She contributed abundant encouragement, time, ideas and enlightenment, not to mention a stereotype-defying sense of humor. I am incredibly thankful to Prof. Dr. Wolfgang Calmano for the trust, kindness, and thoughtful feedback provided over the last six years, as well as to Prof. Dr.-Ing. Mathias Ernst for chairing my thesis committee.

The Alexander von Humboldt Stiftung provided the initial funding for this work and the Bundesanstalt für Gewässerkunde (BfG) funded the majority of the presented here. I would like to thank both organizations for their generous support. Invaluable feedback, suggestions and data were provided by several staff members of the BfG, including Daniel Schwandt, Peter Heininger, Evelyn Claus, Gudrun Hillebrand, and Wilfried Otto.

My sincere thanks go to the Danish Hydraulic Institute (DHI) for making their software available for use in this research. Several people, including Christian Pohl, Tobias Drückler, and Almut Gelfort contributed technical assistance in model development.

I am thankful for the camaraderie and expertise of my working group at the HAW, including Pei-Chi Hsu, Maximilia Kottwitz, Silvia Materu, Kirsten Offermann, Henning Tien, Henning Hermann, and Judith Angelstorf.

Jos Brils (Deltares), Frank Krüger (ELANA), and Burkhard Stachel provided excellent ideas, data, and real-world advice, for which I am sincerely thankful.

Lastly, I would like to thank my family for their love and encouragement. And most of all, Wolf, Leon, and Rosa - none of this would have been possible without you around, and all of it was more fun because you were.

Abstract (English)

Chemical contamination of waterways and floodplains is a pervasive environmental problem that threatens aquatic ecosystems worldwide. The Elbe River is the third largest river in Central Europe, starting in the Czech Republic and running through Dresden and Hamburg before empting into the North Sea. Due to extensive historical contamination and redistribution of contaminated sediments throughout the basin, the Elbe River transports significant loads of contaminants downstream, particularly during flood events. The high mobility of the fine-grained sediments within the basin means that sections of the Elbe River are unlikely to achieve the goals of the Water Framework Directive by 2015 (Zebisch et al., 2005). This study focuses on transport of cohesive suspended sediment and Hexachlorobenzene (HCB), a contaminant of concern in the Elbe River Basin. Sediment-sorbed concentrations of HCB significantly exceed environmental quality criteria and the Elbe River Community (FGG Elbe) has stated that a reduction of 98 % of the sediment-bound HCB load (relative to 2006) would be necessary to achieve all management objectives (FGG Elbe, 2009). To better understand the fate and transport of cohesive sediments and sediment-sorbed HCB, a hydrodynamic and sediment transport model for the reach of the Elbe River basin between Dresden and Magdeburg was developed. An evaluation of impact of the numerous groynes, or spit dykes, along the Elbe, was integrated into the modeling effort.

A quasi-2D model, which includes both a 1D representation of the Elbe between Dresden and Magdeburg and the Elbe's floodplains between Torgau and Magdeburg, was developed. The model was calibrated and validated for hydrodynamics, cohesive suspended sediment and sediment-sorbed HCB. A 2D flexible mesh model was developed between Aken and Barby to evaluate the impacts of groyne fields. The 1D and 2D flexible mesh model allowed for quantification the impact of groyne fields on sediment travel time. Simulations were run to evaluate sediment travel time during high water events.

The impact analysis of Elbe groyne fields showed that they reduce transport times of cohesive material and associated sediment sorbed contaminants approximately 15 % during average hydrodynamic conditions. The quasi 2D model was run under a variety of discharge scenarios to calculate the extent of transport of sediment and sediment-bound HCB to the floodplains (337 km^2) between Torgau and Magdeburg during nine high water events exceeding mean high discharge (MHQ) between 1998 and 2011. Results for sediment and HCB accumulation on floodplains are presented and discussed. A discussion of uncertainty and issues in model development is included. In addition, ample evidence that extreme high water events, such as the August, 2002 floods can have long-term implications on the suspended sediment transport regime and contaminant loads is provided.

A worst case analysis of HCB uptake by dairy cows and beef cattle indicate that significant, biologically relevant quantities of sediment-sorbed HCB accumulate on the Elbe floodplains following flood events. Given both the recent high frequency of floods in the Elbe Basin, and the potential increase in flood frequency due to climate change, an evaluation of source control measures and/or additional monitoring of floodplain soils and grasses is recommended.

Abstract (German)

Die Belastung mit Chemierückständen ist ein allgegenwärtiges Umweltproblem und belastet weltweit aquatische Ökosysteme. Aufgund intensiver Verschmutzung in der Vergangenheit und der Verteilung von belasteten Sedimenten im gesamten Stromgebiet transportiert die Elbe signifikante Mengen an Schadstoffen stromabwärts, insbesondere während Hochwasserereignissen (Heise et al., 2008). Die hohe Mobilität der feinkörnigen Sedimente innerhalb des Stromgebiets wird mit hoher Wahrscheinlichkeit dazu führen, dass Abschnitte der Elbe die in der Wasserrahmenrichtlinie für 2015 festgelegten Ziele nicht erreichen werden (Zebisch et al., 2005).

Die vorliegende Arbeit konzentriert sich auf den Transport von kohäsiven Sedimenten und Hexachlorbenzol (HCB), ein *contaminant of concern* im Einzugsgebiet der Elbe. Sediment-gebundene Konzentrationen von HCB übersteigen in nahezu allen Stromabschnitten Umweltqualitätskriterien, und die Flussgebietsgemeinschaft Elbe stellt in ihrem Hintergrundpapier von 2009 fest, dass eine Reduktion der HCB-Fracht um 98 % (gegenüber 2006) nötig wäre, um alle Bewirtschaftungsziele zu erreichen (FGG Elbe, 2009). Um die Transportwege und den langfristigen Verbleib von kohäsiven Sedimenten und sedimentgebundenem HCB besser zu verstehen, wurde ein quasi-2D-Modell entwickelt, welches sowohl eine 1D-Repräsentation der Elbe zwischen Dresden und Magdeburg als auch des Stromgebiets zwischen Torgau und Magdeburg enthält. Das Modell wurde kalibriert und validiert für Hydrodynamic, kohäsive suspendierte Sedimente und sedimentgebundenes HCB. Ein 2D flexible mesh-Modell deckt die Strecke zwischen Aken und Barby ab und diente der Evaluation der Auswirkungen von Buhnenfeldern, insbesondere die Quantifizierung ihrer Auswirkungen auf das Transportverhalten der Sedimente.

Die Analyse der Buhnenfelder zeigt, dass diese die Transportzeit von kohäsivem Material und den damit verbundenen sedimentgebundenen Schadstoffen während durchschnittlicher hydrodynamischer Bedingungen um rund 15% reduzieren. Das quasi-2D-Modell wurde für Simulationen einer Vielzahl von Abflussszenarien eingesetzt, um das Volumen des Sedimentransports und des Transports von sedimentgebundenem HCB auf die Auen der Elbe zwischen Torgau und Magdeburg während der neun Hochwasser, die zwischen 1998 und 2011 den mittleren Hochwasserstand überschritten, zu berechnen. Die resultierenden Ergebnisse der Sediment- und HCB-Ablagerung auf den Flussauen werden diskutiert. Ebenfalls enthalten ist eine Betrachtung der Unsicherheitsfaktoren und der Schwierigkeiten bei der Modellentwicklung. Nicht zuletzt werden zahlreiche Hinweise vorgestellt, die darauf schließen lassen, dass extreme Hochwasser wie die Flut von 2002 langfristige Auswirkungen auf den Sedimenttransport und die damit verbundenen Schadstoffbelastungen der Auen haben können.

Eine worst-case-Analyse der Belastungen von Milchkühen und Rindern mit HCB läßt darauf schließen, dass signifikante, d.h. biologisch relevante Mengen an sedimentgebundenem HCB während Hochwasserereignissen auf die Auen der Elbe gelangen. Angesichts der recht hohen Frequenz der Hochwasser im Einzugsgebiet der Elbe und einer möglichen Zunahme solcher Ereignisse im Zusammenhang mit dem Klimawandel scheint es angeraten, Maßnahmen zur ständigen Überwachung von Boden- und Vegetationsbelastung in den Elbeauen und/oder Maßnahmen zur Kontrolle der Schadstoffquellen zu evaluieren.

Table of Contents

Acknowledgements ..... **iii**
Abstract (German) ..... **v**
List of Tables ..... **ix**
List of Figures ..... **x**
1 Introduction **1**
2 Background **3**
2.1 Historical and Current Environmental Status 4
2.2 High Water and Flooding Events 8
2.3 Elbe River Geomorphic Features 9
2.3.1 Groynes and Groyne Fields 9
2.3.2 Floodplains 12
2.3.3 Importance of the tributaries Mulde and Saale with regard to Relative Discharge and Suspended Sediments Relationships 17
3 Hydrodynamic and Sediment Transport Modeling **19**
3.1 Transport of Sediment and Contaminants in River Basins 19
3.1.1 Types of Sediment Transport Models 21
3.2 Modeling Sediment Transport in River Basins 22
3.3 Groynes and Groyne Fields 23
3.3.1 Elbe River Groyne Fields: Source and Sink for Particulate-Bound Contaminants 23
3.3.2 Characteristics of Elbe River Groyne Fields 24
4 Model Selection **27**
4.1 MIKE Software Suite 28
4.1.1 MIKE11: Hydrodynamic (HD) Module 29
4.1.2 MIKE11: Advection-Dispersion (AD) Module 30
4.1.3 MIKE11: Ecolab Xenobiotics Module 30
4.1.4 MIKE21FM Hydrodynamic Module (HD) 32
4.1.5 MIKE21FM Mud Transport Module (MT) 33
4.2 Comparison: MIKE Suite vs. SOBEK 33
5 Materials and Methods **34**
5.1 Preliminary Data Analyses 35
5.1.1 Analysis of Long-term Trend Trends in SSC Data 35
5.1.2 Analysis of Long-term Trend Trends in HCB Load Data 36
5.1.3 Rating Curves and Double Mass Curves 37
5.1.4 PCA of Sediment-Sorbed Contaminant Data 38
5.2 Selected Contaminant of Interest: HCB 39
5.3 Modeling: Spatial and Temporal Extents 41
5.3.1 Spatial Extent: Dresden-Magdeburg 41
5.3.2 Temporal Extent 43
5.4 1D Model Data Requirements and Availability 46
5.4.1 Hydrodynamic Model (HD) Module 46
5.4.2 Suspended Sediment/Advection Dispersion (AD) Module 52

5.4.3 Contaminant/Ecolab Model Data Requirements 54
5.5 1D Model Setup 55
5.5.1 1D Hydrodynamic Setup 55
5.5.2 1D Advection-Dispersion Setup 58
5.5.3 1D Xenobiotics (HCB) Setup 60
5.6 1D Model Sediment Package Scenarios 62
5.7 1D Floodplain Model Setup 63
5.8 2D Flexible Mesh Model Setup 69
5.8.1 2DFM Model Bathymetry Setup 69
5.8.2 HD Module Setup 72
5.8.3 MT Model Setup 72
6 Results 74
6.1 Long-Term Trends in Suspended Sediment Loads and Concentration 74
6.1.1 Seasonal Trends 75
6.1.2 Long-Term Trends in the Meissen Suspended Sediment Concentration Data 77
6.1.3 Long-Term Trends in the Magdeburg Suspended Sediment Concentration Data . 78
6.2 Long-Term Trends in HCB Loads 80
6.3 Double Mass Analysis and Rating Curves 83
6.3.1 Double Mass Curves: Dresden and Magdeburg 83
6.3.2 Rating Curves: Dresden and Magdeburg 86
6.4 PCA of Sediment Contaminant Data 89
6.5 Model Calibration 94
6.5.1 Simple Model 94
6.5.2 1D Floodplain Model 100
6.5.3 2DFM Model 105
6.6 Model Validation 110
6.6.1 Simple Model 110
6.6.2 Floodplain Model 112
6.7 1D Suspended Sediment Package 112
6.8 Impact Analysis: Comparison of 2DFM Model and 1D AD Model 116
6.9 Transport and Accumulation on Floodplains 119
6.9.1 Transport and Accumulation of Cohesive Sediment on Floodplains 120
6.9.2 Transport and Accumulation of Sediment-Bound HCB on Floodplains 124
7 Uncertainty Evaluation 126
7.1 Sampling, Measurement and Analysis of Field Data 126
7.1.1 Missing Data Values 128
7.1.2 Data Sampling and/or Measurement Frequency 129
7.2 Model parameter values 129
7.3 Data Interpretation 132
8 Discussion 133
8.1 Trends in Suspended Sediment, Discharge, and HCB 133
8.2 Accumulation of HCB Deposited on Floodplains in Dairy Cows and Cattle 136
8.3 Model Results 138
8.4 Recommendations and Suggestions for Further Work 142

9 Bibliography 144
Appendix A: Ecolab Reference 153
Appendix B: Parameters and Input Values for Hydrodynamic, Cohesive Sediment and HCB Models and Modules 161

List of Tables

Table 1. Contaminant-specific assignment of areas of risk to downstream regions in the German sub-catchment (from Heise at al 2008). 7
Table 2. Width of the active floodplain at different Elbe River cross-sections (IKSE, 2005) 14
Table 3. Count and statistical indicators of sedimentation rates in floodplains of the lower Middle Elbe (data UFZ) based on the averaged sediment records. 15
Table 4. Cumulative discharge and SPM-loads in Rosslau, Mulde, Saale, and Magdeburg during the period of high water discharge in 2006 16
Table 5. Hydrodynamic/sediment transport models 28
Table 6. Availability of gauging, suspended sediment and sediment chemistry data; Elbe River, German border - Schnackenburg 43
Table 7. Ten year load decreases: Zehren to Magdeburg 46
Table 8. Input and calibration parameters for MIKE 11 model 47
Table 9. Hydrodynamic gauging stations 49
Table 10. Suspended sediment gauging stations 53
Table 11. Long-term data gaps in suspended sediment concentration data at Meissen, Barby, and Magdeburg Strombrücke 54
Table 12. Boundary conditions in the 1D model 57
Table 13. Advection-Dispersion module input values 60
Table 14. Simulation periods for the flexible mesh model 72
Table 15. Mud transport module input 73
Table 16. Predicted HCB loads at Schmilka 81
Table 17. Rating curves: Results of least squares regression 89
Table 18. Detection frequency of all analytes included in the PCA 90
Table 19. PCA: Rotated structure matrix 93
Table 20. Calibration statistics for the 1D 'simple' model 94
Table 21. Actual and modeled weir openings and closings 96
Table 22. Discharge scenarios used for validation of floodplain inundation 102
Table 23. Calibration statistics for the 1D simple and floodplain model 102
Table 24. Specifications for the flexible mesh calibration simulation 106
Table 25. Results of the 2DFM MT calibration 109
Table 26. Calibration and validation statistics for the 1D 'simple' model 111
Table 27. Sediment travel times under varying discharge scenarios 115
Table 28. Results of the impact analysis: 1D vs 2D sediment transport times 118
Table 29. Simulaton periods for the floodplain model 119
Table 30. Torgau-Magdeburg: Accumulated sediment on floodplain branches 121
Table 31. Sediment load in g/m^2 in the floodplain near Schönberg Deich 123
Table 32. Torgau-Magdeburg: Accumulated HCB on floodplain branches ($\mu g/m^2$) 124
Table 33. HCB concentrations on Elbe floodplains, from various publications 125

List of Figures

Figure 1. The Elbe River Basin 4
Figure 2. Dresden discharge (1/1/1996-12/31/2011) and related discharge benchmarks..... 9
Figure 3. Magdeburg discharge (1/1/1996-12/31/2011) and related discharge benchmarks 9
Figure 4. Groynes and groyne fields along the Middle Elbe River..... 10
Figure 5. Example groynes and groyne fields, between Barby and Schönebeck 11
Figure 6. Schematic cross section of the Elbe floodplain in the Middle Elbe during lowest (NW) and highest (HHW) water level..... 13
Figure 7. Box and whisker plot of annual discharge (1994-2007) 18
Figure 8. Box and whisker plot of annual suspended sediment loads (1994-2009) 18
Figure 9. Increase in Hg and Cd loads between Magdeburg and Schnackenburg (1994-2009)... 24
Figure 10. Classification of morphological patterns of groyne fields 26
Figure 11. Processes in the xenobiotics template 32
Figure 12. Annual HCB loads (1994-2009) 45
Figure 13. Elbe River and the Pretziener Weir..... 51
Figure 14. Schematic drawing of the floodplain model..... 65
Figure 15. Map showing floodplain branches and connector channels. 'LFloodplain' and 'RTFLoodplain south' are floodplain branches, while channels begin with the word 'Branch'.... 68
Figure 16. Example flexible mesh (upstream of Aken), showing the resolution of the DEM and groynes..... 71
Figure 17. Example interpolated mesh (upstream of Aken), showing flexible mesh resolution 71
Figure 18. Annual suspended sediment concentration at Meissen and Magdeburg 75
Figure 19. Winter and summer SSC at Meissen and Magdeburg..... 76
Figure 20. Meissen SSC (log_{10}), statistically significant groups identified. 78
Figure 21. Magdeburg SSC (log_{10}), statistically significant groups identified. 79
Figure 22. HCB Loads at Schmilka* (1994-2009) 81
Figure 23. HCB loads at Schmilka and Schnackenburg 83
Figure 24. Double mass plot (Dresden) 84
Figure 25. Double mass plot (Magdeburg) 85
Figure 26. Rating curves at Dresden (1995-2001 and 2002-2008, summer and winter) 88
Figure 27. Scree plot for contaminant PCA..... 91
Figure 28. Barby Observed and Modeled Discharge (m^3/s) (1996-2006) 96
Figure 29. Torgau observed and modeled SSC (mg/l) (2000-2002)..... 98
Figure 30. Measured and modeled HCB loads at Dommitzsch in 2006, with SSC for reference 100
Figure 31. Barby observed and modeled discharge (m^3/s) (1996-2006)..... 104
Figure 32. 17 groyne fields used for calibration of the 2DFM MT Module 107
Figure 33. HD simple model validation: 1/1/2007 through 12/31/2009..... 110
Figure 34. AD simple model validation: 1/1/2007 through 5/01/2009. 111
Figure 35. Modeled suspended sediment transport at Dresden during the March, 2006 flood. 113

List of Acronyms

Acronym	Definition
AD	Advection-Dispersion
AMSL	Above mean sea level
ANOVA	Analysis of variation
BfG	Bundesanstalt für Gewässerkunde/Federal Institute of Hydrology
CFL	Courant Friedrichs Lewy
CST	Cohesive Sediment Transport
DBT	Dibutyltin
DDD	Dichlorodiphenyldichloroethane
DDE	Dichlorodiphenyldichloroethylene
DDT	Dichlorodiphenyltrichloroethane
DD_x	DDT and its metabolites, including o,p'-,p,p'-DDT, DDD and DDE
DEM	Digitized Elevation Models
DF	Detection Frequency
DHI	Danish Hydrology Institute
DW	Dry weight
EPA	U.S. Environmental Protection Agency
EQS	Environmental Quality Standards
EU	European Union
FGG	Flussgebietsgemeinschaft
FLYS	Flusshydrologische Software
FM	Frequency Modulation
GDR	German Democratic Republic
GIS	Geographic Information Systems
HAW	Hochschule für Angewandte Wissenschaften Hamburg
HCB	Hexachlorobenzene
HCH	Hexachlorcyclohexane
HD	Hydrodynamic
HHW	Highest Water Level
HQ10	Discharge recurring once in 10 years according to flood statistics
HQ100	Discharge recurring once in 100 years according to flood statistics
HQ20	Discharge recurring once in 20 years according to flood statistics
HQ50	Discharge recurring once in 50 years according to flood statistics
HSPF	Hydrological Simulation Program-Fortran
IKSE	Internationale Kommission zum Schutz der Elbe (International Commission for the Protection of the Elbe River)
ISBN	International Standard Book Number
km	Kilometers
KOW	Octanol-Water Partition Coefficient
LIDAR	Laser Detection and Ranging
LFP	Left Floodplain

Acronym	Definition
M	Meters
MBT	Monobutyltin
MHQ	Mean High Discharge
MHW	Mean High Water
MNW	Mean Low Water
MQ	Mean Discharge
MT	Mud Transport
NA	Not Applicable
NSE	Nash-Sutcliff Model Efficiency
PAHs	Polycyclic aromatic hydrocarbons
PBDEs	Polybrominated Diphenyl Ethers
PCA	Principal Component Analysis
PCB	Polychlorinated Biphenyl
PCDD/F	Polychlorinated dibenzo-p-dioxin and polychlorinated dibenzofuran
PCDDs	Polychlorinated Dibenzo-*p*-dioxins
PCDFs	Polychlorinated Dibenzofurans
PIK	Potsdam Institute for Climate Impact Research
POP	Persistent Organic Pollutant
Q/h	Discharge to Height
QUAL2E	Enhanced Stream Water Quality Model
RFPN	Right Floodplain North of the Umflutkanal
RFPS	Right Floodplain South of the Umflutkanal
SL	Sediment Load
SSC	Suspended Sediment Concentration
SPM	Suspended Particulate Matter
SWAT	Soil Water Assessment Tool
SXE	Dissolved xenobiotics
SXES	Dissolved xenobiotics in sediment
TBT	Tributyl Tin
Tcos	Transfer coefficients
UK	United Kingdom
UNEP	United Nations Environment Programme
US	United States
WASP	Water Quality Analysis Simulation Program
WFD	Water Framework Directive
WSV	Wasser- und Schifffahrtsverwaltung des Bundes. German
XSED	Mass of sediment
XSS	Suspended solids
XXE	Adsorbed Xenobiotics
XXES	Adsorbed xenobiotics in sediment
α-HCH	α-hexachlorocyclohexane
β-HCH	β-hexachlorocyclohexane
γ-HCH	gamma-hexachlorocyclohexane (Lindane)

1 Introduction

The Elbe River is one of the principle waterways in Central Europe, beginning in the Krkonoše Mountains in the Czech Republic, flowing northwest through Germany, before emptying into the North Sea. The Elbe's watershed is the fourth largest in Europe, covering 63% (49,966m^2) and 27% (97,116m^2) of the Czech Republic and Germany's land surface, respectively (IKSE, 2005). The Elbe River has played an important role in the environmental, industrial and agricultural history of Europe, and is vital to the economic success of the Port of Hamburg, the second largest deep-water port in Europe. To convey an idea of scale, the Port of Hamburg was responsible for more than 750 Euros in million tax revenue in 2010 (HPA, 2013).

The water and sediment quality in the Elbe River is influenced by the long history of human industrial development in the Elbe basin, beginning with mining in the 12th century, and continuing to the present day (Hurst, 2002). Waterways, such as the Elbe, commonly attract development due to the ease of access of transport, waste transport, and energy provided by the river. One common consequence of this development is that the contaminants that are the products and by-products of industrial processes and of human development become introduced into the river directly as an effluent stream, or in-directly as waste transported by air, rain, runoff, or direct flow (i.e. tributaries). As a result of these pressures and various transport mechanisms, contamination of river water, sediment, and biota had been a serious issue. However, contaminant levels have improved dramatically since 1989, when East and West Germany were reunited, and both the closure of some factories and diversion of waste helped to slow contaminant inputs to the Elbe River and resulted in improved water quality in most areas. However, exceedances of national and international sediment and biota quality standards are still common (Brügmann, 1995; Götz et al., 1990; Heise et al., 2008; Popp et al., 2000; Stachel et al., 2007).

Elbe River Basin falls under the jurisdiction of the European Union (EU) Water Framework Directive (WFD), which calls for good chemical and ecological status of EU waters by 2015 and serves as the legislative mandate for the strategic management of water bodies within Europe

(Directive 2000/60/EC, 2000). Implementation of the WFD has resulted in increased efforts to evaluate the ecological and chemical status of river basins as well as in the development of integrated basin management plans (Dørge and Windolf 2003; Borja et al. 2004; Moss et al. 2003; Schaumburg et al. 2004). The combined effect of elevated historical levels of contamination within the Elbe River basin, the strong affinity of these contaminants for fine-grained sediments, and the high mobility of the fine-grained sediments within the Elbe River basin means that it is likely that sections of the Elbe River will fail to achieve the goals established by the WFD by the target date (Zebisch et al., 2005).

While the nature and extent of sediment, aquatic, and biota contamination continues to be investigated by various researchers and federal agencies through ongoing monitoring programs, little attention has yet been paid to the basin-scale mechanisms of contaminated sediment transport, and the impact of the numerous groynes, or spit dykes, along the Elbe, on this transport. Additionally, the relatively high frequency of significant flooding events in the past ten years has highlighted the importance of enhancing our understanding of the way water, sediment, and contaminants move throughout the Elbe Basin under extreme conditions. The objective of the present study is to address these knowledge gaps, and to attempt to evaluate key issues relevant to sediment and contaminant transport in the Middle Elbe Basin. More explicitly, the four objectives of this study are:

1. Identify short or long-term trends in concentrations of suspended sediment and sediment-sorbed contaminants in the Middle Elbe
2. Evaluate the impacts of groyne fields on sediment transport
3. Quantify the volume of sediment and sediment-bound contaminant(s) transported to floodplains during high water events
4. Discuss potential ecological and societal impact of sediment contamination, particularly within the context of climate change.

2 Background

The Elbe River is the third longest river in Central Europe, with a length of 1094 km and a total basin area of 148,268 km^2. The Elbe River, or *Labe* in Czech, starts in the Czech Republic and runs through the cities of Dresden, Magdeburg and Hamburg before empting into the North Sea (Figure 1). The river basin is divided between four countries; Germany (65.5%), the Czech Republic (33.7%), Austria (0.6%) and Poland (0.2%) (IKSE, 2005). The course of the Elbe is divided into three geomorphically unique reaches by river kilometer. River kilometers start at zero at the Czech-German border. On the Czech side of the border, the number grows in the upstream direction; on the German side in the downstream direction:

- Upper Elbe - Source waters to the beginning of the North German Lowland at Hirschstein Castle (km -387 to km 96)
- Middle Elbe - Beginning of the North German Lowland at Hirschstein Castle to the Geesthacht weir (km 96 to km 585.9)
- Lower Elbe - Geesthacht weir to the mouth of the North Sea (km 585.9 to km 727.7)

Flow in the Upper Elbe is controlled by reservoirs and several lock and weir system. The Middle Elbe is free-flowing, but flow is affected by approximately 6,900 groynes that line the banks of the River (Sections 2.3.1 and 3.3 provide more information on the groynes and their relevance to the hydrodynamic and cohesive sediment modeling) (IKSE, 2005). The banks of the Upper Elbe are dominated by a steep valley of weathered sandstone, while the Middle Elbe is characterized by broad floodplains, several large meanders and a sloping, level landscape. The Lower Elbe is tidally influenced. For brevity, the term 'Elbe Basin' will henceforth be used to refer to the Elbe River and its tributaries, while 'Elbe' will be used to refer exclusively to the course of the Elbe River itself.

This study will focus on non-tidally influenced area of the Middle Elbe River. Specifically, the modeling discussed in subsequent sections focuses on the area between Dresden (km 55.6) and Magdeburg (km 326.6). The reasons for limiting the study to this area are clarified in Section

5.3. Key tributaries to the Elbe within this area include the Mulde and the Saale Rivers. The confluences of the Mulde and Saale with the Elbe occur at km 259.6 and 290.58, respectively.

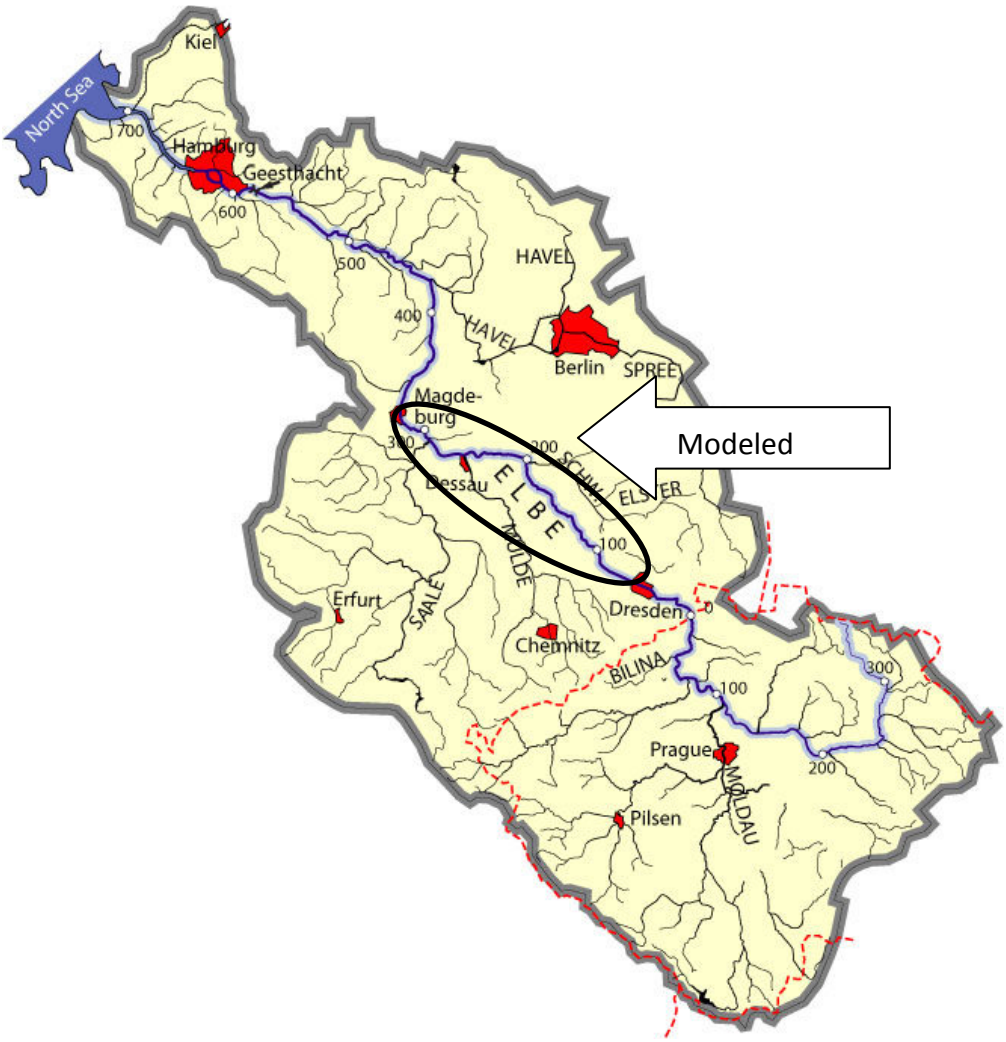

Figure 1. The Elbe River Basin

2.1 Historical and Current Environmental Status

There is an extensive body of literature describing the nature and extent of chemical contamination of the Elbe basin. A summary of relevant literature is provided below.

The Elbe River basin has been settled since prehistoric times, and the Elbe's water and natural resources have been used for mining, domestic, agricultural, and industrial purposes for

hundreds of years (Adams et al., 1996; Guhr, 1995; Schwarzbauer et al., 2000) which resulted in Elbe River becoming one of Europe's most contaminated rivers. The majority of the contamination occurred starting in the mid-20th century, when almost 90% of the Elbe River basin was within the borders of the former Czechoslovakia (1918 – 1992) and the former German Democratic Republic (1949 - 1990). High nutrient loads, elevated concentrations of metals and persistent organic contaminants in biota and sediments, impaired fisheries, and oxygen deficiencies in the tidal area of the Elbe River were documented during this period (Adams et al., 1996; Brügmann, 1995).

Both point and non-point sources contributed to contaminant loads in the Elbe. Non-point sources of contamination included erosion and runoff from intensive agriculture, animal feedlots and roads. The primary point sources of chemical contamination in the Elbe River basin were municipal and industrial waste water effluents. Effluent from chemical, paper, and metallurgical industries in the Saale and Mulde sub-catchments was particularly significant (Vink et al., 1999). The most significant point-sources of chemical contamination in the non-tidal Elbe are described below:

- The heavily industrialized Bitterfeld-Wolfen region, drained primarily by the Spittelwasser Creek, a tributary to the Mulde. The Bitterfeld-Wolfen region was the site of open-pit lignite mining as well as chemical industry production facilities for chloralkali, acetaldehyde, sodium hydroxide, aluminum and magnesium. Evaluations of dioxin data taken from the Elbe River and the Port of Hamburg show that patterns of PCDD/F contamination are similar to those found in the Bitterfeld-Wolfen area (Brack et al., 2003; Götz et al., 2007a, 1998a).
- Mining of tin, silver and uranium in the Erzgebirge (Ore Mountains), which are drained by the Mulde River. This mining has been taking place since the Middle Ages, and contamination resulting from the mining, preparation and smelting of ore has resulted in elevated metal concentrations in floodplain soils and river sediments (Beuge et al., 1999, from Schneider and Reincke, 2006).

- Cold war-era mining and production of uranium and other heavy metals discharged directly into the Elbe River and its tributary, the Saale River (Baborowski and Bozau, 2006; Brügmann, 1995).
- Metals resulting from leather industry production, such as chromium, and arsenic, cadmium, copper, nickel, lead and zinc, resulting from metallurgy and mining industry (Weigold and Baborowski, 2009)
- The chemical factory at Spolana Neratovice, located on the Elbe River in the Czech Republic. Former products included linear olefins, viscose staple as well as the chlorinated herbicide 2,4,5-T ('Agent Orange'). The site is contaminated with dioxins, mercury, and chlorinated aliphatic hydrocarbons (Randak et al. 2009; Stachel et al. 2004).

Water and sediment quality in Elbe River basin began to improve following unification of the East and West Germany in 1990, and the subsequent closure of many factories and large-scale heavy industrial plants (Lehmann and Rode, 2001). Studies conducted in the early 1990s showed a substantial decrease in chlorinated hydrocarbons concentrations, though a less marked decreases in arsenic concentration. Increases in the diversity of benthic organisms, fisheries yield, and decreased contaminant concentration in tissue from fish such as eel and bream were also observed (Adams et al., 1996; Brügmann, 1995; Götz et al., 1998b; Guhr, 1995).

Sediments in the Elbe-watershed still contain high concentrations of contaminants. Particularly during periods of high discharge, sediments can act as a secondary source and contribute significant loads to downstream areas (Baborowski and Friese, 2004; Stachel et al., 2004). When these sediments are resuspended and transported downstream, they potentially endanger river basin objectives (Heise et al., 2008). Work by Heise et al. (2008) quantified the contribution of the different sub-catchments to the overall contaminant load, identifying those which endanger ecosystem services. Within the identified regions/sub-catchments, "areas of risk" from which the contamination originated, were indicated where measures would be most effective. These sub-catchments were identified as the Czech Republic with regard to

polychlorinated biphenyls (PCBs), hexachlorobenzene (HCB), and dichlorodiphenyltrichloroethane (DDT) and its metabolites (DD_X, including o,p'-,p,p'-DDT, DDD and DDE), and Mulde and Saale with the areas of risk for heavy metals, hexachlorocyclohexane (HCH) and dioxins

Table 1. Contaminant-specific assignment of areas of risk to downstream regions in the German sub-catchment (from Heise at al 2008).

Area of Risk	**Inter-regional Risk with High Probability**	**Possible Inter-regional Risk**
MULDE		
Spittelwasser	β-HCH, α-HCH, Dioxins	γ-HCH, DD_X
Region upstream of Jeßnitz		Dioxins
Freiberger Mulde	As, Cd	Pb, Zn
Zwickauer Mulde	Cd	Zn
Cont. Sediment in river bed		Pb
SAALE		
Contaminated sediments in river bed downstream of Bad Dürrenberg	Hg, Zn, Cu, Pb, Cd	DD_X, γ-HCH
Weiße Elster	Zn, Cd	TBT, PCB, Ni
Schlenze, Mansfelder Land	Cu	Cd
Bode		Ni, Cd, PCB, Pb, Cu
ELBE-Main Stream		
Groyne fields	Zn, Pb, Cu, Cd, Hg, HCB, DDD (trend decreasing)	
Triebisch		Cd

Even though there are no target values for the protection of aquatic life for polychlorinated dibenzo-*p*-dioxins and dibenzofurans (PCDDs/PCDFs) and polycyclic aromatic hydrocarbons (PAHs), elevated concentrations are also a concern. For example, sediment concentrations of PCDDs/PCDFs in sections of the Elbe basin significantly exceed background concentrations and contribute to fish tissue concentrations that regularly exceed maximum allowable concentrations established by the European Commission (Götz et al., 1998a, 1998b; Stachel et al., 2007).

2.2 High Water and Flooding Events

Three large floods have occurred in the Elbe Basin in the last ten years; 2002, 2006, and 2011. Figures 2 and 3 show daily discharge at both Dresden and Magdeburg, respectively, with related discharge benchmarks; mean discharge (MQ), discharge recurring once in 10 years (HQ10), and discharge recurring once in 100 years (HQ100). The European-wide flooding that occurred in August, 2002 was the most catastrophic of the three floods, causing approximately $12 billion in Germany and the Czech Republic (Becker and Grünewald, 2003). A record water level of 9.40 meters (m) was recorded at Dresden. The flooding caused significant damage in Dresden, Wittenberg, Dessau and Magdeburg. The 100 year flood caused hydraulic fracture and overtopping of dykes as well as overrun and significant damage to dams (IKSE, 2004). The 2006 and 2011 floods were less significant in Dresden than the 2002 flooding. The 2006 flood, however, exceeded the water level of the flood in 2002 further downstream, in Wittenberge and Neu-Darchau. At both Dresden and Magdeburg, the spring 2006 flood was a 10-year flood, causing significant erosion and damage to dikes incurred. As a result, there was significant flooding of Elbe floodplains (Undine, 2012). A third significant flooding event occurred in January 2011 primarily in the lower half of the Elbe basin. The HQ10 was exceeded at both Dresden and Magdeburg (Figure 3). Further downstream, water height at the Hitzacker (km 522.20) and Lauenburg (km 536.44) gauges surpassed all previous records. However, no damage to dikes or dams was reported within the Elbe basin as extensive improvements on flood safety had been established in the aftermath of 2002.

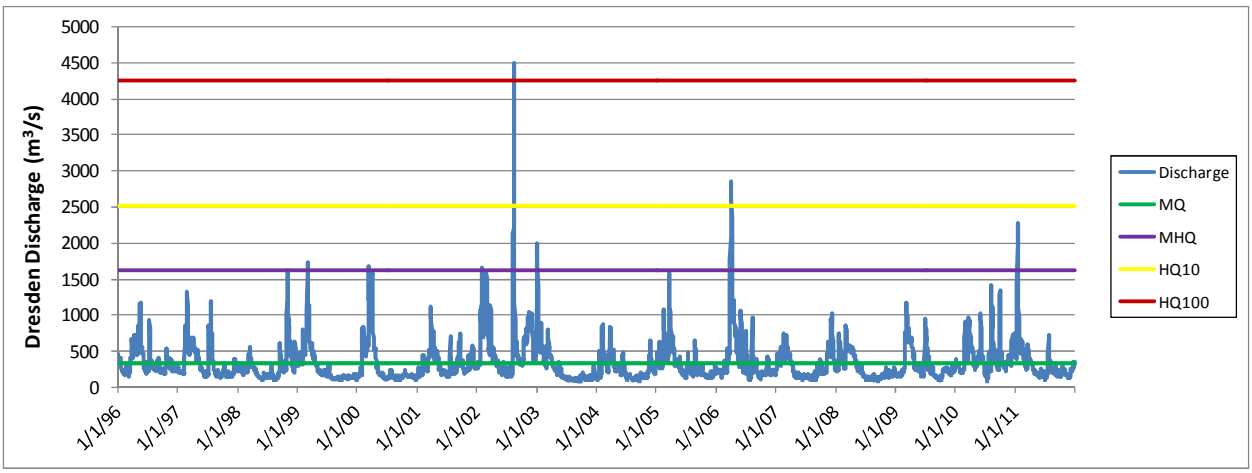

Figure 2. Dresden discharge (1/1/1996-12/31/2011) and related discharge benchmarks (Bundesanstalt für Gewässerkunde, 2009; WSV, 2011)

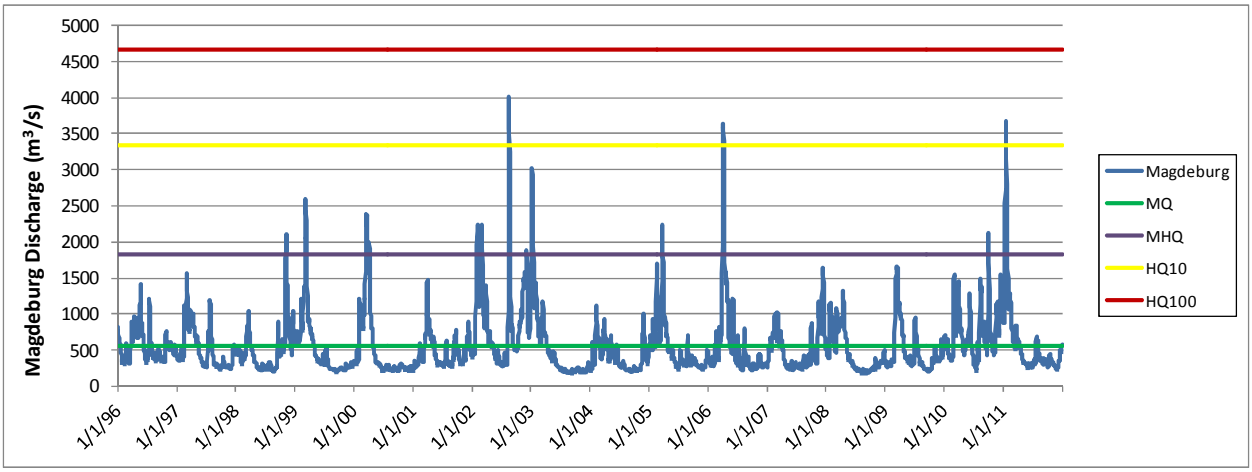

Figure 3. Magdeburg discharge (1/1/1996-12/31/2011) and related discharge benchmarks (Bundesanstalt für Gewässerkunde, 2009; WSV, 2011)

2.3 Elbe River Geomorphic Features

2.3.1 Groynes and Groyne Fields

Approximately 6,900 groynes, or spit dykes, line the banks of the Middle Elbe. Groynes are impermeable fingers of coarse sediment that line the banks of the Elbe River and reach into the main channel (Figure 4) (IKSE, 2005).

Groyne fields are the fine-grained area between the groynes that act as traps for fine-grained sediment and associated contaminants due to lower flow velocities. Due to this trapping effect, groyne fields function as a contaminant sink during periods of low discharge and as a contaminant source during periods of high discharge and/or high erosion.

The Elbe groynes were built starting in the 17th century and have been historically used for flood prevention, protecting river banks against erosion, land acquisition and customs collection. Groynes are actively maintained by the German Water and Shipping Administration (*Wasser- und Schifffahrtsverwaltung des Bundes, WSV*) and their present use is to improve the navigability of the Elbe during low water conditions (Schwartz and Kozerski, 2003). Groyne fields also provide a unique biotope for a variety of flora and fauna as well as provide a biological refuge during high-water events (Falconer and Kozerski, 2003; Sukhodolov et al., 2002).

Figure 4. Groynes and groyne fields along the Middle Elbe River

There are no groyne fields in the Upper Elbe, and the first groyne fields are observed at approximately km 121.5. The dimensions of the groynes and groyne fields along the Middle Elbe are highly variable, as can be seen in Figure 5: the groynes average 20-100 m in length, the groyne heads 5-15 m in width. The spacing between groynes (groyne fields) varies between

approximately 50-400 m. Section 3.3 provides additional information on the hydrodynamic and sediment transport-related significance of the Elbe River groynes as well as summarizes current literature on sediment and contaminant transport in groyne fields.

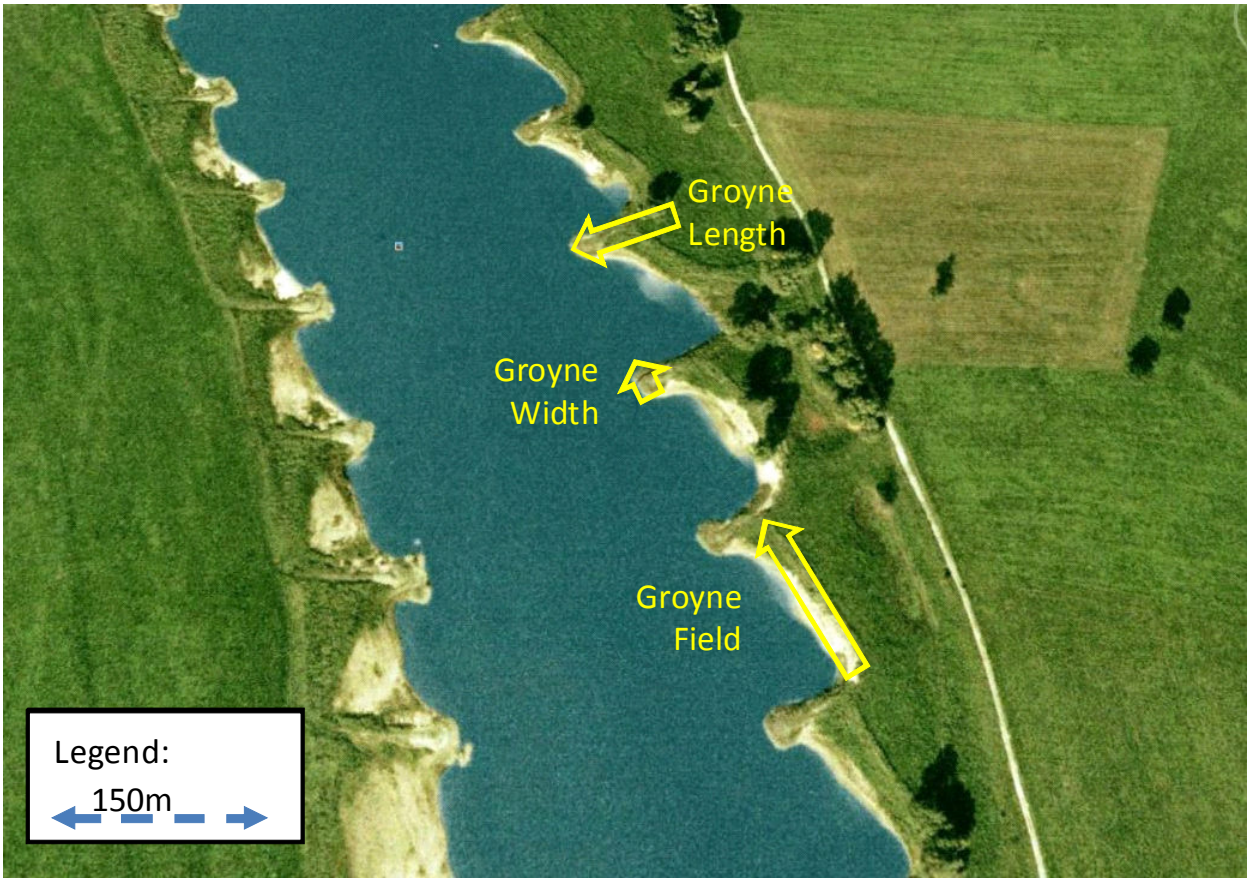

Figure 5. Example groynes and groyne fields, between Barby and Schönebeck (image from Google Earth)

2.3.1.1 Characteristics of Sediment in Elbe River Groyne Fields

Field surveys were conducted during the summers of 2010 (in conjunction with the BfG) and in 2011 to determine chemical and physical characteristics of sediments in Elbe River groyne fields. One of the primary goals of these field surveys was to characterize the suspended material in groyne fields, particularly relative to grain size, and thickness of the sediment layer. The 2010 and 2011 surveys were conducted between km 210-327.3 and km 453-465, respectively. In contrast to the high proportion of groyne fields previously reported to contain thick layers of muddy and silt sediments, only approximately 25% of the sampled groyne fields

were found to contain muddy and silty sediments. The majority of the groyne fields containing a large proportion of fine-grained material are concentrated in the lower part of the Middle Elbe (unpublished data). The sediments in these groyne fields with abundant fine-grained material were found to be very dense. Of the ten groyne fields and small harbors sampled, the median fine grained (<20 µm) was 65% and the median moisture content was 34% (unpublished data).

2.3.2 Floodplains

A floodplain is that part of the river that is affected by the highest water levels and thus not permanently or periodically but eventually exposed to flooding. This zone is called the "morphological floodplain" (Figure 6). Often part of this area has nowadays been cut off from the river dynamic by dikes. What remains behind the dikes is still connected to the river by groundwater, but is only flooded if dikes break ("inactive" or "passive floodplains", acc. to Bretschko 1999). The active floodplain (or "recent" floodplain) is flooded more or less regularly during high water levels. Its area is restricted by the natural morphology or by dikes. The morphological floodplain of the Elbe between Riesa (km 108.4) and Geesthacht (km 585.9) comprises 4360 km^2. The area of the active floodplains has been reduced through dike construction by 76.7 % since medieval times to 1025 km^2 (Simon, 1994). Figure 6 shows the width of the active floodplain at a theoretical cross section of the Elbe River.

Floodplains are considered to be sinks rather than sources of sediment in a catchment. At the lower middle Elbe, the Helmholtz Centre for Environmental Research (UFZ) carried out a number of studies to investigate sedimentation rates in floodplains by the use of sediment traps (Büttner et al., 2006; Baborowski et al., 2007; Randak et al., 2009).

Table 3 gives an overview of the calculated data. Schwarz & Kozerski (2003) calculated an average sediment growth of approximately 1.5 cm/year in the center of a groyne field.

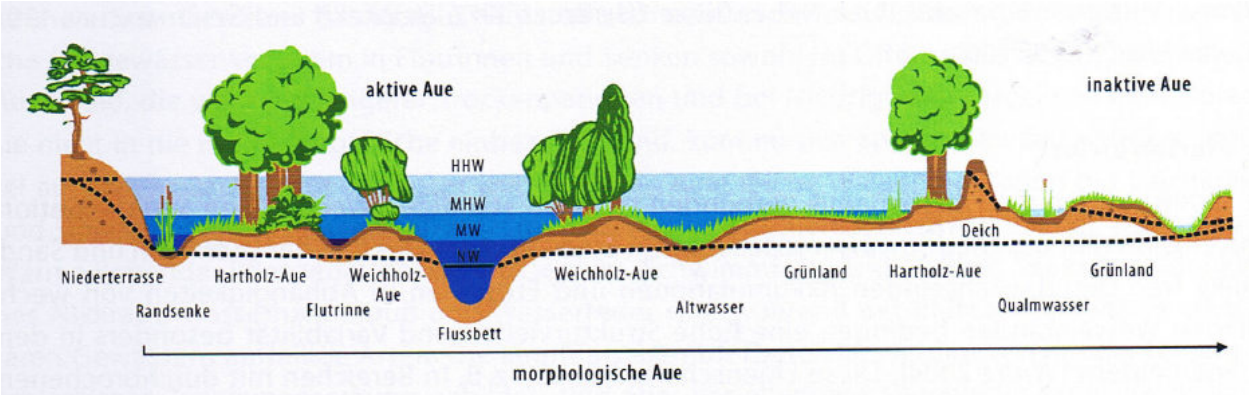

Figure 6. Schematic cross section of the Elbe floodplain in the Middle Elbe during lowest (NW) and highest (HHW) water level
(Graphic: J. Luge, from Scholz et al. 2004)

Table 2. Width of the active floodplain at different Elbe River cross-sections (IKSE, 2005)

Elbe Profile Location	Elbe-km	Floodplain Width [m]
Upstream of Klöden-Bösewig	191	3400
Schwarzen Elster confluence	198.5	3450
Wittenberg	214	2000
Upstream of Coswig	229	5200
Roßlau downstream of der Mulde confluence	256	4100
Downstream of Aken	277	2950
Downstream of the Saale confluence	291	4200
Downstream of Barby (Train tracks)	294	2800
Old Elbe Canel by Pretziener Weir	300.7	3000
Magdeburg-Rothensee/Gerwisch	332	3350
Elbe Descent Channel - Lostau (Old Elbe Canal)	337	3200
Highway Bridge at Hohenwarthe	338.5	1200
Downstream of Rogatz (gravel pit)	354	3000
Buch-Jerichow	383	3300
Arneburg	404	850
Upstream of Werben (to the Havel)	427	2900
Beuster	446	3700
Highway Bridge at Wittenberge	456.3	1400
Cumlosen	469	2700

Table 3. Count and statistical indicators of sedimentation rates in floodplains of the lower Middle Elbe (data UFZ) based on the averaged sediment records.

	SpHW97	SuHW97	H-WHW 98/99	SuHW 02	SpHW 03	SpHW 04	SpHW 05-I	SpHW 05-II
Number	12	9	10	4	6	6	9	13
Min, g/m2	5	11	183	220	60	10	9	50
Median, g/m2	217	27	272	454	82	145	68	214
Average, g/m2	699	75	1258	653	85	167	83	268
Max, g/m2	3810	410	8321	1485	128	468	178	580
Annual suspended sediment load Wittenberge (BfG)	717573			812298	706543	590225	537000*	
Solid particle retention on floodplains between Wittenberge & Hitzacker(65 km, ~12.500 ha)	96828		157219	163250	10566	20826	43869	
Solid particle retention in 12500 ha (% of annual fraction)	13			20	1	4	8	

Note:
*Corrected Value
SpHW-spring floods, SuHW-summer high water, AHW-autumn high water, WHW-winter high water. 2002 data are estimated, due to a lack of available data. Based on different single-site comparisons of values measured in 2002 in comparison with previous years, sedimentation rates in 2002 were assumed to be twice as high as the average value. Translated from Heise et al. 2008, Appendix 10, Table 5-10).

Büttner et al. (2006) used a 2D model to estimate sediment input along a two km^2 floodplain and calculated that about 1000 tons of sediment settled between river km 436 and 440 during a period of high water discharge in 1998. It can be assumed that depending on the total load and the length and level of the high water discharge, between 1 and 13 % of the annual load of suspended matter are contained between Wittenberge and Hitzacker (Heise et al. 2008, Appendix 10).

Analysis of sediment transport during the period of high water discharge in 2006 indicated that 80,000 tons of suspended material was contained between Rosslau and Magdeburg, which equaled the load contributed by Mulde and Saale (Table 4). Considering a floodplain area in the part of the catchment of 125 km^2, this would mean sedimentation of 640 g/m^2 during this period. Major floodplain forests are found between the confluence of the Mulde and of the Saale in the Elbe River, which extend over approximately 40 to 50 km^2 (Heise et al. 2008). The roughness, or frictional resistance of water, of floodplain forests reduce the flow velocity considerably and result in sedimentation of suspended matter. UFZ (Umweltforschungszentrum Leipzig) calculated sedimentation rates of 1400 to 2200 g/m^2 in this area.

Table 4. Cumulative discharge and SPM-loads in Rosslau, Mulde, Saale, and Magdeburg during the period of high water discharge in 2006
(Heise et al. 2008)

Station	Discharge (m^3*10^3)	Load (metric ton)
Rosslau	2,696,597	194,049
Mulde	801,058	18,430
Saale	535,583	52,642
Sum	4,033,238	265,120
Magdeburg	3,907,440	188,621

The floodplains of the Elbe River are today an important resource for agriculture, livestock, industry, and tourism. However, deposits of contaminated sediment particles carried onto floodplains by floods have resulted in elevated contaminant concentrations in holocene soils adjacent to the Elbe River. In particular, metal and arsenic concentrations in these soils

commonly exceeded threshold values established by German soil protection legislation. The contaminated floodplains are commonly used for growing hay or as pasture for cattle, such that transfer of metals and arsenic into the food chain is possible (Kruger et al., 2005; Overesch et al., 2007). However, given its high toxicity and bioaccumulative capacity, contamination of the food chain with dioxin is of even greater concern to farmers (Quast et al., 2011; Taube et al., 2009).

2.3.3 Importance of the tributaries Mulde and Saale with regard to Relative Discharge and Suspended Sediments Relationships

Two large tributaries, the Saale and the Mulde, join the Elbe within the modeled area (defined in Section 5.3.1). Thus, it is important to address the relative contribution of river discharge and sediment from the tributaries to the overall flow and sediment of the Elbe. Figure 7 shows a box and whisker plot of annual discharge for gauging stations in the modeled area for the Elbe, Mulde, and Saale. For the years 1994-2007, the average discharge at Dresden was 345.5 m^3/s. The Mulde and Saale had discharges 16.6 % and 33.6 % of the Dresden discharge, respectively. Thus, while the individual discharge contributions of the Mulde and Saale are small in comparison, they add up to almost half of the flow volume in the Elbe.

Figure 8 shows a box and whisker plot of annual suspended sediment loads for the Elbe, Mulde, and Saale. For the years 1994-2009, the suspended sediment load at Zehren was 244537.5 tons/year. The average Mulde and Saale loads represented 7.4% and 47.2% of the Zehren load, respectively. The Mulde suspended sediment loads, in particular, are relatively small, but the combined input from the two rivers amounts to over half of the total suspended load in the Elbe. Thus, the tributaries have the potential to strongly influence dynamics of suspended sediment, and associated contaminants, in the Elbe.

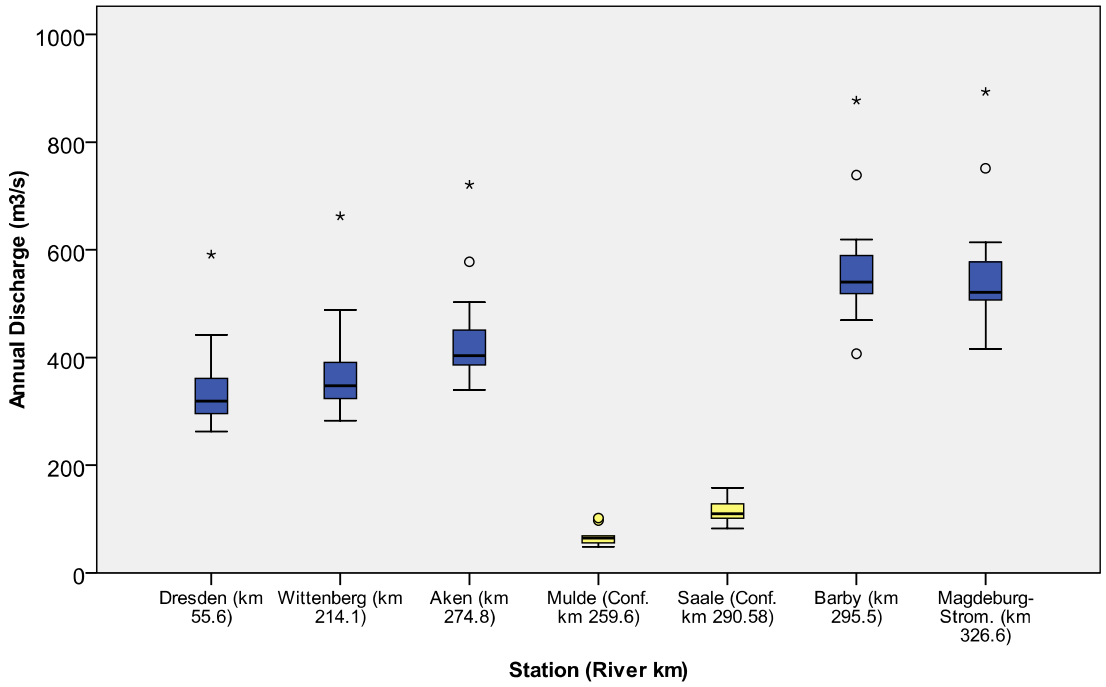

Figure 7. Box and whisker plot of annual discharge (1994-2007) (WSV, 2011)

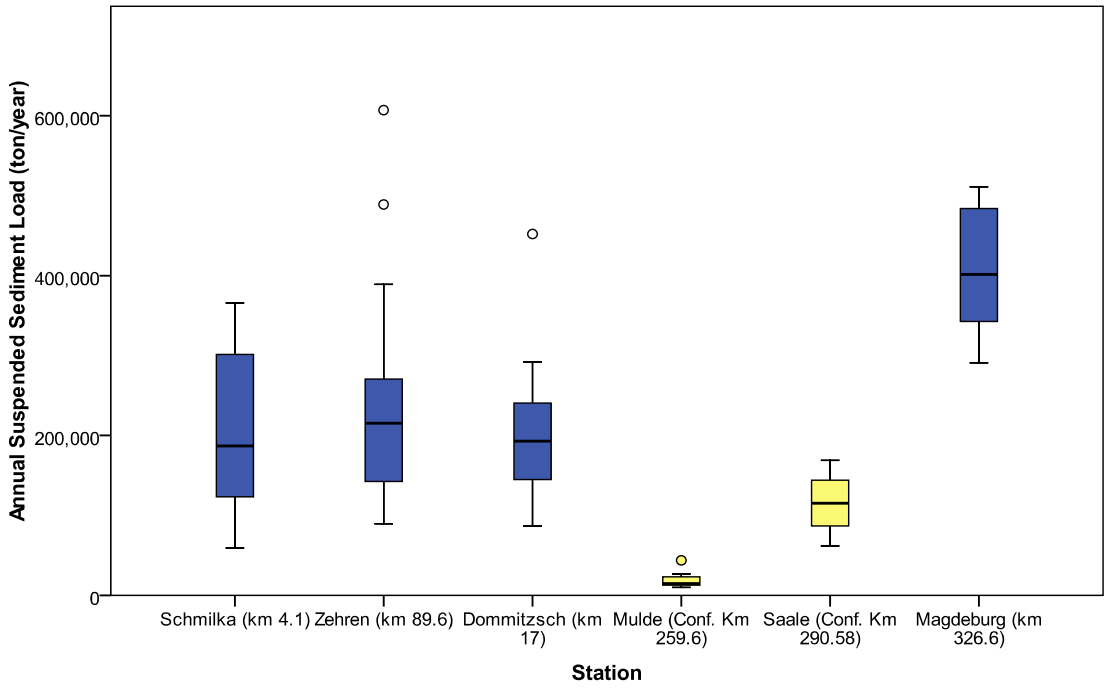

Figure 8. Box and whisker plot of annual suspended sediment loads (1994-2009) (BfG, 2012)

3 Hydrodynamic and Sediment Transport Modeling

Increased awareness of the role of suspended sediments in the fate and transport of environmentally sensitive chemicals has resulted in considerable effort over the last three decades to develop and implement numerical models capable of simulating the transport, erosion, and deposition of sediments (and associated contaminants) in rivers, estuaries, and coastal areas. Efforts to model the hydraulics of water bodies began in the early 1960's, and more complex models simulating water quality parameters and the transport of sediment were developed over the following decades. Recent improvements in computing power has enabled the movement of sediment and water to be investigated at increasing temporal and spatial resolutions (Odd and Owen, 1972; Singh and Woolhiser, 2002; Walling and Kane, 1982).

Hydrodynamic and suspended sediment models have been developed for a diverse array of rivers, estuaries, reservoirs, and oceanic areas. The section below describes approaches to modeling the transport of sediment and sediment-bound contaminants in free-flowing rivers. More information on models in other aquatic environments (i.e. estuaries, reservoirs, etc.) can be found in the following references: Guan, Wolanski, and Dong 1998; Hayter and Mehta 1986; Lumborg and Windelin 2003; Odd and Owen 1972; Wu, Falconer, and Uncles 1999.

3.1 Transport of Sediment and Contaminants in River Basins

Hydrodynamic processes are the dominant mechanism controlling sediment transport; they advect suspended sediments, provide the force necessary to erode bed sediments, and the turbulence they generate plays a significant role in the flocculation of cohesive sediments. Conversely, suspended sediments alter the density and kinematic viscosity of the water body in which they are suspended. Due to the reliance of sediment transport on the fluid in which they are suspended, a calibrated hydrodynamic model is commonly the first step in developing a sediment transport model (Lick, 2008; Liu et al., 2002).

Sediment transport can vary widely within and between rivers, depending on flow rates, bathymetry, sediment properties, and sediment concentration. Sediments originate as material

eroded by wind, storm water or rain. Processes contributing to erosion can be natural (e.g. bank erosion) or driven by human development (e.g. wastewater discharge, mining, construction) (Kalin and Hantush, 2003). Suspended sediments consist of fine-grained material that is light enough to be carried by a river without being deposited. These particles (generally cohesive) consist of a mixture of clay, silt, and organic matter. A key property of the cohesive particles is inter-particle attraction, which is governed by two key processes: cohesion and adhesion. Cohesion describes the attraction between chemically similar particles, such as clays and colliods (Grabowski et al., 2011). More specifically, these particles are bound together by electro-chemical forces, such as van der Waals forces and electrostatic attraction (Pye, 1994). Adhesion is the attraction between particles or substances that are dissimilar. For example, adhesion is the sorption of sediment components by an inter-particle substance, such as organic polymers or iron oxides, by cation bridging or polymerization. Flocculation describes the aggregation of particles by adhesion, and coagulation is when this process occurs via cohesion (Grabowski et al., 2011). Particle flocculation depends on several factors, including sediment type, the type and concentration of ions in the water, and flow conditions (Mehta et al., 1989). Settling velocity is determined by the structure of these flocs (size, density, and shape).

Since cohesive sediments are primarily composed of clay-sized particles, with strong inter-particle forces due to surface ionic charges, clay particles are the primary cause of sediment cohesion. Clays have high surface area to volume ratios, and their flat surfaces, carry strong, generally negative, electro-chemical charges (Partheniades, 2007). As sediment particle size decreases, the inter-particle forces become more important than the gravitational force, and settling velocity is no longer a function of only particle size (Huang et al., 2006).

The cohesive properties of fine-grained sediments also cause heavy metals, hydrophobic organic compounds, and nutrients to adhere preferentially to sediment over water. While the degree of partitioning depends on sediment properties such as age, grain size and type, the colloids and organic matter content of the sediment, as well as properties of the pollutant, contaminants often adhere several orders of magnitude more strongly to cohesive sediments than to water (Lick, 2008). Due to the inability of discrete measurements to capture heterogeneity of natural systems, numerical models are increasingly used to simulate the

transport of sediments and particle- bound contaminants. An overview of the numerous approaches to modeling fate and transport of cohesive sediments and particulate-bound contaminants is provided in the following section. Section 3.3 summarizes existing research approaches to modeling sediment dynamics in groyne fields.

3.1.1 Types of Sediment Transport Models

Based on Wheater et al. (1993) and Merritt et al. (2003), with modifications from C.R.C. Catchment Hydrology (2005a, b), sediment transport models can be classified into three broad categories based on their underlying algorithms:

- **Empirical** – based primarily on response data derived from field or laboratory studies. Empirical model require minimal parameter inputs, and generally simulate a simplified version of the system being studied. Thus, they commonly do a poor job of predicting the implications of extreme events, but are the least computationally intense of the three model types.
- **Conceptual**– more complex than empirical models, generally used to model sediment transport from the upland parts of the watershed. Basic processes such as erosion and runoff are calculated as independent input-output relationships that mimic the functional behavior of the process being modeled.
- **Physics-based, or Process-based** – more complex than conceptual models, and based on fundamental equations for hydraulics and sediment movement (e.g. equations for continuity of mass and/or momentum). Sediment transport is calculated as a function of hydraulic properties of flow. Given the heterogeneity of natural systems, physics-based models require numerous parameter inputs.

Other considerations when selecting a model include how data are represented (stochastic vs. deterministic), the number of space and time dimensions, how the model represents spatial detail (lumped vs. distributed), and the method used to quantify processes affecting sediment transport (e.g. erosion, deposition grain size distribution, settling speeds, flocculation, etc.) (C. R. C. C. R. C. Catchment Hydrology, 2005; C. R. C. Catchment Hydrology, 2005; Lick, 2008;

Mehta et al., 1989). Alternatives for space dimensionality include one-dimensional (1D), two-dimensional (2D), or three-dimensional (3D), or a combination thereof. While 1D models provide results along a single axis (Lin et al., 1983), two-dimensional (2D) and three-dimensional (3D) provide results along two and three-axes, respectively (Ariathurai and Krone, 1976; Edelvang et al., 2002; Hayter and Mehta, 1986; Lindenschmidt et al., 2008). Spatially lumped models aggregate the modeled area into a single unit and average variability over the entire unit. Spatially distributed models divide the modeled area in discrete units, enabling spatial heterogeneity to be represented with a broad array of model inputs.

While numerous sediment transport models are available, the fundamental theories on which they are based are often quite similar. The differences between models often come from differences in the modeling approach or minor differences in algorithms used to simulate individual processes (C. R. C. Catchment Hydrology, 2005). Comprehensive reviews of available commercial software packages are available in Horn et al. (2004), Kalin and Hantush (2003) and Merritt et al. (2003).

3.2 Modeling Sediment Transport in River Basins

The majority of descriptions of sediment transport models found in the literature are for estuaries or reservoirs (Bever et al., 2009; Guan et al., 1998; Hayter and Mehta, 1986; Lumborg and Windelin, 2003; Odd and Owen, 1972; Wu et al., 1999). Literature detailing results of sediment transport models in large river basins are less common (Edelvang et al., 2002; Peckham, 2003; Saleh et al., 2000). This disparity is due to both the importance of estuaries in retaining fine grained sediment and the large amount of data needed to adequately characterize sediment and hydrodynamics in large river basins. Since the ongoing sources of contamination within the Elbe River basin are distributed throughout the watershed, a broad-scale approach is required to accurately detail both the diversity of contaminant and sediment sources and temporal aspects of contaminant transport.

3.3 Groynes and Groyne Fields

The primary purpose of groynes is to maintain adequate navigation depths in the Elbe River. The bottleneck effect of the reduced channel cross-section between the groyne heads causes higher flow velocities, which increases bedload erosion. Conversely, flow velocity decreases downstream of the groyne head and between groynes which increases hydraulic retention time in the groyne field. Thus, the morphological structure of the groynes causes the river banks to be areas of increased sedimentation rather than increased erosion. During high water conditions, groynes are typically submerged, and flow proceeds directly over the groynes. Partially submerged groynes result in eddies that move through the groyne field and govern the amplitude variations of the flow over the groyne (Ockenfeld et al., 2003; Uijttewaal, 2005).

Even though groyne fields are a commonly used river training structure within Europe, sediment deposition and transport patterns within groyne fields are not well understood (Sukhodolov et al., 2002). The section below summarizes the current state of knowledge on the Elbe River groynes and groyne fields as well as parameters measured or calculated in previous studies that will be used to calibrate or validate the model that is the focus of this study.

3.3.1 Elbe River Groyne Fields: Source and Sink for Particulate-Bound Contaminants

Groyne fields cover almost 92% of the banks of the Middle Elbe River, and are of key importance to the transport of particle bound substances within the river basin. Several authors have identified the fine- grained sediments that accumulate in groyne fields as an important source and sink for contaminants for the Elbe River, depending on flow conditions (Baborowski et al., 2007; Götz et al., 1998b; Heise et al., 2008; Schwartz and Kozerski, 2003; Schwartz, 2006; Weigold and Baborowski, 2009). The contribution of groyne fields to downstream contaminant loads is illustrated particularly well in Figure 9, which shows the increase in Cd and Hg loads between the monitoring station by Magdeburg (km 318.1), located downstream of all significant tributaries to the Elbe River, and Schnackenburg (km 474.6). No known sources of Cd and Hg between Magdeburg and Schnackenburg exist, yet the Cd and Hg

concentrations increase between approximately 0.25 and 2.5 fold. This trend decreases somewhat in 2001.r

Other potential causes of this trend may be incomplete mixing that occurs between the two locations. This may be an indication of contaminated material being resuspended on that stretch from groyne fields, but other explanations are also possible, such as incomplete mixing that occurs between the two locations.

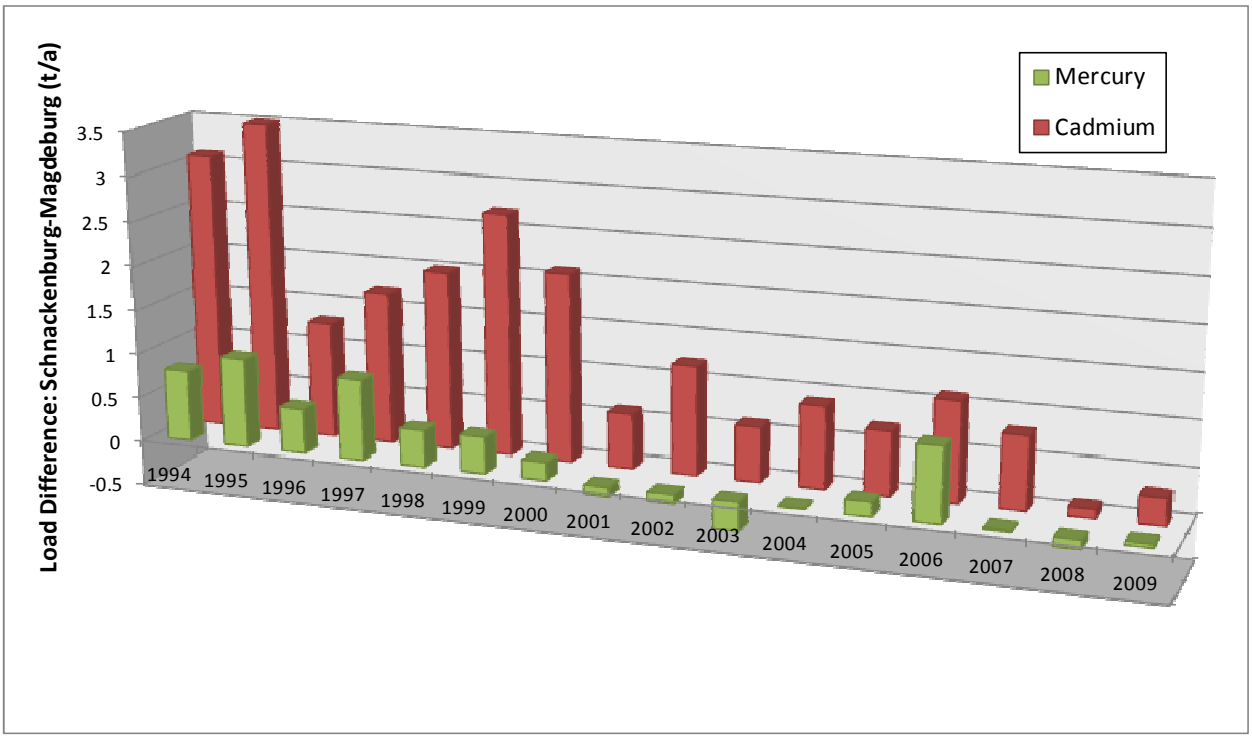

Figure 9. Increase in Hg and Cd loads between Magdeburg and Schnackenburg (1994-2009) (Bergemann, 2011)

3.3.2 Characteristics of Elbe River Groyne Fields

Recent detailed research has evaluated the hydraulic and sediment characteristics of typical groyne fields in the Elbe River basin. Study results have provided insight into (1) physical and chemical properties of groyne fields, (2) deposition patterns in groyne fields, and (3) significance of shear stress inputs in estimating erosion in groyne fields. Study results are summarized below.

Flow velocity and discharge within groyne fields are significantly lower than in the main channel. To estimate the rates of hydraulic exchange between the groyne fields and the main channel of the Elbe River, Kozerski et al. (2006) used tracer experiments (single point dye injections) to show the mean characteristic time, or time to decay of the tracer, within five groyne fields near Havelberg in the Middle Elbe to be between 15 and 69 minutes, and to be uncorrelated with water level. However, the authors found the tracer studies can overestimate hydraulic residence due to incomplete mixing of tracer substances within the groyne field. Schwartz and Kozerski (2003) and Schwartz (2006) evaluated the physical-chemical characteristics of groyne fields and determined the groyne fields to be dominated by cohesive sediments (<63 µm). Prior to the 100-year flood that occurred in August, 2002, surficial concentrations of nutrient and contaminant were significantly elevated relative to main channel sediments. Following the August, 2002 flood, surface sediments were generally less contaminated, but contaminant concentrations remained elevated at depth. This change corresponded to a post-flood coarsening of groyne field sediments caused by the downstream transport of fine sediments by floodwaters downstream and onto floodplains (Schwartz and Kozerski, 2002; Schwartz, 2006). Two studies have measured sedimentation rates in groyne fields (Brügmann, 1995; Schwartz and Kozerski, 2003). Brügmann (1995) found the sedimentation rate to be between three and four cm per year, while Schwartz and Kozerski (2003) measured sedimentation rate in one groyne field to be 1.5 cm per year.

Sukhodolov et al. (2002) describe a classification system for groyne fields that divides groynes into seven morphological classes based on sediment deposition patterns (from (Hinkel, 1999). Aerial analysis showed that 49 and 21 percent of the Elbe River groyne fields fall into the 'uniform partial deposition' and 'upstream wave-shaped' deposition categories, respectively, indicating low ratios of lateral (Lg) to longitudinal (Lf) groyne length (Figure 10). The authors also evaluated sediment accumulation and flow patterns in two typical groyne fields located along the Middle Elbe (river km 317 and 420). They determined that one-gyre circulation pattern was dominant when the ratio Lg/Lf fell below a critical value of 0.5, and a two-gyre circulation dominated when the ratio exceeded 0.5. This study also showed suspended sediment concentrations (SSC) leaving and entering the groyne field to be equivalent.

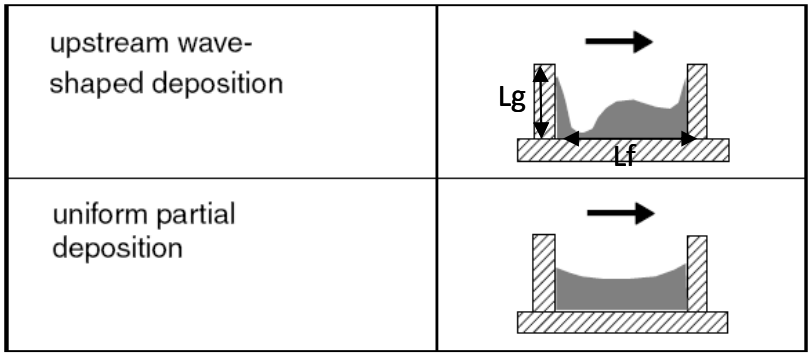

Figure 10. Classification of morphological patterns of groyne fields
Modified from Sukhodolov et al., (2002), based on Hinkel (1999)

Two studies have measured erosional shear stress in groyne fields. Schwartz (2006) measured critical shear stress for erosion and evaluated the *in situ* relationship between critical shear stress for erosion and flow velocity. The author found critical shear stress in one groyne field (km 420.9) varied between of 0.5 and 3.5 N/m^2 (Pa), and found that an effective flow velocity of approximately 41 cm/s is required to erode upper sediment layers (approximately 0 to 5cm) and that an average flow velocity of 88 cm/s is required to erode the deeper, more consolidated layers. A flow velocity of 122 cm/s was necessary to erode the most consolidated layers, a value which was only achieved during extreme events, such as the August, 2002 flooding (Wirtz, 2004). More recent work investigating shear stress in three groyne fields in the Elbe River has shown mean critical shear stress of 3 N/m^2 (average of 94 measurements) (Prohaska et al., 2008). These measurements were conducted using sediment cores in a laboratory setting, utilizing the SETEG system (Kern et al., 1999).

Prohaska et al. (2008) also developed a 1D multi-strip model for the Elbe River from Wittenberg (km 214.6) to Magdeburg (km 326.6) using stochastic inputs of critical erosion shear stress from three groyne fields (Coswig (km 235.0), Steckby (km 280.0), and Fahlberg (km 318.0)) to estimate the probability of groyne field erosion at different flood discharges. The authors found treating critical erosion shear stress values as stochastic variables with associated probabilities to be more effective than a deterministic method in estimating erosion of groyne field sediments.

4 Model Selection

Numerous commercial software packages models are available for simulating hydrodynamics, water quality, and sediment transport within riverine systems. Model selection for this project was completed by first establishing a list of model selection criteria, and then comparing the characteristics of a set of commonly used hydrodynamic/sediment transport models to the criteria list. Models were evaluated according to the following criteria:

- Suitable for the morphologic and hydrodynamic heterogeneity of the Elbe River basin
- Capable of simulating the hydrodynamic and sediment transport interactions between the main channel and groyne fields
- GIS Integration
- Availability of technical documentation and/or support
- Data requirements
- Cost and availability
- Ease of use

Section 4.2 provides a brief comparison between MIKE and SOBEK, the modeling package currently used by the BfG for modeling hydrodynamics, sediment transport, and flooding scenarios for German rivers. Table 5 lists the eight models considered for this project. Given the subjectivity of some of the model selection criteria, a qualitative, rather than quantitative, comparison between model selection criteria and available models was conducted. MIKE 11, and SOBEK, two of the modeling packages listed in. Section 4.2 provides a brief comparison between MIKE and SOBEK, the modeling package currently used by the BfG for modeling hydrodynamics, sediment transport, and flooding scenarios for German rivers.

The MIKE suite of software (Danish Hydraulics Institute) was ultimate selected for a variety of reasons including: ability to couple 1D/2D models, high likelihood of accurately simulating hydraulic and sediment dynamics in groyne fields, the potential for integrating this model with

an already existing MIKE model for the tidal Elbe, widely accepted model structure, the presence of a local DHI office with staff members available for meetings and one-on-one assistance. A description of the MIKE modeling system is provided in Section 4.1. Section 4.2 provides a brief comparison between MIKE and SOBEK, the modeling package currently used by the BfG for modeling hydrodynamics, sediment transport, and flooding scenarios for German rivers.

Table 5. Hydrodynamic/sediment transport models

Model	Model Type (See Section 3.1.1)	Reference
ANSWERS	Physical	Beasley, Huggins, and Monke 1980
CE-QUAL-W2	Conceptual	Cole and Wells 2002
HSPF	Conceptual	Wool et al. 2001
MIKE 11	Physical	Havnø, Madsen, and Dørge 1995
QUAL2E	Conceptual	Brown and Barnwell 1987
Sednet	Empirical/Conceptual	Wilkinson, Henderson, and Chen 2004
SOBEK	Conceptual	Delft Hydraulics 1996
WASP	Physical/ Conceptual	Wool et al. 2001

4.1 MIKE Software Suite

The MIKE software suite consists of 1D (MIKE11) and 2D flexible mesh (MIKE21FM) components. MIKE11 and MIKE 21FM have been used simulate hydrology, hydraulics, water quality and sediment transport in estuaries, rivers, and other inland waters worldwide (Edelvang et al. 2002; Havnø, M. N. Madsen, and Dørge 1995;(C. B. Pedersen et al.; Jayatilaka et al., 1998; Niedbala et al., 1999; N. H. Pedersen et al., 2005; Thompson et al., 2004). Both MIKE11 and MIKE 21FM are described in detail below. Model variables, algorithms and their interdependencies of the one- and two-dimensional models and their composite modules are detailed in the DHI, 2010, 2011a, and 2011b.

4.1.1 MIKE11: Hydrodynamic (HD) Module

MIKE11 has a base hydrodynamic module (HD) that uses an implicit, finite difference scheme for the computation of unsteady flow. MIKE 11 simulates changes in water depth and flow velocity in space and time in response to variation in flow rate and/or water surface elevation at boundaries for given bottom morphology and initial conditions. The models provides a full solution of the Saint Venant equations for continuity and momentum (shown below in Equation 1 and Equation 2, respectively), plus many process modules for advection-dispersion (AD), water quality and ecology, sediment transport, and rainfall-runoff.

Equation 1: $$\frac{\partial q}{\partial x} + \frac{\partial A_{fl}}{\partial t} = q_{in}$$

Equation 2: $$\frac{\partial q}{\partial t} + \frac{\partial\left(\alpha \frac{q^2}{A_{fl}}\right)}{\partial x} + gA_{fl}\frac{\delta h}{\delta x} + gA_{fl}I_f = \frac{f}{\rho_w}$$

where: q = discharge, A_{fl} = cross section area, q_{in} = lateral inflow (per length unit), h = water level, α = momentum distribution coefficient, I_f= flow resistance, f= momentum forcing (per length unit), and ρ_w = density of water.

The module used to simulate the transport of sediment and other non-degrading substances, is based on the one-dimensional equation of conservation of mass of dissolved or suspended material (advection-dispersion equation) as reported in Ariathurai and Krone (1976) and Mehta et al. (1989). The model includes description of sediment settling with different settling velocities (flocculation), hindered settling and a combination of currents and waves to calculate the bottom shear stress. For the floodplain and river profile, flooded area versus elevation curves are computed to quantify the storage capacity of sections of the floodplain, and are also exported to a MIKE 11 cross-section database.

4.1.2 MIKE11: Advection-Dispersion (AD) Module

The advection-dispersion (AD) module is used to model transport of cohesive sediment, defined as sediments smaller than 63 µm. The CST model solves the advection-dispersion equation, shown in Equation 3:

Equation 3: $\frac{\partial AC}{\partial t} + \frac{\partial QC}{\partial x} - \frac{\partial}{\partial x}\left(AK\frac{\partial C}{\partial x}\right) = S_e - S_d$

where *Q* = discharge, *A* = cross-sectional flow area, *C* = cross-sectional average sediment concentration, *K* = dispersion coefficient, *Se* = erosion (resuspension) flux, and *Sd* =deposition flux. Erosional flux is expressed following Equation 4:

Equation 4: $S_e = \frac{M^*}{D}\left[1 - \left(\frac{U}{U_{ce}}\right)^2\right], U \geq U_{ce}$

where *M** = erodibility of bed, *D* = flow depth, *U* = cross-sectional average flow velocity, and U_{ce} = critical erosion velocity. Depositional flux is expressed following Equation 5:

Equation 5: $S_d = \frac{wC}{D^*}\left[1 - \left(\frac{U}{U_{cd}}\right)^2\right], U \leq U_{cd}$

where *w* = mean settling velocity of suspended particles, *D** = average particle settling depth and U_{cd} = critical deposition velocity.

The AD module can also simulate the transport, erosion and deposition of non-cohesive sediments based on the one-dimensional equation of conservation of mass of a dissolved or suspended material (i.e. the advection-dispersion equation). The AD module uses as input discharge, water level, cross-sectional area and hydraulic radius output by the HD module. The advection-dispersion equation is solved numerically using an implicit finite difference scheme which is, in principle, unconditionally stable and has negligible numerical dispersion.

4.1.3 MIKE11: Ecolab Xenobiotics Module

Ecolab is a numerical template for ecological and contaminant modeling. The template can be customized to model water quality, eutrophication, heavy metals, organic contaminants and

ecology. The module describes the chemical, biological, ecological processes and interactions between state variables, or variables that describe the mathematical "state" of a dynamic system. State variables included in ECO Lab can either be transported by advection-dispersion processes based on hydrodynamics, or have a more fixed nature (e.g. rooted vegetation).

The transport of xenobiotics discharged into the aquatic environment or from polluted sediment can be modeled by simulating mechanisms controlling the movement of xenobiotics within the environment. These mechanisms are abundant, but in a macroscopic scale a limited number of overall processes govern transport processes. (Anderson et al., 1987; Honeyman and Santschi, 1988), from (DHI, 2011). These seven processes are listed below:

1. The adsorption and desorption of xenobiotics
2. The sedimentation and resuspension of particle-bound xenobiotics
3. The diffusive transport of dissolved xenobiotics at the sediment/ water interface
4. Biodegradation
5. Photolysis
6. Hydrolysis
7. Evaporation of dissolved xenobiotics
8. The transport of dissolved and particulate xenobiotics in the water column by advection and dispersion.

The xenobiotic ECO Lab template itself accounts for the first seven processes detailed above, while the advection-dispersion process is calculated by MIKE 11. Figure 11 details the interactions between these processes, in both the sediment and water phases. Appendix B details mathematical formulations behind the Ecolab template.

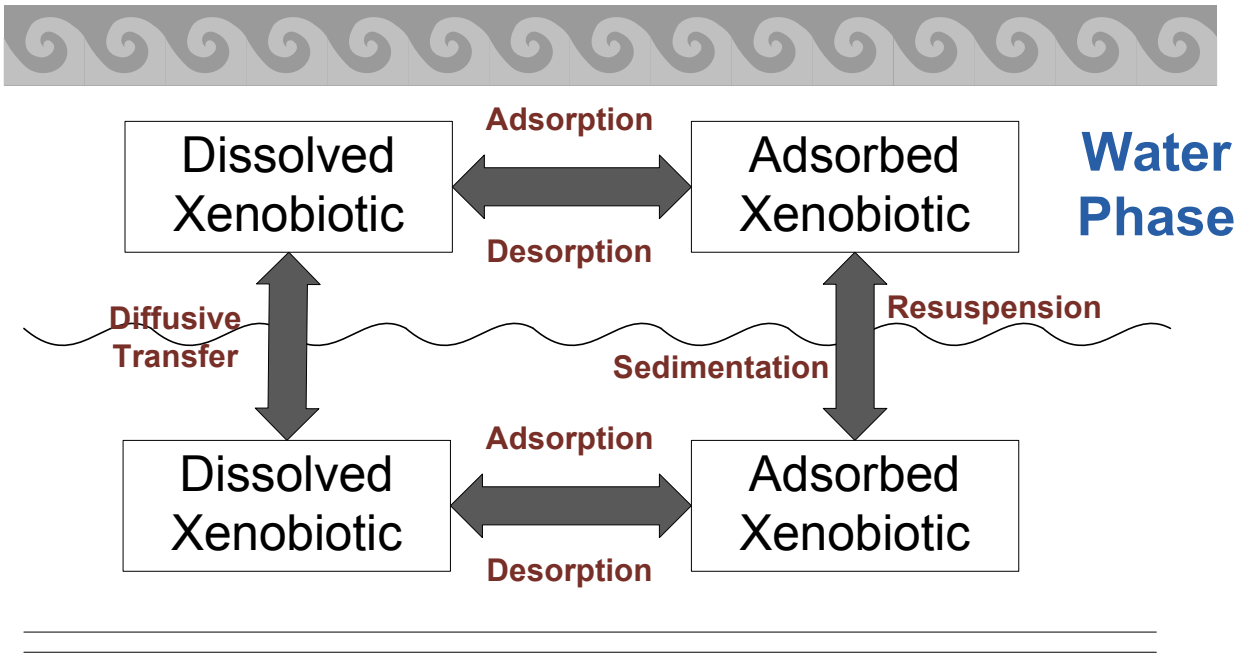

Processes:

- Adsorption/desorption from particulate matter
- Sedimentation/resuspension of particulate matter
- Optional: Biodegradation, photolysis, hydrolysis, evaporation

Figure 11. Processes in the xenobiotics template

4.1.4 MIKE21FM Hydrodynamic Module (HD)

The FM Hydrodynamic Module is based on the numerical solution of the two-dimensional shallow water equations; the depth-integrated incompressible Reynolds averaged Navier-Stokes equations. The model solves equations for continuity, momentum, temperature, salinity and density using a cell-centered finite volume method. The model consists of an unstructured grid composed of triangles or quadrilateral elements in the horizontal plane. An explicit scheme is used for time integration. An approximate Riemann solver is used for computation of convective fluxes, making discontinuous solutions possible. Manning's bed roughness and eddy viscosity are the two primary calibration parameters.

4.1.5 MIKE21FM Mud Transport Module (MT)

The Mud Transport (MT) module describes erosion, transport and deposition of mud or sand and mud mixtures under the action of currents and waves. Sand transport can be simulated using this module, but only sand assumed to be transported via suspended transport (i.e. bedload transport is not simulated). The FM Hydrodynamic module provides the hydrodynamic basis for the MT module. Processes simulated in the model include: morphological update of the bed resulting from erosion and deposition, description of settling processes, flocculation and wave forcing processes. The sediment bed is assumed to be layered and is characterized by its density and shear strength. Dispersion and critical shear stress for deposition are the key parameters for calibration.

4.2 Comparison: MIKE Suite vs. SOBEK

SOBEK (Delft Hydraulics) is an integrated software package for river, urban or rural management. SOBEK is used to model 1D flow in channels, rivers, and urban drainage networks as well as simulate water quality parameters, sediment transport, and 2D overland flow. Like MIKE, SOBEK solves the one-dimensional Saint Venant flow equations using a staggered grid. Both models can analyze and solve nearly all typical hydraulic modeling applications for multiple rivers, sinuous rivers, split flow, and flow diversions. The major differences between MIKE and SOBEK are the coupling between 1D and 2D models, interpolation of cross-sections, ease of use, availability of documentation, and technical support. Given that the Elbe River groynes are smaller than the width of the main channel, the distinct advantage of the MIKE software is that it allows for the coupling of 1D/2D models at a resolution that will facilitate modeling of sediment transport interactions between the main channel and the groyne fields.

5 Materials and Methods

This section describes the development of the hydrodynamic, suspended sediment and contaminant models, as well as details the multiple steps that carried out as precursors to model development. Key amongst these initial steps were compiling, processing, and analyzing the existing suspended sediment, discharge, and contaminant databases. As described in Section 3, in support of model development, the initial goal of this study was to develop a better understanding of any trends or relationships in or between the vast databases of discharge, SSC, and sediment-sorbed contaminants in the Middle Elbe. This was accomplished by conducting three preliminary analyses:

1. Long-term trend analysis of existing sediment data, with respect to season and annual variability
2. Relationship between discharge and suspended sediment, using double mass analysis and rating curves
3. Principle component analysis (PCA) of existing sediment contaminant data. This technique was used to evaluate relationships between contaminants. This analysis was also used to aid in selecting a contaminant to model, as well as identify contaminants that are correlated with the modeled contaminants.

More detail on the statistical techniques and methods used for the long-term trend analysis, double mass analysis/rating curves, the PCA are described in Sections 5.1.1, 5.1.3, and 5.1.4, respectively. All three of these analyses were used to aid and inform the process of model development, as well as provide perspective on model input and output data. All statistical analyses were performed using SPSS version 16 or Microsoft Excel (Microsoft, 2007; SPSS Inc., 2007).

The goal of model development was to enable robust simulations of sediment-bound contaminants throughout the reach of the Elbe between Dresden and Magdeburg, including the floodplains. The steps to achieving this are as follows: First, by establishing the contaminant to be modeled and the time and space over which to model. Second, by

developing a modeling strategy that incorporates adequate simulations of groyne fields, as well as transport to floodplains. Lastly, by calibrating and validating the model, or models. More details on model development and calibration are provided in the following sections.

Once the contaminant of interest and spatial and temporal scales were established, the model development strategy involved a multi-step process. First, a 1D model (HD, AD, and xenobiotics) that did not include floodplains was developed and calibrated. Floodplains were excluded to allow for faster calibration. Second, a 1D model (HD, AD, and xenobiotics) that did include floodplains was developed and calibrated. Information learned from the first step was incorporated into this second model. Third, it was anticipated that a 1D model will not be adequate to simulate the complex hydrodynamic and sediment transport that occur both within groyne fields and between groyne fields and the main channel. Even though a 2D model covering the entire length of the modeled area would be ideal to simulate the groynes, the quantitative limitations of most computers preclude this possibility. Therefore, the third step was to select a smaller stretch of the Elbe between Aken (km 274.8) and Barby (km 294.8), and model that in 2D over a short period of time. The last step in this process was to conduct an impact analysis, comparing the results of the 1D and 2D FM model to determine the influence of the groynes on sediment transport times.

5.1 Preliminary Data Analyses

5.1.1 Analysis of Long-term Trend Trends in SSC Data

Knowledge of trends in erosion, transport, and deposition of SSC and loads in the Elbe was considered an important first step in model development, due to the importance of suspended sediment to contaminant transport. Thus, long-term, regional and seasonal trends in the suspended sediment datasets from Meissen and Magdeburg-Strombrücke (model boundaries) were investigated between 1/1/1995 and 12/31/2008. This was completed by first carrying out an analysis of missing data, and then evaluating data for temporal and spatial trends. There are three reasons for missing suspended sediment data: missing weekend data, which are interpolated over the weekends, missing data in mid-December to early-January holiday period,

which begin in 2002, and longer-term gaps in the record due to either malfunctions at the sampling station and/or the need for station repair. For the purposes of this analysis, missing weekend data were ignored since they occur at all stations, and only issues related to the December/January and longer-term data gaps were investigated. Between 1995 and 2008 (inclusive), 7.9% of the Meissen, and 3.2% of the Magdeburg Strombrücke data record are missing. While the relatively small percentage of missing data from Magdeburg Strombrücke is unlikely to influence statistical results, the missing data from Meissen has the potential to cause spurious results, particularly due to the fact that the post-2002 data are always missing from the same time period (mid-December to early January). Of particular interest in this analysis was whether any observed short- or long-term trends in SSC or loads could be identified. Results from this analysis were key in guiding model development, and are presented in Section 6.4.

5.1.2 Analysis of Long-term Trend Trends in HCB Load Data

As discussed in Section 2.1, loads of many contaminants in the Elbe have decreased dramatically over the past 20 to 30 years. Since the annual loads of many contaminants display a decreasing historical trend, it is possible to use linear regression to predict future contaminant loads. For this analysis, long-term HCB[1] loads at Schmilka (km 3.9) and Schnackenburg (km 474.5) were analyzed to estimate future loads at Schmilka and the resulting load downstream in Schnackenburg under scenarios of (1) natural attenuation (no management measures) and (2) source control. These two stations were selected because Schmilka is closest to the Czech/German border and thus most representative of HCB loads travelling downstream from the Czech Republic. Schnackenburg is the sampling station closest to the weir at

[1] Load data were provided by Bergemann (2011)

Geesthacht, thus the reach between Schmilka and Schnackenburg is representative of most of the non-tidal Elbe within German borders.

An important source of uncertainty in these predictions, particularly given the high variability in contaminant loads, is the rate of HCB load decrease (i.e. the slope of the regression line). To address this uncertainty, this analysis incorporated a probabilistic approach to predicting future contaminant loads in the Elbe using Monte Carlo simulation techniques. A stochastic approach was particularly appropriate for these calculations due to the high heterogeneity as well as spatial and temporal variability in contaminant concentrations. This analysis was only possible to conduct on contaminants with a statistically significant trend of historical decrease. All statistics were conducted on $\log_{10}$ normalized variables to satisfy the assumption of normality. Monte Carlo simulations were generated using the Excel add-in Crystal Ball.

Regression coefficients were used to predict contaminant loads at 10-year intervals (2020 through 2060). Monte Carlo simulations were then used to simulate confidence intervals (CIs). The key assumption in these simulations is the slope of the line and the y-intercept. The distribution for the slope and y-intercepts were assumed to be normal, with a defined standard deviation. The standard deviation for the distribution of the slopes and y-intercepts was equivalent to the standard deviation of the $\log_{10}$ normalized contaminant data. 1000 trials were then run and the certainty of pre-determined load decreases within a specific timeframe was recorded. A 75% CI was ultimately selected because this presents a good balance between a scenario that is just as likely to happen as not (50% CI) and a scenario that encompasses almost all possibilities (96% CI).

5.1.3 Rating Curves and Double Mass Curves

The relationship between SSC, discharge, and yield are key factors to understanding sources, sinks, and trends in the fate and transport of sediment and sediment-sorbed contaminants within the Elbe Basin. However, the relationship between SSC and discharge is often highly variable. This variability is caused by a number of factors including: flow hysteresis, seasonal effects of vegetation and water temperature, temporal changes in particle origin, changes in

land use and/or land cover, as well as rainfall patterns. The SSC and discharge relationships at both Dresden and Magdeburg were investigated to determine if long-term and/or seasonal relationships exist within the dataset. Two methods were used to investigate trends in discharge and SSC: double mass curves and rating curves.

Double mass curves plot cumulative discharge against the cumulative sum of SSC over the same time period, and are often a first step in developing rating curves. The theory behind double mass curves is that by plotting the accumulation of two quantities, the data will plot as a straight line, and the slope of this line will represent a constant proportionality. Breakpoints, or changes in slope, indicate a change in the constant of proportionality and the consistency of data over time (Searcy and Hardison, 1960; Wigbout, 1973). Reasons for breakpoints can include changes in sediment or discharge transport regime, morphological changes, and land-use changes.

Sediment rating curves are most often used to estimate an empirical relationship between discharge and SSC, often in the absence of measured data. They can also be used to further investigate seasonal and long-term patterns in the sediment/discharge relationship. A poor correlation between discharge and SSC does not necessarily signify that a relationship does not exist, but rather that patterns may be obscured by seasonal variation, hysteresis, or the resolution and variability of the data (Asselman, 2000; Cigizoglu and Alp, 2006; Horowitz, 2002). Results of the double mass analysis and rating curve are presented in Section 6.3.

5.1.4 PCA of Sediment-Sorbed Contaminant Data

In this study, PCA was used as a first step to aid in analyzing trends and relationships in sediment contaminant data. PCA is a multivariate statistical technique commonly used to reduce the dimensionality of datasets with many correlated variables, and to group similar data. In PCA, correlated variables are transformed to a new set of uncorrelated reference variables, called principle components (PCs). The PCs accounting for the largest percentages of the variance in the original data can be used as a proxy for the original data (Murphy and

Morrison, 2007). When a small number of PCs (e.g. three to five) represents most of the variability in a dataset (e.g. 70 to 100%), the PCA can be assumed to be successful.

PCA was used primarily to identify patterns in sediment-sorbed concentrations of organic contaminants. The secondary goal of this analysis was to describe relationships between contaminants as well as to identify any contaminants correlated with HCB, the contaminant which is focused on in this study. The dataset consisted of concentration of contaminants associated with sediment particulate matter (FGG Elbe, 2012). These data are discussed in Section 5.4.2. For this analysis, sediment from only the Zehren sampling station (Km 89.6) were used, as they represent the input from the Czech Republic, free from the influence of the Saale or Mulde Rivers. Only organic contaminants were included in this analysis.

Prior to evaluating statistical relationships, the detection frequency of all sediment analytes was calculated. Detection frequency is defined as the ratio of the frequency the analyte is detected above the limits of detection to the total number of times the analyte was analyzed for by the laboratory. The basis for this analysis is that the contaminant data are left-censored (i.e. the concentration of each contaminant is below an arbitrary limit, equivalent to the limit of detection). If a majority of the results for any given contaminant are found to be below this limit, statistical analysis of this analyte may create spurious results. Therefore, this analysis was initially limited to analyses with minimum detected frequency of 50%. The decision to exclude all analytes with a detection frequency of less than 50% was based primarily on the available data, but also on recommendations from other authors (Antweiler and Taylor, 2008; Helsel, 2005; Taylor and Cihon, 2004).

5.2 Selected Contaminant of Interest: HCB

A diversity of contaminants contribute to interregional risk in the Elbe River Basin (Table 1). Thus, a key step in setting up the model was deciding which of these contaminants to model. All contaminants that were previously identified as “substances of concern” within the Elbe River Basin and those that were identified as Elbe relevant contaminants by the IKSE were considered (Heise et al., 2008). However, it was decided to initially complete the modeling with

one contaminant, and due to the strong affinity of organic contaminants for sediments and organic material, organic contaminant would be most appropriate. The contaminant modeling focused on HCB due to:

- Sediment concentrations of HCB in sections of the Elbe River basin significantly exceed maximum allowable concentrations established by the European Commission (Heise et al., 2008). HCB is also of high societal and environmental interest.
- HCB is a highly representative contaminant. Following the results of the PCA (methods described in Section 5.1.4 above, and results in Section 6.4) patterns in sediment-sorbed HCB concentrations are associated with other Elbe relevant contaminants including p,p´DDT, PCB 28, and pentachlorobenzene and several chlorinated benzenes. Trends in HCB concentration can then be assumed to function as a proxy for several other contaminants.
- HCB is toxic to aquatic life, persistent in the environment and bioaccumulative (D'Eugenio, 2005; Egeler et al., 1997; Niimi and Cho, 1980).
- The log K_{OW} of HCB is 5.31, indicating strong binding to suspended matter, and relatively little remobilization to the water phase (EPA, 2002).
- HCB is listed as a WFD priority hazardous substance (COM(2011)876, 2012; Directive 2000/60/EC, 2000) as well as a persistent organic pollutant (POP) by the United Nations Environment Programme (UNEP, 2004).
- Availability of concentrations of sediment bound HCB over a broad geographic area and time period. While other contaminants (i.e. dioxins) are of high societal interest and political relevance, no long term monitoring program exists that would provide the necessary data for modeling such a broad geographic area.
- There are sufficient historical and current data on sediment-bound HCB concentrations within the area of interest. More information on availability of HCB data is provided in Section 5.4.3.

- Contaminants with multiple metabolites and isomers (DD_x, HCH) or congeners (PCB) were excluded from the list of potential substances to be modeled due to their complexity.

5.3 Modeling: Spatial and Temporal Extents

Determining the spatial and temporal extent of the modeling was a key step in model development. It was ultimately decided to model the reach of the Elbe between Dresden and Magdeburg, and use the period between 1996-2006 to calibrate the model. The justification for these two decisions is described in the following sections.

5.3.1 Spatial Extent: Dresden-Magdeburg

The first key constraint of the model was that the modeled area should be free from tidal influence and the weir at Geesthacht (km 585.9), as well as within German borders (due to the availability of data). Further, sufficient discharge, suspended sediment, and contaminant input data should be available to establish boundary conditions for the HD, AD, and xenobiotic modules. Table 6 details the availability of each of these three data types over the 16 year period from 1996-2009 (See Section 5.3.2) for the German reaches of the Elbe upstream of Geesthacht. As shown in this table, while long-term discharge data are available at many locations along the Elbe, suspended sediment and sediment chemistry data are available less frequently, and often not at the same locations. Additionally, given computational limits, modeling the entire stretch of the Elbe is not possible.

The stations of Dresden (km 55.6), Meissen (km 82.2), and Zehren (89.6) were chosen to provide the upstream boundary data for discharge, suspended sediment, and sediment chemistry, respectively. One potential concern is that the Dresden gauging station is 34 km from the Zehren sediment chemistry monitoring station and thus companioning data from all locations would not be appropriate. However, the flow velocity of the Elbe at Dresden at mean discharge (MQ) is roughly 56 km per day, meaning it would take approximately half of a day for water to flow between Dresden and Zehren (Simon, 2005). If mean high water (MHQ) is assumed (approximately 1500 m^3/s), travel time is approximately six hours, well within the

bounds of uncertainty for the sediment chemistry data, which are collected monthly (Simon, 2005). Magdeburg Strombrücke was selected as the downstream boundary due to the availability of all three data types as well as its location downstream of two key tributaries to the Elbe, the Mulde and Saale Rivers. The total length of the modeled area is thus 271.4 km.

Table 6. Availability of gauging, suspended sediment and sediment chemistry data; Elbe River, German border - Schnackenburg.

Location	River	River km	Discharge[1] (WSV, 2011)	Suspended Sediment Concentration (BfG, 2012; FGG Elbe, 2012)	Sediment Chemistry (FGG Elbe, 2012)
Schoena/Schmilka	Elbe	2.1/4.1	Yes		Yes
Pirna	Elbe	34.7			Yes
Dresden	Elbe	55.6	Yes		
Meissen	Elbe	82.2		Yes	
Zehren	Elbe	89.6			Yes
Riesa	Elbe	108.4			
Torgau	Elbe	154.6	Yes		
Dommitzsch	Elbe	172.6	Yes		Yes
Wittenberg	Elbe	214.0	Yes	Yes	
Priorau/Dessau	Mulde	23.9/7.6	Yes	Yes	Yes
Mulde	Confluence	259.0			
Dessau	Elbe	261.0	Yes		
Aken	Elbe	274.8	Yes	Yes	
Calbe/Rosenburg	Saale	19.0/4.5	Yes	Yes	Yes
Saale Confluence	Confluence	290.5			
Barby	Elbe	294.8	Yes	Yes	
Schoenebeck	Elbe	312.0	Yes		
Magdeburg Alte Elbe	Elbe	326.6	Yes		
Magdeburg Strombrücke	Elbe	327.0	Yes	Yes	Yes
Niegripp-AP	Elbe	344.0	Yes		
Rogaetz	Elbe	351.0	Yes		
Tangermünde	Elbe	388.0	Yes	Yes	
Wittenberge	Elbe	454.8	Yes		Yes
Schnackenburg	Elbe	474.5	Yes		Yes

Note:

1. As noted in Section 5.4.1.2, discharge is calculated from observed water height. Discharge is not calculated for all stations, but as it is required for the upstream boundary (water height is used for the downstream boundary), it is used here to summarize all potential data.

5.3.2 Temporal Extent

Given the many uncertainties in modeling contaminant transport and the heterogeneity inherent in both suspended sediment and contaminant concentration data, it was clear that the model development strategy should maximize the accuracy and precision of the contaminant

transport component of the model. Data availability is discussed in detail below, but an important issue in model development is the varying temporal resolutions of the hydrodynamic, suspended sediment, and sediment chemistry data. Hydrodynamic data are available daily, suspended sediment data are measured Monday through Friday (and interpolated on weekends), and sediment chemical data are collected and analyzed on a monthly basis. Due to the low resolution of the available sediment chemistry data and the importance of the chemistry data to the project objectives, a modeling strategy was developed that maximized the utility of available data. The key concept of this strategy was to utilize the well documented, long-term decrease in the load of sediment-sorbed contaminants to calibrate the contaminant transport module of the model. Namely, to use the ten year load decrease between the up-and downstream model boundaries to calibrate the model. Since contaminant transport is ultimately based on concentrations of suspended sediment, which is in turn based on the output of the hydrodynamic module, the long-term calibration of contaminant fractions will also help minimize variability and uncertainty in the modeling.

Figure 12 shows annual HCB loads at Dresden and Magdeburg between 1994 and 2009. A clear and statistically significant (α=0.05) decreasing trend is observable at both stations. From these data, ten year decreases between Dresden and Magdeburg were calculated (e.g. the difference in load between what enters the system in Dresden in 1995 and what flows through Magdeburg in 2005). It should be noted that the monitoring station at Zehren was out of order for an extended period during both 1995 and 2006. The average ten year decrease across all years was 50.7±46.1%, or approximately 5% a year. The next step was to select a ten year period to use for model calibration. Due to the problems with the monitoring station, and the fact that the data are visually inconsistent with previous and subsequent years, 1995 was excluded as a possibility. However, 2006 remained a possibility since it was consistent with adjacent years. With the exception of the 1999-2009 and 1995-2005 difference, the remaining ten year differences are relatively consistent (mean of 78.0 ±7.8%). Thus, any of the ten year periods could theoretically be selected for calibration. However, due to the missing six months of data during 1995 from Zehren, when loads were relatively high, both 1994 and 1995 were excluded. Therefore, the next ten year period (1996-2006) was selected to use as the

calibration period. It should, however, be noted that the flooding in 2002 and 2006 may potentially impact the reliability of the load calculations. In particular, the 2002 flooding resulted in physical damage to dams and dikes, as well as overtopping of hydraulic control structures, so values calculated during this time period may not be accurate. The 2006 load data are less likely to be impacted by reliability issues since there was no physical damage to flood control structures.

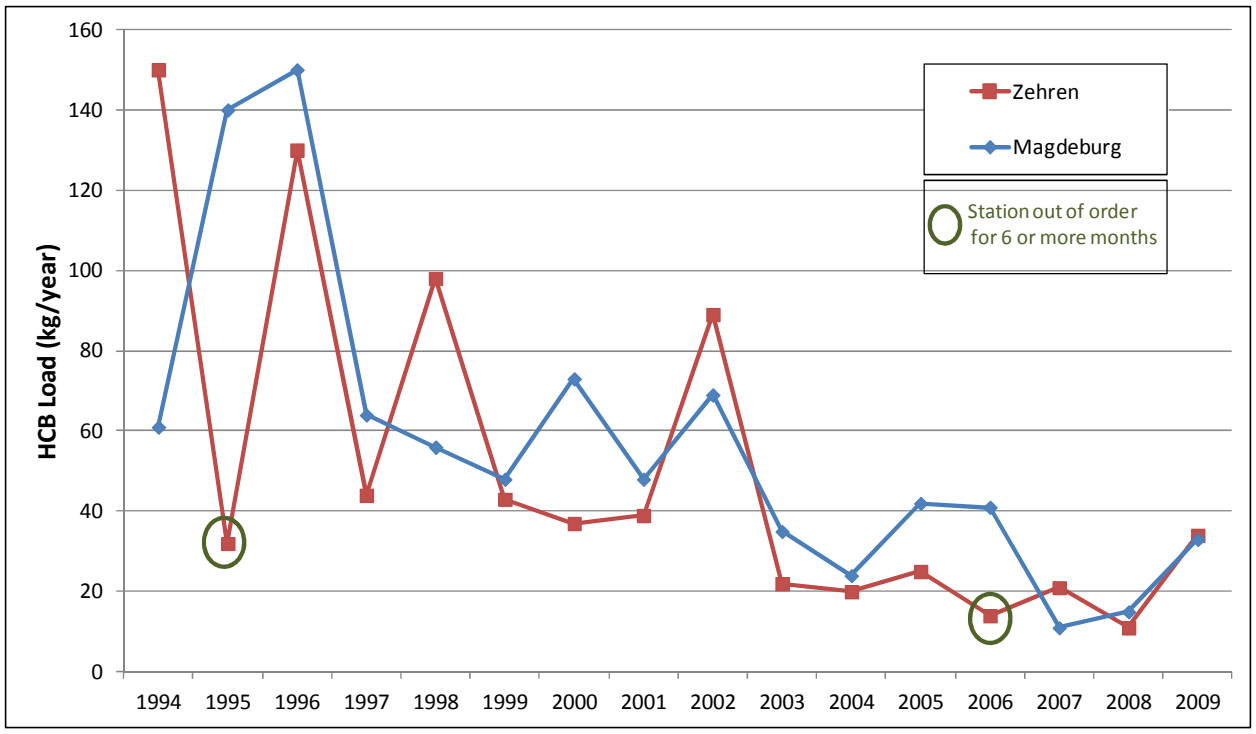

Figure 12. Annual HCB loads (1994-2009)

Table 7. Ten year load decreases: Zehren to Magdeburg

Year	Load Decrease: Zehren to Magdeburg(%), averaged over a 10-year period
1994-2004	84
1995-2005	-31.3
1996-2006	68.5
1997-2007	75
1998-2008	84.7
1999-2009	23.3

5.4 1D Model Data Requirements and Availability

These following sections describe both data requirements and availability development of the 1D hydrodynamic, suspended sediment, and contaminant transport model. The model makes use of an extensive network of data collected by multiple sources, including the Federal Institute of Hydrology (Bundesanstalt fuer Gewässerkunde (BfG)), the Elbe River Community (Flussgebietsgemeinschaft Elbe (FGG Elbe)), the Waterway and Shipping Administration (Wasser- und Schifffahrtsverwaltung des Bundes (WSV)), and individual German Federal States.

5.4.1 Hydrodynamic Model (HD) Module

Data required to simulate river hydrodynamics include river bathymetry, floodplain geometry, information on physical structures (e.g. weirs and dams), hydrographs for the upstream boundary, water level for the downstream boundary, as well as for any internal boundaries within the system. More detail on each of these data types are provided in Table 8.

Table 8. Input and calibration parameters for MIKE 11 model

Model	Module	Input Data	Calibration Parameter
MIKE 11	Hydrodynamic (HD)	Discharge and/or water level at model boundaries	Friction number (Chezy, Manning)
		Cross-sections, generated from digital elevation model (DEM)	
	Advection-Dispersion (AD)	SSC at upstream boundary	Dispersion coefficient, erodibility coefficient, critical shear stress for erosion and deposition
		Sediment characteristics: fall velocity, grain size, etc.	
		Initial bed height of sediment	
	Ecolab (Xenobiotics)	Xenobiotic concentration in water and sediment	Process rates
		Xenobiotic constants (Koc, Kw, etc.), sediment characteristics, decay rate, etc.	

5.4.1.1 River Bathymetry and Floodplain Geometry

In MIKE 11, river and floodplain cross-section profiles can be extracted from a bathymetry file. River bathymetry data were obtained from two meter DEM (2004, WSV – BfG). The DEM covers the length of the Elbe River within Germany, most of the Elbe River's floodplain, and sections of major tributaries leading up to the confluence with the Elbe River. The DEM file was developed from three data sources; multibeam echosounder covering the main stem of the river (resolution of 1.0m), digital photogrammetry of near-shore areas including groyne fields (resolution of 1.0m), and LIDAR data (resolution between 0.5m and 1.0m) for the floodplains (2004, WSV – BfG).

5.4.1.2 Hydrodynamic Data

Most morphological models, including MIKE 11, require an upstream discharge boundary and a downstream water level boundary. Additional discharge and water height data are also required within the system for model calibration. Gauge height and discharge measurements are available for gauges located throughout the Elbe Basin. Table 9 summarizes the main gauging stations within the study area. Unless otherwise noted, gauges are referred to by the

name of the closest city (i.e. the Magdeburg gauge is located adjacent to the city of Magdeburg). Table 9 also identifies the gauging stations that were used to establish boundary conditions for the hydrodynamic model, including Dresden discharge at the upstream boundary, Magdeburg discharge/gauge height relationship at the downstream boundary, and discharge from Mulde and Saale from the Priorau and Calbe-Grizehne gauges, respectively.

Discharge is calculated from stage height by the WSV based on a standard discharge-stage height (Qh) table. To develop the Qh table, the WSV regularly conducts measurements of flow velocity at the cross-section adjacent to each gauge, at high, medium and low water levels. Additional measurements are conducted after major floods, which may also alter the river profile. If the discharge/stage height relationship has been altered, than the Qh table is modified to match the new conditions. The frequency with which a Qh table is adjusted varies from gauge to gauge (Schwandt, 2012a) .

Table 9. Hydrodynamic gauging stations
(BfG, 2012; FGG Elbe, 2012; WSV, 2011)

Gauge	River	River KM	Discharge (Q)[1]	Water Height (h)[1]	Used for Boundary?	Used for Calibration?
Dresden	Elbe	55.6	1/1/1994-Present	1/1/1994-Present	Yes - Q	
Meissen	Elbe	82.2	NA	1/1/1994-Present		
Riesa	Elbe	108.4	1/1/1994-Present	1/1/1994-Present		
Torgau	Elbe	154.6	1/1/1994-Present	1/1/1994-Present		
Wittenberg	Elbe	214.1	1/1/1994-Present	1/1/1994-Present		
Aken	Elbe	274.8	1/1/1994-Present	1/1/1994-Present		
Barby	Elbe	295.5	1/1/1994-Present	1/1/1994-Present		Yes
Magdeburg	Elbe	326.6	1/1/1994-Present	1/1/1994-Present	Yes - Q/h	
Priorau	Mulde	23.9	6/1/1995-Present	6/1/1995-Present	Yes - Q	
Calbe-Grizehne	Saale	17.6	1/1/1994-Present	1/1/1994-Present	Yes - Q	

Notes:
1: Gauging data may exist prior to 1/1/1994, but are considered outside the timeframe of interest

5.4.1.3 Data gaps in the Hydrodynamic Data

One substantial data gap exists in the hydrodynamic data: the Priorau (Mulde) discharge data are missing between 8/1/2004 and 11/30/2005 (inclusive). A number of methods to substitute the missing data, including simple substitution of the average of Priorau discharge (67.2 m^3/s), were considered. The relationship between the Priorau and Calbe-Grizehne discharge data were found to be the strongest. As the discharge data from both stations were strongly left skewed, a log transformation was applied to both datasets (i.e. a power transformation). This resolved the skewedness, and both datasets were then considered normal both by visual inspection of histograms. Even though log-normalized datasets were considered non-normal

according to the Shapiro-Wilk test (α=0.05), linear regression is relatively robust to slight deviations from normality. Linear regression between the Priorau and Calbe-Grizehne (Saale) data was statistically (R^2= 0.78, p < .001) significant. Thus, the missing Priorau discharge data were substituted using the Calbe-Grizehne discharge data, following Equation 6:

Equation 6: Priorau Q = (0.3412 *Calbe Q) $^{1.1067}$

5.4.1.4 Flow Control Structures

Weirs and dams are flood control structures that can alter natural flow regimes, and are therefore important to consider when developing hydrodynamic models. While there are several dams located both upstream and downstream of the study area, there are no dams within the study area. There is, however, one weir that is used to contain flood waters and channel them downstream. The Pretziener Weir (described below) is located upstream of Magdeburg and is essential to protecting the city of Magdeburg from high water conditions.

5.4.1.4.1 Pretziener Weir

The Pretziener Weir is located downstream of a three km long canal that diverges from the Elbe at km 300.7, near Pretzien. The Pretziener Weir is located at the head of the 'Elbe bypass canal' (“Elbeumflutkanal”), as illustrated in Figure 13. The 25 km long Elbe bypass canal rejoins the Elbe downstream of Magdeburg, at km 336.7. The Weir is 162.8 m long, 7.5 m wide, and 3.8 m high and is composed of nine iron gates between ten sandstone pillars. Each gate is 5.75 m high and 12.55 m wide, resulting in a useable flow width of 112.95 m (Simon, 2010a).

Figure 13. Elbe River and the Pretziener Weir
(source: Google Earth)

Even though the primary function of the Pretziener Weir is to serve as pressure relief valves during high water conditions, it also has important functions during lower water conditions. The functions of the weir during various water conditions are summarized below:

- At low and medium water levels, the Pretziener Weir dams off the Elbe River and prevents water from flowing into the *alte Elbeniederung* east of Magdeburg as well as helps to maintain adequate water depth for navigation in Schönebeck and Magdeburg.
- For small and medium flood events, the Weir protects the dam from flooding the transport infrastructure between the routing dikes of the Elbeumflutkanal
- For larger floods, the Weir is opened, and roughly 1/3 of the total Elbe discharge is diverted into the Elbe Bypass Canal, protecting the cities of Schönebeck and Magdeburg from flooding until the water level lowers.

To achieve these objectives, the Pretziener Weir is opened when the water level at the Barby gauge (km 294.8) is at 550 cm and is projected to reach 592 cm. The Weir is closed again once the water level falls below the level 525 cm at the Barby gauge. Weir openings take several hours and require the closing of multiple highways (Simon, 2010b).

5.4.2 Suspended Sediment/Advection Dispersion (AD) Module

Required input data for the AD module include: SSC at upstream boundary, sediment characteristics including fall velocity and grain size, as well as the initial bed height of sediment. Suspended sediment data were obtained for 13 sampling stations in the Elbe watershed from the BfG (Schwandt, 2009). Sampling stations within the modeled area are listed in Table 10. Suspended sediment samples were collected Monday through Friday using gravimetric filtration with 'Melitta' paper filters. The average pore size of the filters is approximately about 6.1 microns, but may vary due to slight manufacturing differences (DVWK, 1986; Naumann et al., 2003; Otto, Wilfried, 2012a). This sampling method produces values that are internally consistent, but not necessarily highly accurate (Otto, Wilfried, 2012b).

The BfG suspended sediment dataset does not include any data for the Mulde. The only alternative long-term dataset is from the FGG Elbe long-term monitoring of suspended sediments. FGG Elbe samples sediments using flow-through sedimentation tanks, from which sediments are composited and measured on a monthly basis. Even though the methods and sampling frequency vary between the two sampling programs, since the FGG Elbe are the only available, they were used in establishing model boundary conditions.

5.4.2.1 Data Gaps in the Suspended Sediment Record

All sampling stations have data records with missing values that cover between 1 and 20% of the sampling period (Table 10). Two different types of data gaps exist in the suspended sediment record; missing weekend data, and longer gaps (weeks to month) that occurred either caused by the inaccessibility of the sampling location due to high water, insufficient personnel during holiday (Christmas/New Year) periods or unknown causes. Data gaps over weekends were easily resolved by interpolation. However, for the longer data gaps which generally

consisting of multiple days or weeks, interpolation was not a feasible substitution method. Rather, the mean of all results for that station was initially used to substitute for any missing values. However, as this method has the potential to dramatically underestimate SSC during high water events, other substitution methods are considered below.

Table 10. Suspended sediment gauging stations (BfG, 2012)

Sediment Sampling Station	River (River km)	Date		Percent of Missing Values
		Minimum	Maximum	
Pirna	Elbe (34.7)	1/1/1992	Present	7%
Meissen	Elbe (83.4)	1/1/1995	Present	8%
Torgau	Elbe (154)	1/1/1994	Present	4%
Wittenberg	Elbe (216.3)	1/1/1992	Present	3%
Aken	Elbe (274.8)	1/1/1992	Present	4%
Dessau[1]	Mulde (7.6)	1/8/1985	Present	NA
Calbe	Saale (20)	1/1/1992	Present	1%
Barby	Elbe (294.8)	1/1/1992	Present	3%
Magdeburg Alte Elbe	Elbe (326.6)	1/1/1992	Present	20%
Magdeburg Strombrücke	Elbe (327)	1/1/1993	Present	3%

Note:
1. Bimonthly data from FGG Elbe, as no other datasets are available.

Table 11 details the beginning and end date of the long-term data gaps for Meissen, Barby, and Magdeburg Strombrücke as these stations were used either to establish boundary conditions or for calibration. As shown in this table, data gaps generally increase in frequency starting in 2001 and frequently occur over the Christmas/New Year period, but also during high water periods. While populating missing data with the average station concentration can be assumed to be an adequate method for most dates, it is not sufficient during high water events. Gaps in the SSC record occur during two high water events; in August, 2002 at Meissen and December 2002/January 2003 at both Meissen and Barby. Since Barby was used for calibration, no data substitution was required for this station, but due in particular to the importance of the August, 2002 flooding, substitute data were needed for the other data gaps.

Table 11. Long-term data gaps in suspended sediment concentration data at Meissen, Barby, and Magdeburg Strombrücke

Sampling Station	Data Gap (High Water Period in *Italics)*
Meissen (km 82.20)	9/8/2001-9/25/2001, 12/22/2001-1/1/2002, *8/13/2002-8/25/2002, 12/21/2002-1/5/2003,* 12/20/2003-1/4/2003, 12/24/2004-1/2/2005, 6/1/2005-8/21/2005, 12/24/2005-2/13/2006, 12/21/2006-1/1/2007, 5/16/2007-5/31/2007, 10/20/2007-1/1/2008, 5/31/2008-6/30/2008, 12/11/2008-4/30/2009
Barby (km 295.5)	12/21/2001-1/1/2002, *12/24/2002-1/1/2003*, 6/1/2005-8/10/2005, 1/3/2006-1/30/2006, 11/1/2006-1/1/2007
Magdeburg Strombrücke (km 326.6)	6/1/2005-8/10/2005, 11/1/2006-1/1/2007, 3/28/2007-4/17/2007, 12/22/2007-1/1/2008

The optimal alternative to substituting these data would be to use data from adjacent stations; concentration data measured either at Pirna (km 34.67) or Torgau (km 154.15), approximately 47 kilometers upstream and 72 kilometers downstream, respectively, of Meissen. Data were missing from Pirna during the August, 2002 high water and from both Pirna and Torgau during the December, 2002 high water. Therefore, the Torgau data were evaluated to determine if using them was preferable to an average for the August, 2002 high water. To assess the suitability of using Torgau to substitute the missing values, if a flow rate of between 2.0 to 2.34 km/h are assumed, and it was assumed that suspended sediment travels at the same velocity as the main flow; it would take the suspended material approximately 30 and 36 hours to travel between Meissen and Torgau (IKSE, 2005). Second, the data were evaluated graphically and there was found to be a moderate relationship between the two stations. Thus, Torgau data were used for Meissen during the August, 2002 high water period. For the 12/2002 missing data, no applicable dataset were available and thus the average value was used.

5.4.3 Contaminant/Ecolab Model Data Requirements

The Ecolab xenobiotics template requires the initial and boundary concentrations of state variables, as well as discharge magnitudes and concentrations for pollution sources. Additional inputs value include process rates (i.e. desorption rates in sediment and water, K_{oc}, etc.), some

of which are governed by calibration, and others that are based on literature values or laboratory measurements. Due to the complexity of the interactions between contaminants and both the solid and aqueous phases of rivers, data requirements for the Ecolab model are extremely complex, and many of the individual variables have high uncertainty. Appendix B lists all of the Ecolab input parameters.

Concentrations of sediment-bound HCB are available from the FGG Elbe for stations on the Elbe, Mulde and Saale. Within the context of the FGG monitoring program, composite data are collected over approximately four weeks in a settling basin and a variety of organic and non-organic contaminants are analyzed. The sampling stations relevant to this study are listed in Table 6.

Field surveys were conducted by the BfG and HAW during the summer of 2010 to evaluate contaminant concentrations in seven groyne fields and ten harbors (unpublished data) between river kilometers 221.0 and 327.3. The median of the groyne field and harbor HCB concentrations was 74 and 80.5 ug/kg, respectively.

5.5 1D Model Setup

Two 1D models were developed; a first, simpler model that excluded floodplains (and thus had a shorter runtime) was used to calibrate the HD, AD, and Ecolab modules. The second 1D model included floodplains, and calibration values were taken from the first setup. The section below describes setup of both 1D models. Calibration results for the simple 1D and floodplain 1D models are provided in Section 6.4.

5.5.1 1D Hydrodynamic Setup

Once the main river channel between Dresden and Magdeburg and the section of the Elbe bypass canal upstream of the Pretziener Weir (called 'Umflutkanal' in the model) were delineated, cross-sections were automatically generated every 250 m, and the channel geometry was extracted from the processed 3 m digital elevation model (DEM). More cross-

sections were added as needed in locations with complex river morphology (i.e. meanders or tributary confluences). Uniform resistance was assumed at all cross-sections. Cross sections were individually examined to ensure no errors occurred during automatic generation and the positions of markers indicating left and right low flow bank were added to each cross-section where necessary.

As described in Section 5.4.1.2 , boundary conditions must be defined where river reaches start and end, and where additional inflows are included in the model. The hydrodynamic boundary conditions included open boundaries at the up and downstream ends; discharge at Dresden, and a Qh relationship at Magdeburg. Both the Mulde and Saale were included as discharge point inputs (Table 12). Initial water level was established at 2m throughout the model. The model was setup to run in an unsteady state. Model stability is an important issue when dealing with unsteady models that simulate time-varying flow behavior. Instabilities can result from the solution scheme incorrectly balancing modeling equations between computation points at the selected computational time step. Thus, an order to achieve a stable model, it is critical that an appropriate time step for flow computations is selected. In selecting the time step, resolution of results, model run time, geometry and construction of the model, and the finite difference solution scheme were considered. In addition, the Courant number can be used to calculate the appropriate time step given a specific grid. The Courant equation is defined in Equation 7.

Equation 7: $$Cr = \frac{\left(v + \sqrt{gD}\right)\Delta t}{\Delta x}$$

Where, Cr is the Courant number, v is velocity, Δ*x is* the distance between cross sections, Δ*t is* the time step, where g is gravity, and D is the mean water depth. For optimal model results, the Courant number should be kept as small as possible (ideally close to one), but a small number of grid points with Courant values between ten and 20 is acceptable (DHI, 2011).

In order to satisfy the demands of the model construction, the model was initiated with a four day 'hotstart' during which a five second time step was used. The four day period was sufficient

to 'fill up' the model. After this warm-up period, a five minute time step was used. This time step caused no obvious stability issues, and maintained a Courant number under one.

Table 12. Boundary conditions in the 1D model

Location	Boundary Type	Elbe Model Chainage (m)	Input
Dresden	Open	0	Dresden Q
Magdeburg	Open	269337.63	Q/h Relationship
Saale confluence	Point Source	202290	Calbe Q
Mulde confluence	Point Source	233583	Priorau Q

A control structure was inserted at the end of the 'Umflutkanal' branch to represent the Pretziener Weir. The control structure details are as follows:

- Gate type: Overflow
- Number of gates: 1
- Gate width (m): 112.95
- Sill level (m): 48.044
- Max speed (m^3/s): 0.001

A control strategy, which governs how the weir gate level changes, was established for the Pretziener Weir. The control strategy effectively raises or lowers the gate at the Pretziener Weir, or target point', depending on a value at the control point, or the Barby gauge. In the model, this control point is expressed in terms of water height, or elevation above datum, rather than water depth, or vertical distance between river surface and river bottom. However, the available data for the Pretziener Weir only express the control strategy in terms of water depth above an arbitrary control point. Establishing an initial water height was complicated by the fact that the river bed in the Elbe can vary dramatically, particularly during high water conditions. Thus, an initial value for the Pretziener Weir control point was calculated as follows: The initial value for the Barby gauge zero point (with a reference datum of above mean sea level, or AMSL) at Barby is 46.11m (WSV, 2012). Detailed bathymetry indicates that the Elbe bottom depth near the gauge is approximately 44.57m AMSL. Since the Pretziener Weir is opened when water depth at Barby reaches 5.5 m, the initial value for the Barby control point

was 51.61m AMSL. This value was then altered once the model was calibrated to best replicate known historical weir openings and closings that occur during the calibration period.

5.5.2 1D Advection-Dispersion Setup

Once the hydrodynamic model was calibrated, the results were saved in five minute time steps, and the AD module was setup and calibrated. Boundary conditions for the AD module were established using daily suspended sediment data from Meissen, Magdeburg, and Calbe (Saale River), and bimonthly data for Dessau (Mulde River), as explained in Section 5.4.2 (BfG, 2012; FGG Elbe, 2012).

To achieve model stability in the AD module, the time-step had to be reconsidered since concentrations in the AD module are calculated at both discharge and water height calculation points. Therefore, the Δx is half the distance between two water height points used when calculating the AD Courant number (i.e. every 250m). The model was found to be stable at a time step of one minute, with only 0.18 % of the data points having a Courant number exceeding one. The hydrodynamic results were interpolated using one-minute time steps. The AD module was setup with one component, a single layer of cohesive sediment. The input parameters for cohesive sediment transport are listed in

Table 13, and a brief explanation of the reasoning for each input value is provided below. More information on each parameter is provided in DHI (2011).

- Sediment (dry) density: Assumed to be 550 kg/m^3. During field investigations in summer 2010 and summer 2011, groyne sediment was investigated with manual sediment probe and found to be highly consolidated to stiff. Following guidance from DHI, 2011 density values of 400-550 kg/m^3 should be used to represent a highly consolidated (one year) bed and values of 550-650 should be used to represent stiff mud (10 years). The DHI values were taken from Van Rijn et al., (1993). While no values for dry weight (dw) sediment density were found in the literature, wet weight densities for sediments from one groyne field (km 420.9) of between approximately 1100 and 1118kg/m^3 are published in Schwartz, 2006). Using Equation 8, and

assuming moisture content of 34% (Section 0), this yields a density of 834 kg/m^3. This value is significantly above the suggested values for consolidated to stiff sediments, and given that it is from only one sample, a value of 550 kg/m^3 was used.

Equation 8 $$\rho_d = \frac{\rho_w}{1+moisture\ content}$$ where:

$$\rho_d = dry\ density, \rho_w = wet\ density$$

- Settling Velocity: Only one paper on settling velocity of Elbe sediments was found, which provides a small set of example values, all of which fell below the suggested input range (Cornelisse, 1996). The author was contacted, but was unable to provide any additional data due to the long time that has elapsed since the study was originally conducted (Cornelisse, 2009). Therefore, the mean of the suggested range equivalent to 0.00625 m/s was used.
- Critical shear stress for deposition: The suggested range is: 0.03 -1.00 N/m2 (DHI, 2011). The mean of these two values, 0.515 N/m^2, was used.
- Time centering: The mean of the suggested range, 0.75 N/m^2, was used.
- Critical shear stress for erosion: Prohaska et al. (2008) investigated critical erosion shear stress in three Elbe groyne fields using SETEG, a laboratory channel device between 2002 and 2006. The minimum, mean, and maximum of 94 measurements in the three groyne fields is 0.28, 3.04, and 12.27 N/m^2, respectively. Visual inspection of the authors' data show that the majority of results are roughly an order of magnitude larger than the suggested range for the model (Prohaska et al., 2008). In addition, Schwartz (2006) reported critical shear stress values between approximately 0.5 N/m^2 and 3 N/m^2. This disparity not surprising given both the *in situ* heterogeneity and the well documented disparity between different methods of estimating critical shear stress (Bohling, 2009; Jepsen, 2006; Tolhurst et al., 2000a, 2000b; Widdows et al., 2007). Due to this disparity, the maximum of the suggested range, 0.1 N/m^2, was used.
- Erosion coefficient: The mean of the suggested range, 0.35 g/m^2/s, was used.

- Erosion exponent: The mean of the suggested range, 2.5, was used.

Table 13. Advection-Dispersion module input values

Input Parameter	Units	Suggested Range (DHI, 2010)	Initial Value	Final Value
Volume of sediment/length of river	NA	NA	10	
Density	kg/m3	NA	550	550
Free settling velocity	m/s	0.0025 - 0.01	0.00625	
Critical shear stress for deposition	N/m2	0.03 -1.0	0.515	
Time centring	NA	0.5-1.0	0.75	0.75
Critical shear stress for erosion	N/m2	0.05 - 0.10	0.075	
Erosion coefficient	g/m2/s	0.20 - 0.50	0.35	0.35
Erosion exponent	NA	1.0 -4.0	2.0	2.0

5.5.3 1D Xenobiotics (HCB) Setup

Following calibration of the HD and AD modules, the xenobiotics template was added to the model. The input parameters in the xenobiotics template are both numerous and complex, and consist of: state variables, constants, forcing, auxiliary variables, and processes. The state variables and processes are discussed below, and all other inputs are summarized in Appendix B, along with initial values for each parameter.

The xenobiotics template consists of six state variables: dissolved xenobiotics (SXE), adsorbed xenobiotics (XXE), dissolved xenobiotics in sediment (SXES), adsorbed xenobiotics in sediment (XXES), suspended solids (XSS), and the mass of sediment (XSED). Due to the relatively high log Kow of HCB, suspended sediment is considered to be the only transport vector for HCB. The input values for each of the state variables are detailed below:

- SXE and SXES: Boundary and initial concentrations for the dissolved fractions were considered to be essentially zero, but were set to an extremely low number ($7x10^{-8}$

mg/L and g/m^2) because of mathematical issues (e.g. dividing by zero) that could be caused by using a zero input value (D'Eugenio, 2005).

- XSS: Boundary and initial concentrations was taken from the results of the AD module
- XSED: calculated by assuming a potentially resuspendable sediment depth of 15 cm. With a wet bulk density of approximately 2.2 g/cm^3 (Lichtfuss and Brümmer, 1981), this yields a sediment mass of roughly 330 kg/m^2.
- XXE and XSS: Initial concentrations for XXE and XSS were assumed to be identical, assumed to be 0.041 (mg/L and g/m^2), the mean HCB concentration at Zehren, calculated from the FGG database of pollutants in particulate matter (FGG Elbe, 2012). Boundary conditions were established using monthly HCB concentrations from Zehren and Magdeburg Strombrücke, also available from the FGG database of pollutants in particulate matter (FGG Elbe, 2012). These data were first arranged to assign the monthly concentration to each day of the sampling month, and then the data were interpolated to five minute time steps.

Model time-step and stability were reassessed at this point, due to the long run-times that were observed by initially using a one minute time step. Balancing model run-time and Courant number proved difficult due to the complexity and slow run times of the xenobiotics template, so the calibration was conducted on a slightly modified version of the 1D simple model, where the cross-sections were 4000 m apart rather than 250 m. This yielded a Courant number larger than one at 78% percent of the data points. However, 80% of these Courant values were still below two and no values were above twenty.

As illustrated in Figure 11, there are multiple processes available in the xenobiotics template, but not all processes were simulated. Since HCB has a relatively high log Kow, is considered to be almost insoluble, and no known rates of hydrolysis or photolysis exist, the process of diffusion, photolysis, evaporation, biodecay, and hydrolysis were not simulated. All other processes (adsorption, desorption, production of suspended solids, sedimentation, and resuspension) were simulated.

5.6 1D Model Sediment Package Scenarios

Suspended sediment loads and transport rates in the Elbe Basin vary spatially and temporally by orders of magnitude. Physical controls such as discharge conditions, channel-boundary materials, land use, channel stability, and the type and timing of precipitation events complicate the prediction of sediment transport rates. Potential model-based methods to determine sediment transport rate include stochastic particle tracing and the use of synthetic discharge and suspended sediment concentration (SSC) data combined with actual flood data to estimate the travel time between two specific locations. A key assumption in this alternative is that since HCB is strongly bound to suspended material (Koc =4-5), suspended sediment rates and HCB transport rates can be considered to be equivalent.

To evaluate the feasibility of this alternative, both the particle tracking and synthetic data-approach were briefly evaluated. The particle tracking approach was found to be possible over small distances (i.e. Aken to Barby), but ultimately be too time intensive over the long distances, such as Dresden to Aken, or Magdeburg. Thus, the alternative of using synthetic datasets to simulate transport time was decided on. This modeling was completed by using actual, measured paired SSC and discharge data measured during various discharge scenarios (MNW, MQ, MHQ, etc), and then coupling these data with balanced loads under average conditions before and after the high water event. To clarify, the input data at the upstream end of the model would then have three periods:

1. A 'warm-up period' using average SSC and discharge data (synthetic data)
2. Measured, paired SSC and discharge from an actual high water event
3. A 'warm-down' period of average SSC and discharge data (synthetic data). The 'warm-down' period allows for static conditions so the transport time of the flood-event data can be simulated and measured.

For the warm-up and warm-down periods, input data were established by balancing suspended sediment loads at model boundaries, following Equation 9:

Equation 9 : QDresden*SSCDresden + QMulde*SSCMulde+ QSaale*SSCSaale= QMagdeburg*SSCMagdeburg

Equation 9 can be solved for SSCMagdeburg using discharge equivalent MQ, which yields At all other boundary locations, SSC from either an average, or rating curve, as appropriate were used. For these simulations, discharge and SSC in the Mulde and Saale were constant at the MQ and average SSC.

5.7 1D Floodplain Model Setup

The objective of the 1D floodplain model was to replicate the spatial detail available from a 2D model in one dimension. In this approach, often referred to as quasi-2D modeling, floodplains are modeled as a network of theoretical river channels on the floodplains that are connected to the main river via theoretical connector branches that transfer water from the main channel upland to the theoretical river channels. Cross-sections along both the theoretical river and connector branches allow for the quantification of storage of water, sediment, and HCB on the floodplains (water levels, volumes and spatial extent). The 1D floodplain model was setup by using identical boundary and bathymetric data to the 1D simple model, but the physical setup of the model was altered to allow for the transport of water, sediment and HCB to the floodplains to be simulated. The section below describes modifications to the simple model.

The first step in modifying the simple 1D model was to depict the Elbe basin floodplains in GIS. Spatial data delineating flooded areas under HQ100 were exported from Flusshydrologische Software (FLYS) and used to represent the floodplain (Bundesanstalt für Gewässerkunde, 2009). The area of the modeled floodplain between Torgau (km 154.16) and Magdeburg (km 326.6) was measured in ArcGIS and found to be 337.6 km^2. Given that the floodplain in the southern half of the model is extremely narrow, due to the sandstone cliffs, only floodplains downstream of Torgau were modeled (km 154.16). This decision was secondarily a practical one, as including floodplains in the model significantly increase runtimes, and it was preferable to model the downstream floodplains, which are considerably wider than the upstream floodplains, as accurately as possible.

Before the theoretical floodplains were delineated, the potential for physical structures, such as bridges, to encroach on the floodplain was investigated. Bridges can increase upstream flooding by narrowing the channel width and increasing the channel's resistance to flow. This results in a higher water level upstream of the obstruction, creating a backwater effect that can inundate upstream areas. In total, there are eight bridges downstream of Torgau (km 154.16):

- Straßenbrücke Torgau/ Torgau Bridge (km 154.5)
- Eisenbahnbrücke/Torgau Railway Bridge (km 155.53)
- Eisenbahnbrücke Wittenberg/Wittenberg Railway Bridge (km 213.73)
- Straßenbrücke Wittenberg/ Wittenberg Highway Bridge (km 213.79)
- Autobahnbrücke Vockerode/ Vockerode Highway Bridge (km 246.52)
- Straßenbrücke Roßlau/ Roßlau Bridge (km 257.65)
- Eisenbahnbrücke Roßlau/ Roßlau Railway Bridge(km 257.65)
- Straßenbrücke Schönebeck/ Schönebeck Bridge (km 311.77)

The encroachment potential of the eight bridges was visually investigated; first in Google Earth (Google Earth, 2012), and then in FLYS (Bundesanstalt für Gewässerkunde, 2009). The FLYS program was used to evaluate interactions between bridges and floodplain hydrological boundaries under four different discharge conditions: MQ, MHQ, HQ20, and HQ100. The investigation showed minor influence of the bridges, but the effect was not significant enough to delineate separate theoretical floodplain channels.

To modify the 'simple' model to include floodplains, theoretical river channels were generated in GIS, at roughly the midpoint between the middle line of the Elbe, and the outer extent of the floodplain. Three theoretical floodplain branches were generated, one representing the entire left floodplain (LFP), and two representing the right floodplain; one downstream, or south, of the Umflutkanal (RFPS), and one upstream, or north, of the Umflutkanal (RFPN). The left and right floodplains begin at approximately river kilometer 157.5 and 160.5, respectively. The downstream ends of the left and right floodplains reconnect with the Elbe just downstream of

Magdeburg, at approximately river kilometer 324 and 326.5, respectively. Figure 14 illustrates this setup in a simplified manner.

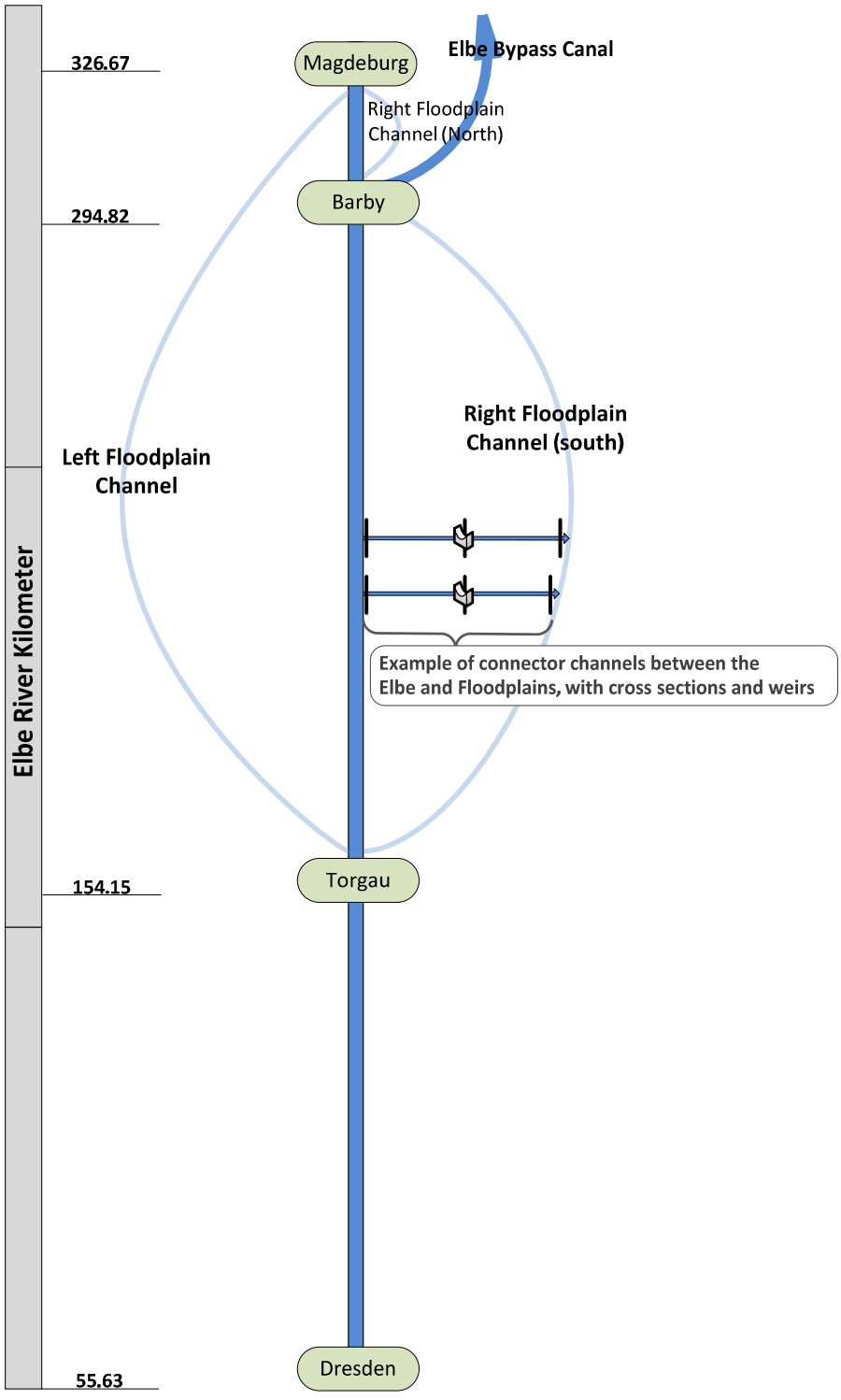

Figure 14. Schematic drawing of the floodplain model

The next step was to create branches connecting the main channel to the LFP, RFPS, and RFPN. Connector channels were drawn approximately every one kilometer, with more branches in larger meanders, and less where the floodplain narrows (also shown in Figure 14). Whenever possible, connector branches were drawn along existing flow paths, if they were obvious from the DEM. Cross-sections were drawn every 700-1000m on the floodplain branches, and at the beginning, end, and at approximately the boundary between levees and the floodplain on the connector channels. The cross-sections on floodplain branches extend the width of the floodplain, while the connector channels cross-sections are approximately 150 m. Cross-sections were always drawn perpendicular to the flow direction. In anticipation of model instability caused by the slight difference in bed level between the Elbe cross-sections and the first cross-sections of the connector channels (chainage 0.0), the bed level of the connector channels cross-sections were adjusted slightly to the bed level of the Elbe. A similar adjustment was made to the end cross section of connector channels, where they meet theoretical floodplain channels. These adjustments generally consisted of changes on the order of one cm to 50 cm on the beginning of connector channels one cm to two m at the ends. This difference is due to the fact that floodplain elevations vary more than Elbe bottom elevation.

Figure 15 shows a detailed example of how the floodplain branches, connector channels, and related cross sections were developed. Due to the large area integrated in floodplain modeling, a map showing all floodplain and connector channels is not possible at this scale. In total, 152 connector channels were included on the left floodplain and 122 on the right floodplain. The left and right floodplain connector channels had an average length of 458m and 377m, respectively.

Flow between the main stem of the Elbe floodplains is controlled in the model by a single "mathematical" weir, located at the middle cross-section of every connector channel. These weirs effectively form a control point for flow, keeping water from entering the floodplains until the weir level is exceeded. All weirs were defined as broad-crested weirs and their hydraulic characteristics described by the stage/flow-width relationship that is determined from the cross section geometry at the weir location. MIKE 11 then calculates the appropriate discharge to

associate with each stage of flow based on the stage/flow-width relationship and the adjacent cross sections.

As with the MIKE 11 'simple' model, Manning's bed roughness (M) is the primary method of model calibration. An initial bed Manning's M of 15 (n=0.06) for the floodplain was selected, which assumes mixed pasture land with a moderate to high grass height, with light brush and trees (Chow, 1959). For all other parameters, initial values were identical to the simple model. The model was initiated with a water height of 0.2 m in all channels.

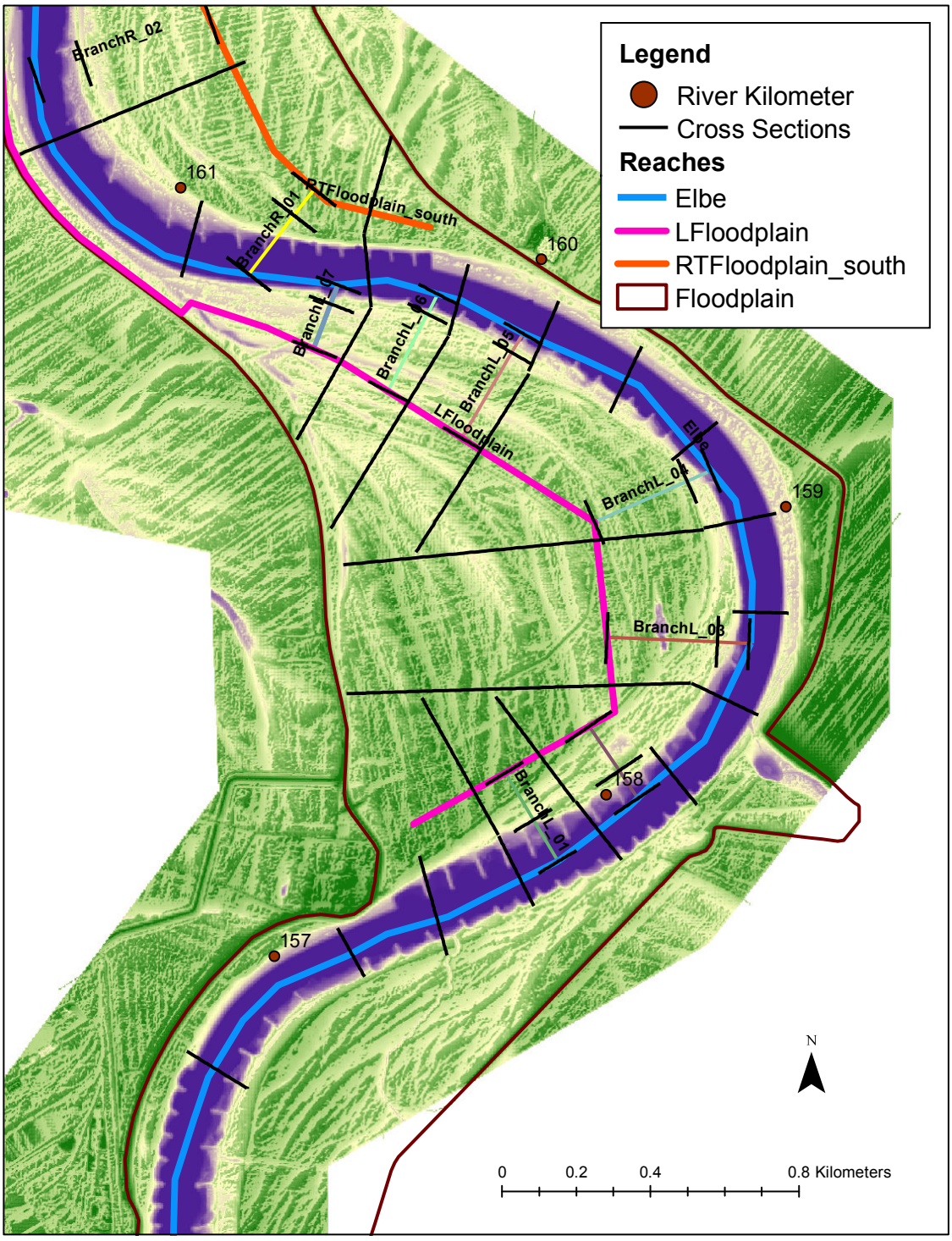

Figure 15. Map showing floodplain branches and connector channels. 'LFloodplain' and 'RTFLoodplain south' are floodplain branches, while channels begin with the word 'Branch'

5.8 2D Flexible Mesh Model Setup

As detailed in Section 5, a 2DFM model was developed for the stretch of the Elbe between Aken (km 274.8) and Barby (km 294.8). The goal of this model was to determine the role of groynes in governing the transport rate of cohesive sediments. Any groyne-mediated influence on suspended sediment transport can then be integrated into the 1D simple and/or floodplain models. Development of the flexible mesh model involved several steps, which are described below. Many of the same datasets were used as in the 1D model, but varying assumptions were made due to added dimensionality of the model.

5.8.1 2DFM Model Bathymetry Setup

MIKE Mesh Generator is a tool used to creating digital mesh files for use in FM models. Setting up a mesh includes appropriate selection of the area to be modeled, adequate resolution of the bathymetry, and defining boundaries and boundary conditions. Furthermore, the resolution in the geographical space must be selected with respect to ensure model stability. Mesh development includes three steps: import of bathymetry data, generation of a depth-independent mesh framework, and interpolation and refinement of the mesh.

The first step in the 2DFM model setup was to delineate a depth-independent framework for the mesh, dividing the area of interest into polygons. Each polygon contains either triangular or quadrangular elements, depending on the level of detail that is required. Rectangular elements are generally larger than triangular elements, and thus triangular elements are used to cover areas where more detail is required. Since the primary interest in the Elbe River is the transport of water and sediment in the groyne fields, triangular elements were used to cover the area of the Elbe River between the main channel and the banks. The quadrangular elements were used to cover the main channel, where uniform directional flow is expected. Once this is completed, the three m DEM coverage was used create a computational mesh. Development of the mesh framework requires establishing a balance between elements small enough to provide adequate detail, and large enough to allow for reasonable model run times. Once the mesh was generated, element shapes were refined to optimize for model run-time.

For example, model run-times are minimized when the quadrangular elements have 90° angles. Thus, the depth-independent mesh framework was manually edited according to these considerations. Multiple mesh generation trials were conducted, and an optimal size of quadrangular and triangular elements was established. Figure 16 shows an example of what the mesh coverage looks like for an approximately 1-km section of the Elbe. The last step in mesh generation is to interpolate the bathymetry to the depth-independent mesh framework. A nearest neighbor algorithm was used for this interpolation. Figure 17 shows the interpolated mesh for the same section of the Elbe River shown in Figure 16. The next step is to develop a depth-independent framework for the mesh. The area of interest is divided into polygons, and each polygon contains either triangular or quadrangular elements, depending on the level of detail that is required.

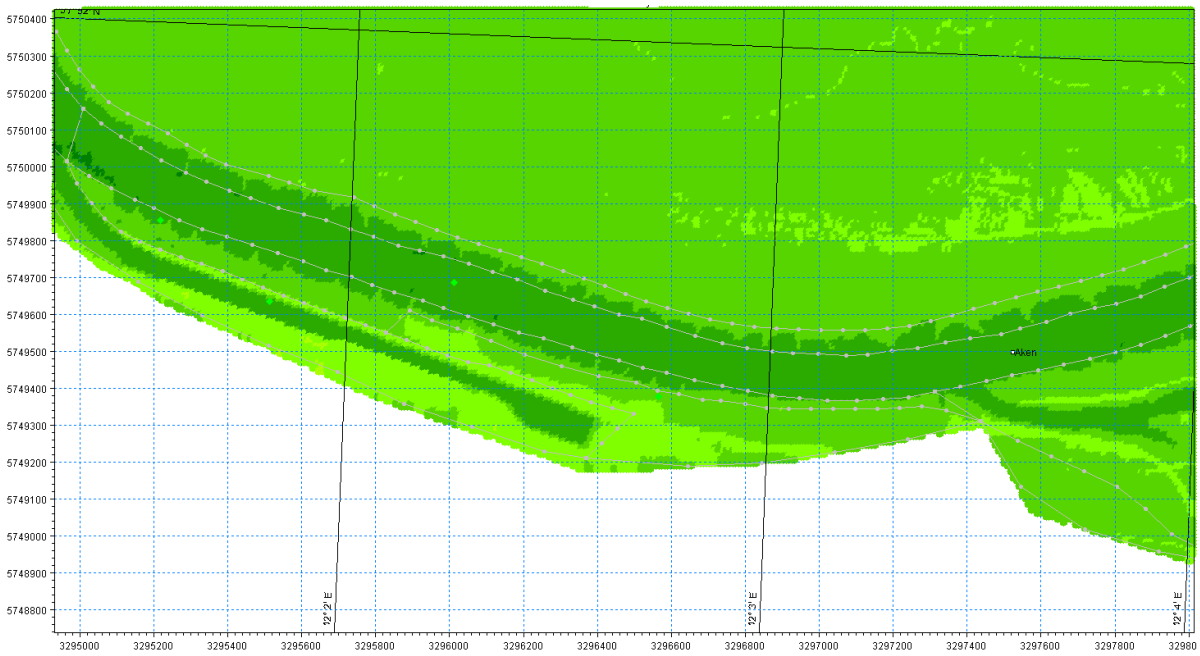

Figure 16. Example flexible mesh (upstream of Aken), showing the resolution of the DEM and groynes

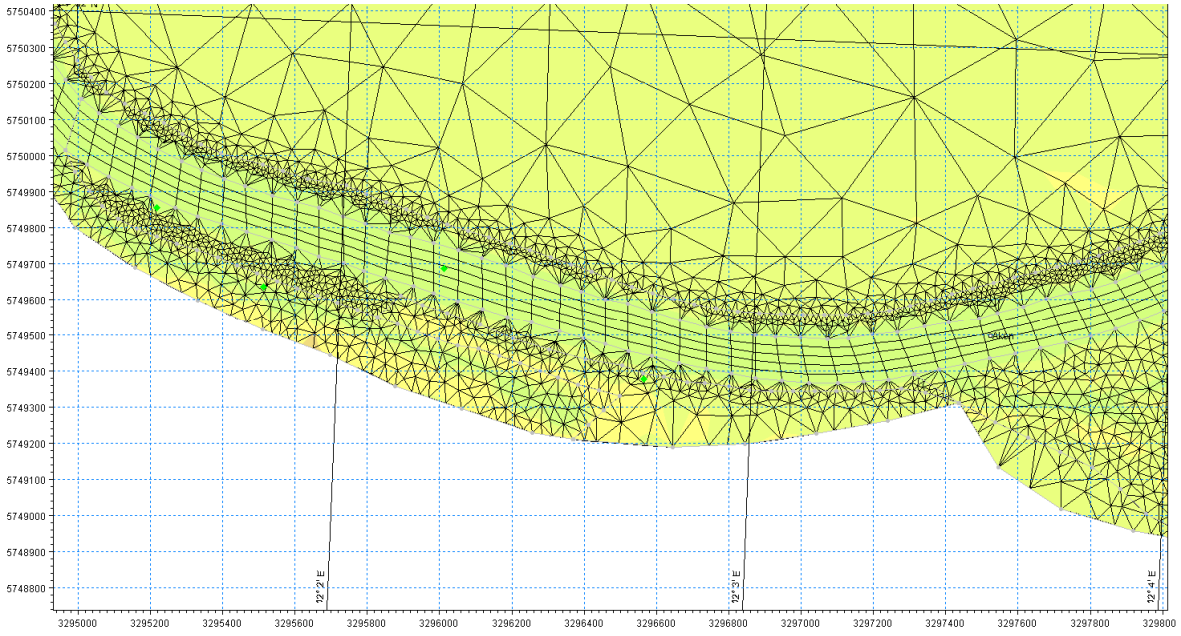

Figure 17. Example interpolated mesh (upstream of Aken), showing flexible mesh resolution

5.8.2 HD Module Setup

The HD module boundary conditions were established using daily discharge and water height data from Aken and Barby, respectively. Input from the Saale River was setup as a point source using daily discharge data. Both the discharge and water height data datasets were interpolated to five minute time-steps. Three, two-week simulation periods were selected, a low, moderate, and high flow period at the Aken gauge. These were selected by finding two week simulation periods which approximately averaged to the mean low water (MNW), MQ, and mean high water (MHQ) at Aken, which are 168, 463, and 1851 m^3/s, respectively. These simulation periods are detailed in Table 14.

Table 14. Simulation periods for the flexible mesh model

Benchmark	Benchmark Discharge (m3/s)	Simulation Period	Number of days
MNW	168	7/28/1999-8/10/1999	14
MNW	168	6/13/2000-6/26/2000	14
MQ	436	10/29/1996-11/11/1996	14
MQ	436	3/7/2001-3/18/2001	14
MHQ	1851	3/15/2000-3/28/2000	14
MHQ	1851	3/24/2006-4/6/2006	14

Initial input values for the 2DFM model are shown in Table 24. Of key importance are the time-step interval and the resistance number. A time step interval of 60 seconds allowed adequate run-times, while maintaining Courant numbers close below two. The resistance number was taken from the 1D HD model (Section 5.5.1).

5.8.3 MT Model Setup

The primary input for the MT module was the output from the HD module. The MT boundary conditions were established using daily (Monday-Friday, interpolated weekends) SSC data from Wittenberg, (km 214.1) and Barby (km 295.5). The daily data were interpolated to five minute

increments for consistency with the time-step interval of the HD model. Inputs to the MT module are summarized in Table 15.

Table 15. Mud transport module input

Condition	Setting
Fractions	The number of grain size fractions and bed layers in the simulation, set to 1
Water Column Parameters	Sand fractions not included and constant settling velocity. Flocculation is simulated. Density of sediment and concentration for flocculation set to 2200 kg/m3 (Lichtfuss & Brümmer, 1981) and 0.01 kg/m3, respectively. Critical shear stress for deposition set to 0.515 is N/m^2, following recommended values (generally less than the critical shear stress for erosion).
Bed Parameters	Critical shear stress for deposition set and density set according to Section 5.5.2. Bed roughness set to 0.001, the recommended value for fine sediment. Bed density (dry weight) set to 250 (kg/m3), the recommended value for medium consolidated bed sediments.
Forcings	No waves
Dredging	No dredging
Dispersion	Scaled eddy viscosity formation, scaling factor = 1.
Sources	No additional sources of suspended sediment included
Morphology	Morphological impact on the hydrodynamics taken into consideration

6 Results

Results of both the preliminary data analysis and model development are detailed below. In Section 6.1, the long-term SSC data are evaluated with respect to seasonal and/or long term trends. The potential implications of missing data are also assessed. In Section 6.3, SSC and discharge data are analyzed concurrently to conduct a double mass analysis and establish rating curves. In Section 6.4, the SSC data are combined with contaminant concentration data to conduct a PCA. The results of the calibration, validation and various scenarios of the hydrodynamic, suspended sediment and HCB models are presented in Sections 6.5 through 6.8. Section 6.8 discusses the results of the groyne impact analysis. Note that all analyses discussed below, with the exception of the 2011 flood modeling, were conducted prior to the 2011 data becoming publically available, so they are not included in the results.

6.1 Long-Term Trends in Suspended Sediment Loads and Concentration

Both the Meissen and Magdeburg SSC data display trends that are important for a holistic understanding of sediment transport in the Middle Elbe. Two general trends can be observed from visual inspection of graphical data:

1. A long-term trend of decreasing SSC at Magdeburg and Meissen, within the timeframe of the available dataset (1/1/1995-4/30/2009) is discussed in Sections 6.1.2 and 6.1.3. This trend can be seen in Figure 18.
2. Higher SSC in summer than winter, as shown in Figure 19 (discussed in Section 6.1.1). For the purposes of this analysis, summer is defined as April through September and winter as the remaining months.

The statistical significance of these two trends was evaluated for both sampling stations using independent-samples t-tests and one-way analysis of variance (ANOVA ($p<0.05$), and the results are detailed in the following sections. As the datasets from both stations have significant data gaps, amounting to 8% of the Meissen data, and 3% of the Magdeburg data (and 2009 is only a

partial dataset), the implications of missing data to the long-term trend analysis are also discussed.

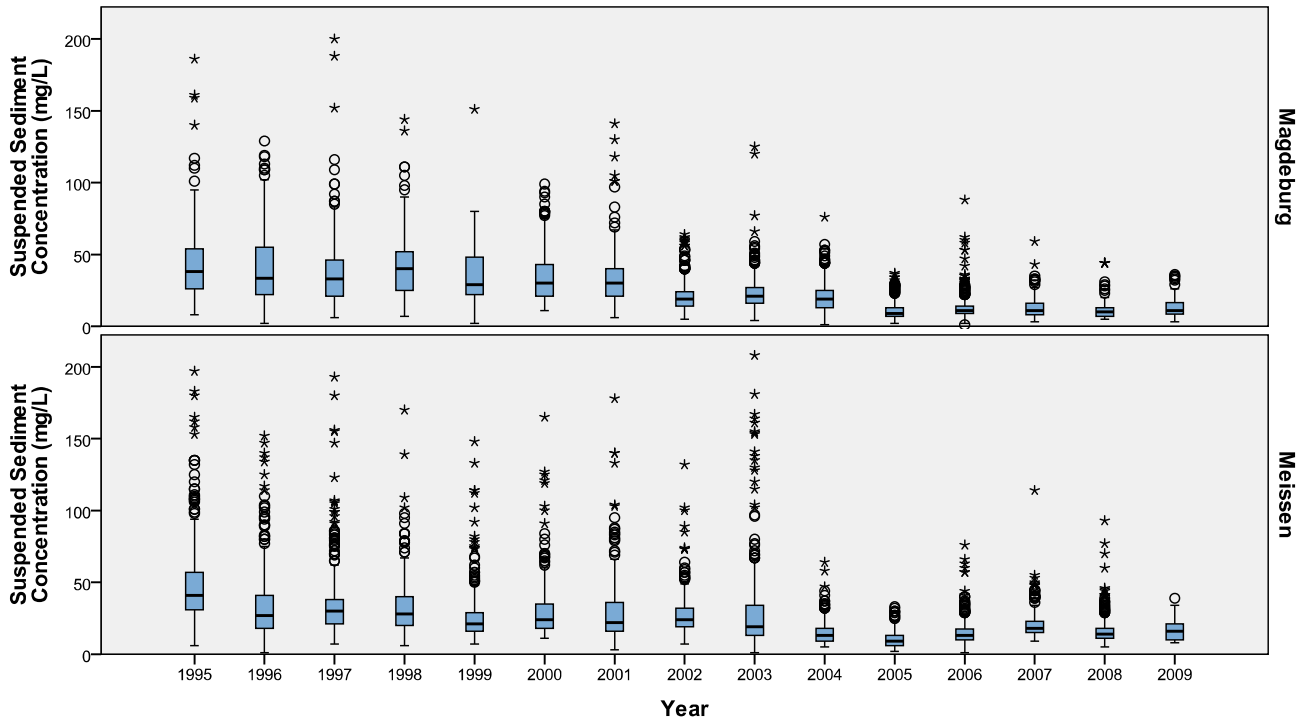

Figure 18. Annual suspended sediment concentration at Meissen and Magdeburg
(Note: 7 outliers with values above 200 were excluded from the Meissen plot to improve readability).

6.1.1 Seasonal Trends

The Meissen and Magdeburg SSC data were assessed to determine if there was a statistical difference between concentrations in winter (October through March) and summer (April through September). Winter and summer SSC at Meissen and Magdeburg are shown in Figure 19, wherein the summer concentrations are noticeably elevated relative to winter at both locations, likely due to both seasonal variations in discharge and phytoplankton blooms related to warmer temperatures (Engelhardt et al., 2004; Karrasch et al., 2001).

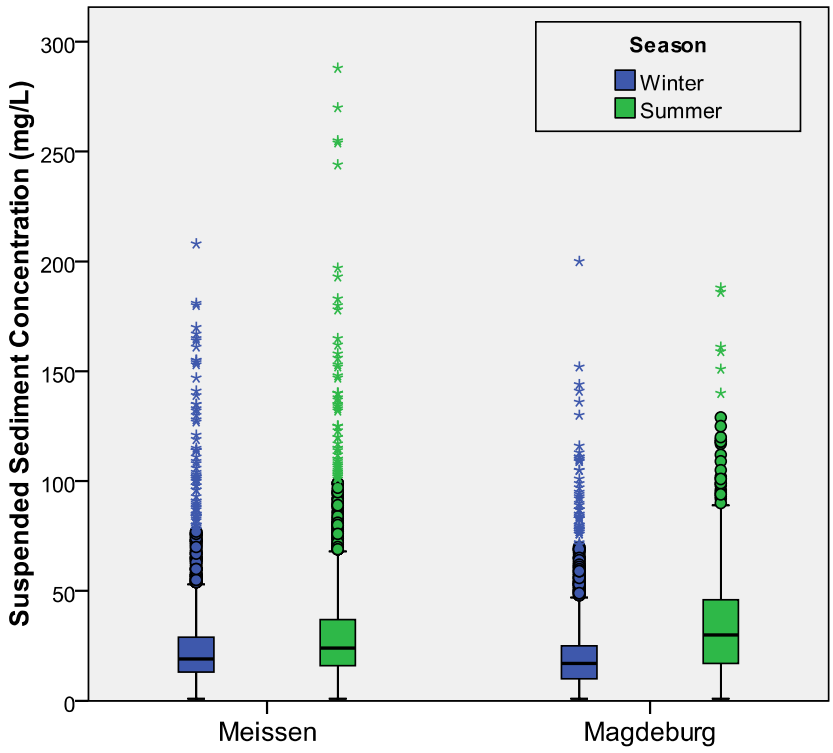

Figure 19. Winter and summer SSC at Meissen and Magdeburg

To evaluate whether the observed difference between the seasons is statistically significant, the distributions of the Meissen and Magdeburg SSC datasets were assessed using histograms and Q-Q plots and determined to be log-normal. Data from both locations were log-normalized, and even though the Kolmogorov-Smirnov test of normalized data was significant, box plots and Q-Q plots showed that the data is approximately normal. Therefore parametric independent-samples t-tests were used to evaluate statistical significance at the two sampling stations. The log-normalized data displayed homogeneity of variances for both the Meissen and Magdeburg data, as assessed by Levene's Test for Equality of Variances (p = .239 and p = .240, respectively). For the Meissen data, there was a statistically significant difference in SSC scores between summer and winter, with summer displaying a higher mean, $p < 0.05$. The Magdeburg data also displayed a statistically significant difference in SSC scores between summer and winter, with summer displaying a higher mean, $p < 0.05$.

This analysis shows that at both Meissen and Magdeburg summer SSC concentrations are significantly elevated relative to winter. As discussed above, this trend is likely caused by summer low water periods which encourage phytoplankton growth, and thus a subsequent increase in SSC.

6.1.2 Long-Term Trends in the Meissen Suspended Sediment Concentration Data

The objective of this analysis was to determine if there was a statistically significant decrease in Meissen SSC over the time period of the available dataset (1/1/1995-4/30/2009). Figure 18 shows the SSC concentrations for 1995 through 2009 at Meissen. As discussed in Section 6.1.1, the SSC data were found to be log-normal, so the dataset was initially $\log_{10}$ transformed.

One-way ANOVA revealed a statistically significant difference in SSC between years (1995-2009) ($p < .005$). Homogeneity of variances was violated, as assessed by Levene's Test of Homogeneity of Variance ($p < .005$). Games-Howell *post-hoc* analysis revealed approximately five sets of stations that group together. These groups are summarized below and identified graphically in Figure 20, but it should be noted that the *post-hoc* results are complicated, given the 14 years being compared. Thus, the groups listed below are based on both statistical significance and visual assessment of annual data:

- Group 1: 1995
- Group 2: 1996-1998, 2000-2002
- Group 3: 1999, 2003, 2007
- Group 4: 2004, 2006, 2008, 2009
- Group 5: 2005

The statistical results show a significant trend of decreasing mean SSC concentration over time. However, given that the data gaps start in 2001, there is the potential for the missing data to skew the results. Importantly, the missing data occur with a higher frequency in winter (65% in winter, 35% in summer), and since winter SSC concentrations are known to be lower (Section

6.1.1), the missing data are more likely to cause the existing dataset to be skewed towards higher SSC. This should somewhat alleviate concerns that the gaps in measured data are causing an unrealistic representation of actual values. A further discussion of potential error from measurement methods is provided in Section 7.1.

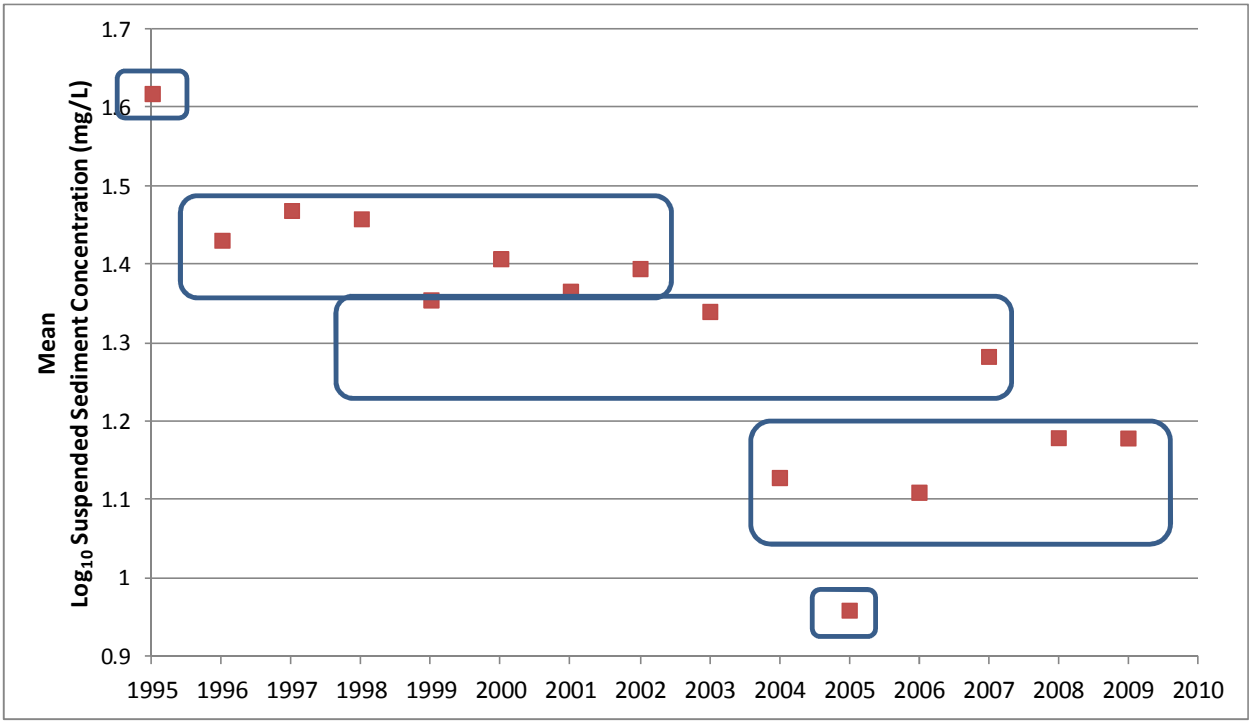

Figure 20. Meissen SSC (log_{10}), statistically significant groups identified.

6.1.3 Long-Term Trends in the Magdeburg Suspended Sediment Concentration Data

The objective of this analysis was to determine if there was a statistically significant decrease in Magdeburg SSC over the time period of the available dataset (1/1/1995-4/30/2009). Figure 18 shows the SSC concentrations for 1995 through 2009 at Magdeburg. As discussed in Section 6.1.1, the data were found to be log-normal, so the dataset was initially log_{10} transformed. One-way ANOVA revealed a statistically significant difference in SSC between years (1995-2009) ($p < .005$). Homogeneity of variances was violated, as assessed by Levene's Test of Homogeneity of Variance ($p < .005$). Games-Howell *post-hoc* analysis revealed four groups of stations, each group statistically different from the other groups. These groups listed below in order of decreasing mean SSC, and illustrated graphically in Figure 21. However, it should be

noted that the *post-hoc* results are complicated, given the 14 years being compared. Thus, the groups listed below are based both on statistical significance and visual assessment of annual data:

- Group 1: 1999 and 1995
- Group 2: 1996, 1999, 2000, and 2001
- Group 3: 2002, 2003 and 2004
- Group 4: 2005, 2006, 2007, 2008 and 2009

As with the Meissen SSC data, the Magdeburg data also have significant missing data. The largest gap occurs 6/1/2005-8/10/2005, which likely cause the SSC mean to be artificially lower, and 11/1/2006-1/1/2007, which likely has the opposite effect. Only a partial dataset was obtained for 2009, but the data were still included in the analysis. These data gaps need to be considered when interpreting statistical results, although the missing data from 2005 and 2006 are unlikely to affect data grouping due to the reasoning described previously.

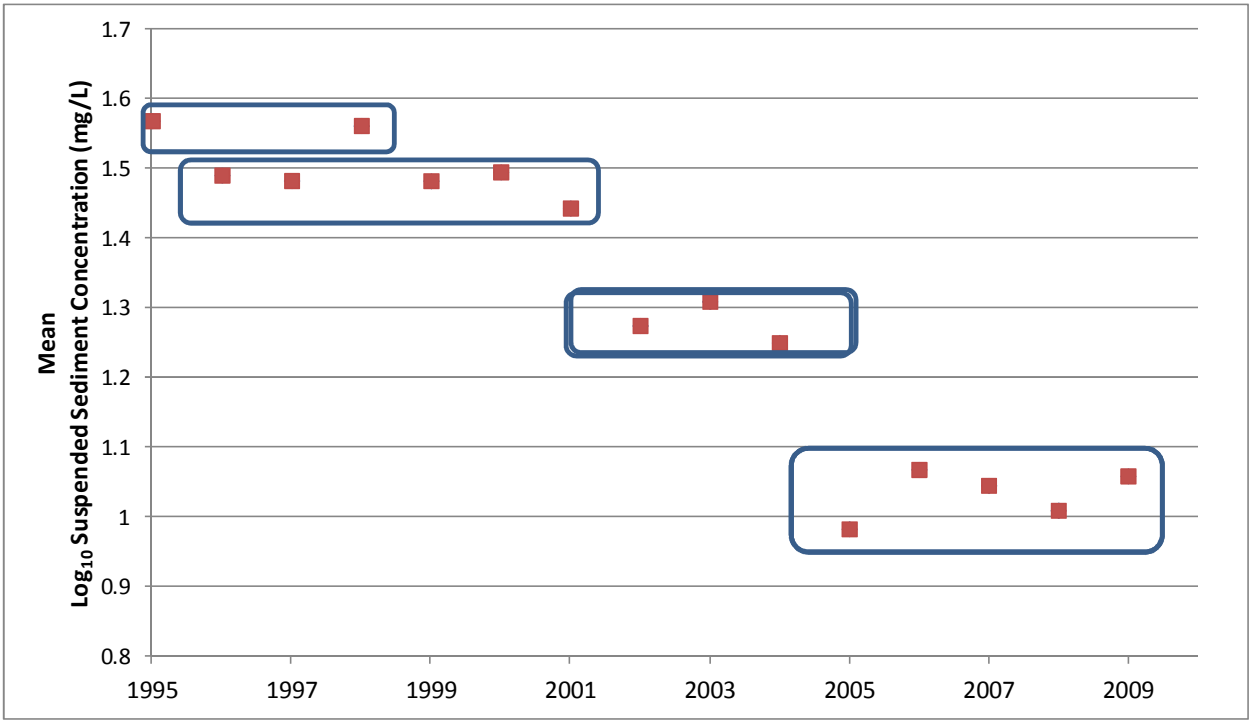

Figure 21. Magdeburg SSC (log_{10}), statistically significant groups identified.

6.2 Long-Term Trends in HCB Loads

As detailed in Section 5.1.2, the objective of this analysis was to evaluate long-term (1994-2009) trends in HCB loads by (1) predicting future loads at Schmilka under scenarios of both natural attenuation (i.e. no source management measures) and source control and (2) using these predictions to estimate the future impact of both scenarios at Schnackenburg. The implications of analysis results are discussed in Section 8.1.

The Schmilka load data were evaluated in two ways. The first explores future HCB loads under the assumption that future loads will continue to decrease at a rate consistent with historical loads (1994-2009). The second method takes into consideration the results discussed in Sections 6.1 and 6.3, namely that the August, 2002 floods precipitated a change in the volume of suspended sediment in the Elbe, and that the suspended sediment load data can thus be separated into two distinct time periods; 1994-2002 and 2003-2009. In the second analysis, data from these two time periods are analyzed separately. An important assumption in both methods is that future loads can only be predicted if there is a statistically significant decrease in load over time.

The HCB loads at Schmilka, shown in Figure 22, display a statistically significant decrease between 1994 and 2006 (R^2 =0.6146 , $p<0.001$). Thus, the regression equation could be used to predict future loads at ten-year intervals (2020 through 2060). Once these predictions were complete, probability forecasts were generated for 75% confidence intervals, which are shown in Table 16. This table presents both a predicted load at each of the 10-year intervals, and a probabilistically simulated 75% CI around the predicted load. For example, the deterministic regression model indicates that the HCB load at Schmilka will be 0.087 kg/year in 2040, representing a 99.57% decrease from present conditions (defined as the average of 2003 through 2009 loads). Once uncertainty is incorporated, there is a 75% chance that the load will be between and 1.70E-03 kg/year and 4.79 kg/year in 2040. Therefore, the worst case scenario under present conditions is that the HCB load at Schmilka in 2040 will be 4.79 kg/year. These calculations and simulations assume that HCB loads will to decline at present rates, consistent with exponential decrease.

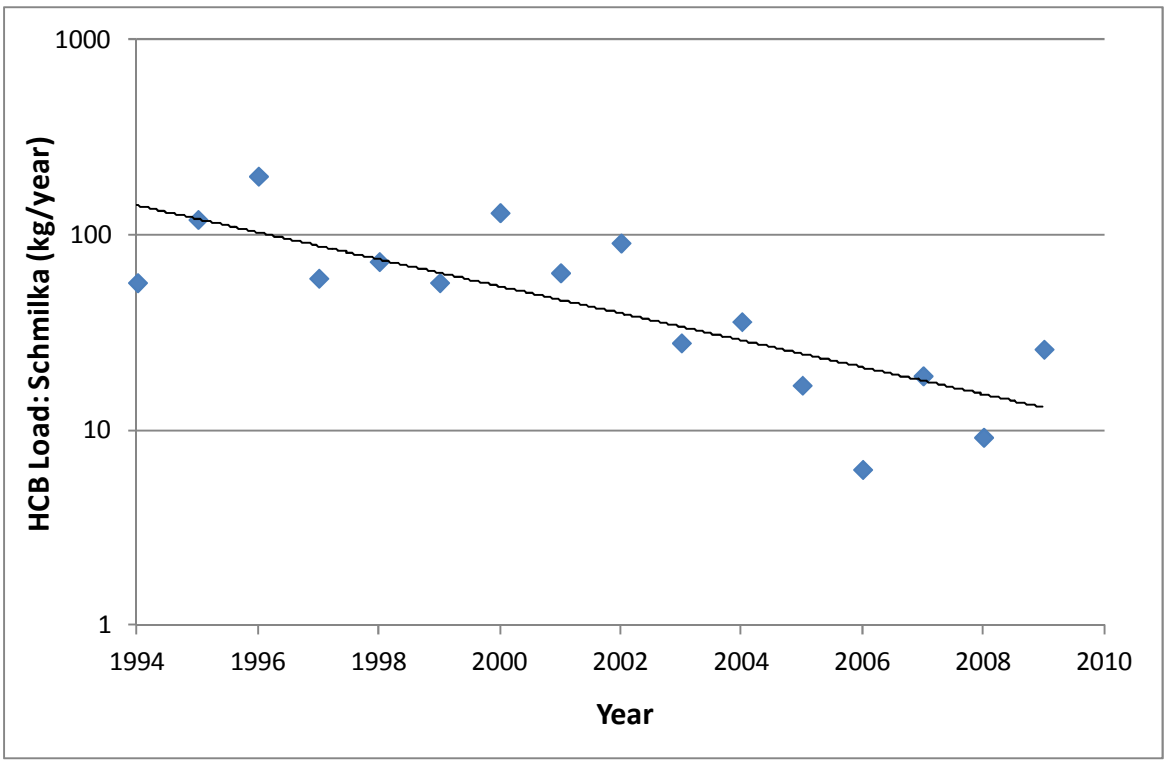

Figure 22. HCB Loads at Schmilka* (1994-2009)
Note: *The Schmilka measuring station was out of service for 8 months in 2002. Thus, the actual load is probably higher.

Table 16. Predicted HCB loads at Schmilka

Contaminant	Location	Year	Standard Deviation	Load Units	Predicted Load	% Decrease from Average (2003-2009)	75% Confidence predicted value is between…	
							Lower	Upper
HCB	Schmilka	2020	0.42	kg/year	1.999	90.11%	0.04	77.62
		2030	0.42	kg/year	0.416	97.94%	0.01	23.44
		2040	0.42	kg/year	0.087	99.57%	1.70E-03	4.79
		2050	0.42	kg/year	0.018	99.91%	4.79E-04	0.93
		2050	0.42	kg/year	3.91E-03	99.98%	8.32E-05	0.19

The HCB load data were then divided into two groups (1994-2002 and 2003-2009) with the intent of conducting an analysis identical to the one described above. However, neither of these groups showed a statistically significant decrease over time. Rather, ANOVA failed to

detect a statistically significant relationship with time in both datasets (p= 0.807 and p=0.443 for the 1994-2002 and 2003-2009 subsets, respectively). Thus, loads within each group can be assumed to be equivalent. Since neither of these data groupings display decrease in load over the time period of the historical data, it is not possible to predict future load decrease. The data from these two time periods only display a statistically significant decrease when evaluated simultaneously, the sub-groups do not.

The next analysis focused on evaluating the impact in Schnackenburg of any HCB load decreases measured 470.6 km upstream at Schmilka. As shown in Figure 23, there is a strong relationship between HCB loads at Schmilka and Schnackenburg ($R^2 = 0.7719$, $p<0.001$). This figure also shows while Schmilka loads are higher in some years (1996, 2000, 2002), neither of the stations has a consistently higher load than the other. Schmilka loads exceed those measured at Schnackenburg by the largest magnitude in 2000 and 2002, despite the Schmilka station being out of order for eight months in 2002. However, paired t-tests (by year) failed to detect any significant difference between the loads at the two locations (p=0.438). Thus, the loads at each station can be considered equivalent in any given year.

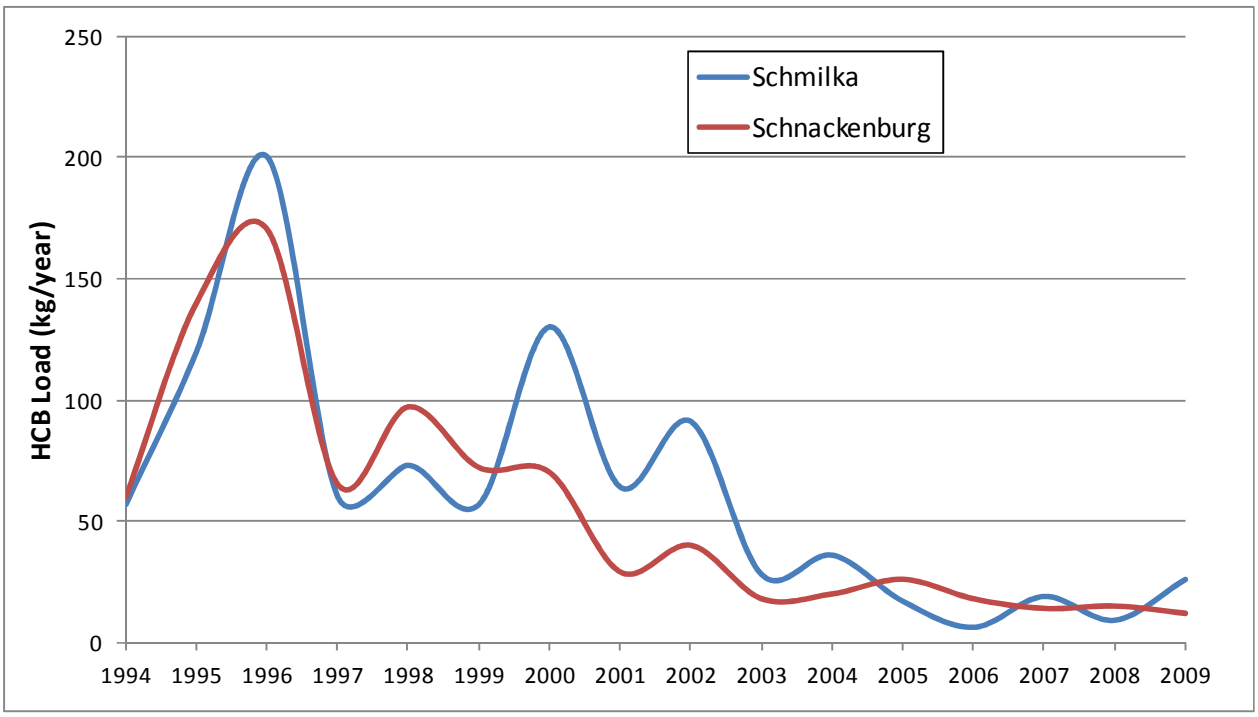

Figure 23. HCB loads at Schmilka and Schnackenburg

6.3 Double Mass Analysis and Rating Curves

6.3.1 Double Mass Curves: Dresden and Magdeburg

To complete the double mass analysis, cumulative SSC was calculated at Dresden/Meissen and Magdeburg using data collected 1/1/1995 through 12/10/2008 and 1/1/1993 through 12/31/2008, respectively. All dates with missing suspended sediment data were removed from the dataset. The double mass plots for Dresden and Magdeburg are shown in Figure 24 and Figure 25, respectively. As discussed previously, the double mass plots give a long-term perspective on the relationship between SSC and discharge, which can be expressed by alterations in the slope of the graph. Changes in slope of the line indicate that the relationship between sediment and discharge have changed over time (e.g. sediment concentrations are higher or lower relative to discharge).

The graphs from Dresden and Magdeburg show relatively consistent slopes for the first years of the record, with noticeable changes in inflection first occurring in 2002, roughly at the same time as the 100-year flood that occurred in 2002. This shift is particularly obvious at

Magdeburg (Figure 25), but can also be observed at Dresden (Figure 24) and suggests a transition to lower sediment concentrations and/or higher discharge. Indeed, the 2002 marks a clear transition in the average annual SSC. For all years following 2002, SSC at Magdeburg continue to be lower than in previous years (Figure 25).

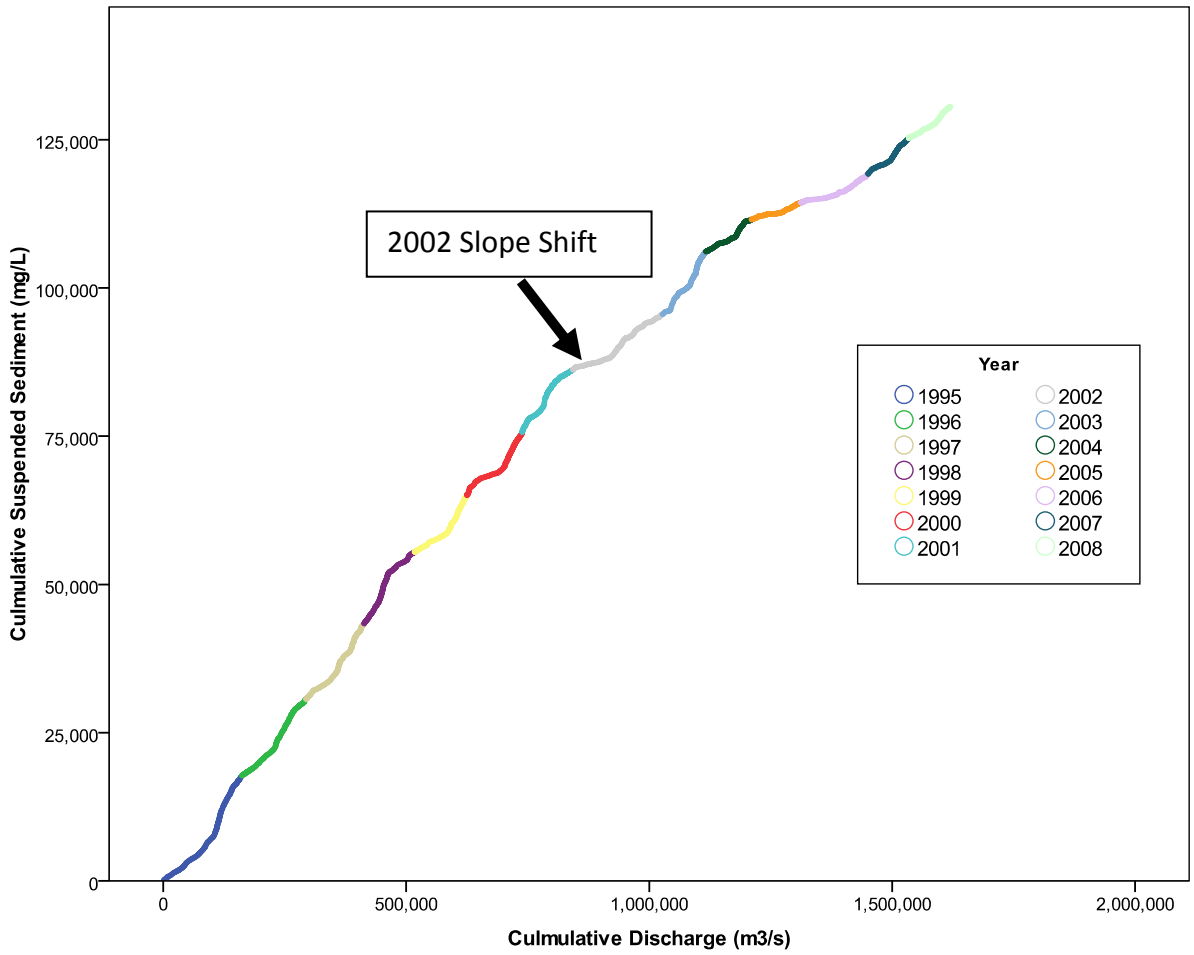

Figure 24. Double mass plot (Dresden)

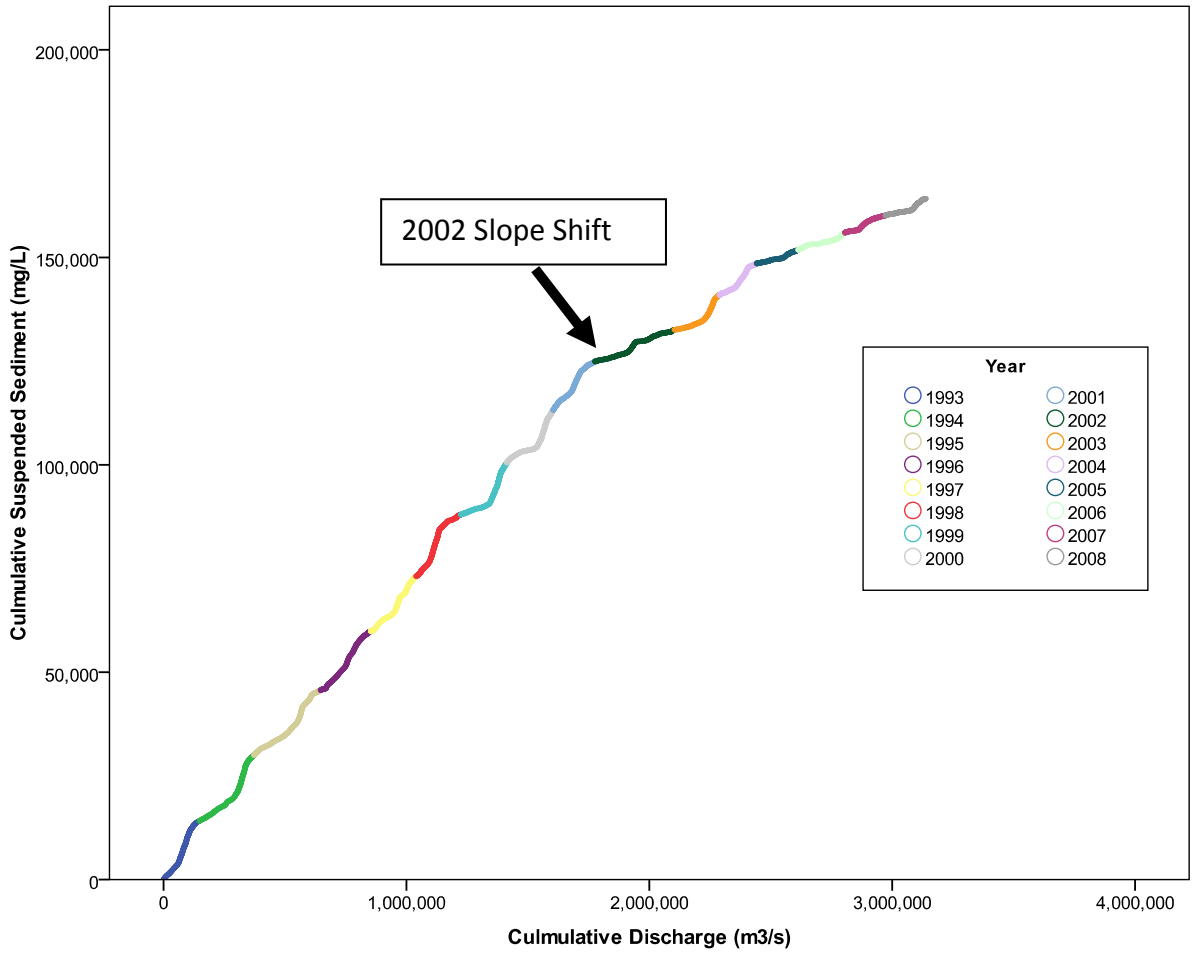

Figure 25. Double mass plot (Magdeburg)

A second breakpoint is clear at Dresden in late 2003/early 2004 and again in early 2006. At Magdeburg, a second breakpoint can be observed in late 2004/early 2005. However, it should be noted that the WSV recalculated Q/H relationships in 2006 which may be responsible for observed differences in the plots (Schwandt, 2012b).

Since differences in the long-term relationship between suspended sediment and discharge data can be observed in the double mass plots, the next step was to determine (a) if seasonal and or temporal patterns might be responsible for this change (b) if those relationships are statistically significant and (c) where the differences lay. A confounding factor in this analysis, however, are the missing SSC data, from periods when either sampling crews were unable to collect data, or the sampling station was not functioning. These questions are explored more

quantitatively via the development of sediment rating curves (Section 6.3.2) and a statistical evaluation of the long-term dataset and missing data (Section 6.1).

6.3.2 Rating Curves: Dresden and Magdeburg

Sediment rating curves were evaluated for both Dresden and Magdeburg according to the following data groupings: All data, winter, summer, pre-2002 (summer and winter), and post-2002 (summer and winter). The seasonal groupings are based on the analysis of seasonal trends (Section 6.1.1) and the well documented summer phytoplankton blooms in the Elbe which can result in increased SSC (Engelhardt et al., 2004; Karrasch et al., 2001). For the purposes of this analysis, summer is defined as April through September and winter as the remaining months. The data were also divided into two groups, 1995-2002 and 2002-2008, based on the results of Sections 6.3.1 and 6.1, which show that there is likely a change in the relationship between sediment and discharge related to the August, 2002 flooding event.

For this analysis, all paired discharge and SSC data were included (1/1/1995 through 12/31/2008 for Dresden and 1/1/1993 through 12/31/2008 for Magdeburg), and if either the discharge or SSC were missing from any sampling date, all data from that date were excluded (i.e. missing values were not substituted). The discharge and SSC from both Dresden and Magdeburg were strongly positively skewed, and were thus $\log_{10}$ transformed. Following $\log_{10}$ transformation, both variables were approximately normally distributed, as assessed by visual inspection of their histograms. All statistics were conducted on $\log_{10}$ transformed data. Discharge and SSC data were fit to a linear model using least squares regression on logarithms of concentration and discharge data. This equation can then be transformed power function in the form $C=aQ^b$, where C is SSC (mg/l), Q represents discharge (m^3/s), and a and b are regression coefficients (Walling and Webb, 1988; Walling, 1977).

Results of the least squares regression are presented in Table 17. Even though the R^2 values are very low for some of the rating curves, all curves were statistically significant at p= 0.05 due to the large sample size, which ranged between 1139 and 5722, depending on data grouping. The R^2 values range between 0.15 and 0.003 for Dresden (1995-2001 Winter) and Magdeburg (all

data), respectively. In general, the correlation coefficients between SSC and discharge are higher at Dresden than at Magdeburg, and the winter data are always more strongly correlated than the summer data (Table 17). Potential reasons for this observed phenomenon are detailed in the discussion, Section 8.1. However, the R^2 are still overall quite low, with the highest value explaining only 15% of the variability in SSC.

Since the correlations between discharge and SSC are generally stronger at Dresden, Figure 26 is included to illustrate the high degree of scatter around regression line as well as the steepness of the slopes. The slopes of the established rating curve slopes are generally steeper at Dresden than Magdeburg, and are usually steeper in winter than in summer. The largest slope change between pre-and post-2002 flooding occurs at Dresden, where the slope is distinct flatter following the flooding. The Dresden summer and winter, and Magdeburg summer and winter groups all decrease in slope following the August, 2002 flood. This analysis highlights the differences in the SSC/discharge relationship between summer and winter, between Dresden and Magdeburg, as well as alterations in sediment transport potentially resulting from the August, 2002 flooding event.

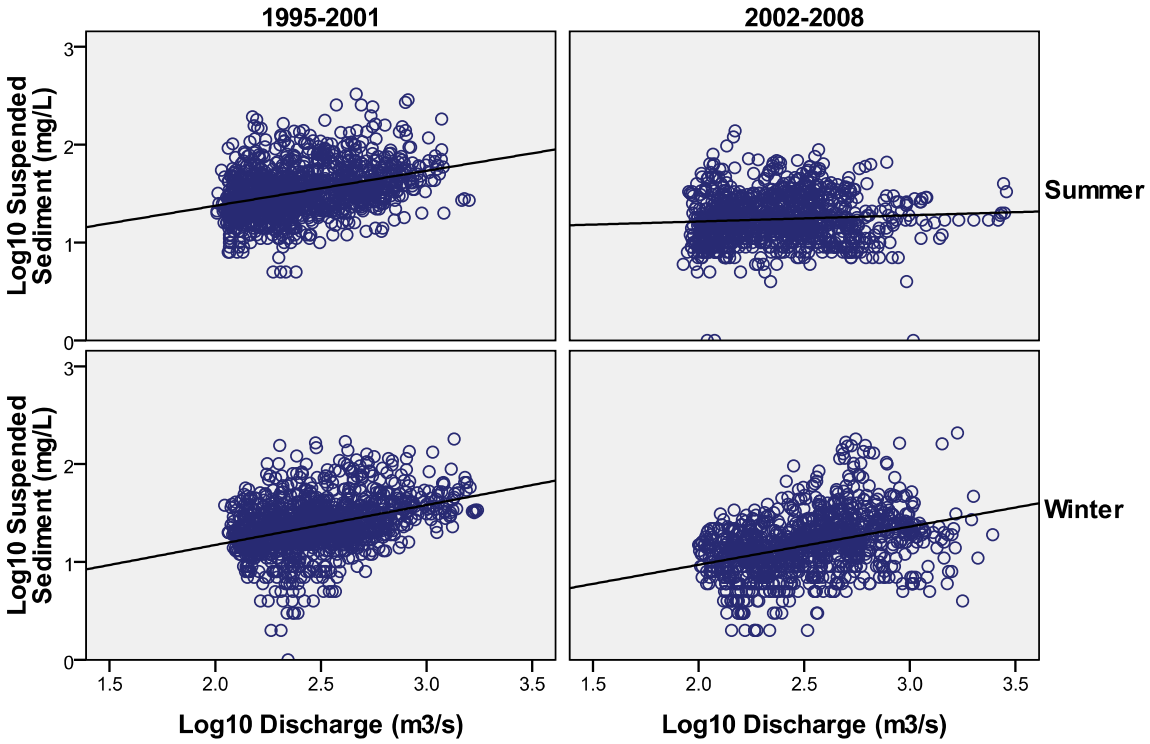

Figure 26. Rating curves at Dresden (1995-2001 and 2002-2008, summer and winter)

Table 17. Rating curves: Results of least squares regression

Location	Dataset	n	Slope	R^2	p-Value
Dresden	All	4766	0.2224	0.067	<0.005
	Winter	2364	0.2988	0.11	<0.005
	Summer	2402	0.0598	0.036	<0.005
	1995-2001 Winter	1266	0.3648	0.1489	<0.005
	2002-2008 Winter	1298	0.354	0.1381	<0.005
	1995-2001 Summer	1263	0.3648	0.1348	<0.005
	2002-2008 Summer	1139	0.0053	0.006	0.014
Magdeburg	All	5722	0.0199	0.0007	0.05
	Winter	2855	0.1991	0.0581	<0.005
	Summer	2367	-0.0303	0.0016	0.30
	1993-2001 Winter	1640	0.3409	0.1211	<0.005
	2002-2008 Winter	1215	0.3025	0.0905	<0.005
	1993-2001 Summer	1647	-0.158	0.11	<0.005
	2002-2008 Summer	1220	-0.1222	0.021	<0.005

6.4 PCA of Sediment Contaminant Data

Of the 84 organic contaminants contained in the FGG sediment sorbed contaminant database (FGG Elbe, 2012), 48 were excluded from this analysis because they had detection frequencies below 50%, were sums of other contaminants already included on the analytes list (e.g. PAHs), or were analytes only measured in recent years, such as polybrominated diphenyl ethers (PBDEs) and butyltins (TBT, DBT, MBT), and were thus not measured frequently enough to be included in the PCA. The primary objective of these exclusions was to reduce the likelihood that PCA results are skewed by non-detects or values used to substitute for analytes that are not frequently measured. The remaining 36 analytes and their detection frequencies (DFs) are shown in Table 18.

Prior to conducting the PCA, data were transformed using an autoscale transform (See Equation 10). Non-detects were included in the analysis at a values of one-half of the detection limit. The suitability of PCA was assessed prior to analysis by testing variables for outliers using box plots.

Equation 10: $Z_{ij} = \frac{x_{ij} - \bar{x}_j}{s_j}$

where: X is the matrix, $\bar{X}_j$ is the calculated mean, and S_j the standard deviation in each column (j=1,2...n).

Table 18. Detection frequency of all analytes included in the PCA

Parameter	Number of Times Detected Above Detection Limit	Number of Times Analyzed	Detection Frequency
1,2,3-Trichlorbenzen	155	185	84%
1,2,4-Trichlorbenzen	180	186	97%
1,2-Dichlorbenzen	148	174	85%
1,3,5-Trichlorbenzen	100	186	54%
1,3-Dichlorbenzen	153	174	88%
1,4-Dichlorbenzen	160	174	92%
Acenaphthen	140	140	100%
Acenaphthylen	140	140	100%
Anthracen	140	140	100%
Benzo(a)anthracen	140	140	100%
Benzo(a)pyren	140	140	100%
Benzo(b)fluoranthen	140	140	100%
Benzo(g,h,i)perylen	140	140	100%
Benzo(k)fluoranthen	131	131	100%
Chlorbenzen	146	174	84%
Chrysen	140	140	100%
Dibenz(a,h)anthracen	140	140	100%
Fluoranthen	140	140	100%
Fluoren	140	140	100%
Hexachlorbenzen	185	185	100%
Indeno(1,2,3-cd)pyren	140	140	100%
Naphthalen	140	140	100%
o,p'-DDD (2,4-DDD)	180	186	97%
o,p'-DDT (2,4-DDT)	174	186	94%
p,p'-DDD (4,4-DDD)	186	186	100%
p,p'-DDE (4,4-DDE)	183	186	98%
p,p'-DDT (4,4-DDT)	179	186	96%
PCB-101	178	186	96%
PCB-138	177	177	100%
PCB-153	186	186	100%
PCB-180	185	186	99%
PCB-28	166	186	89%
PCB-52	171	186	92%
Pentachlorbenzen	149	177	84%
Phenanthren	140	140	100%
Pyrene	140	140	100%

Once all components were extracted, scree plots, which plot total variance explained by each component against its respective component, and the proportion of total variance accounted

for by each component, were used as decide how many components to retain. The inflection point of the scree plot shown in Figure 27 begins at the fifth component, would lead to the retention of the first four components (Cattell, 1966). Additionally, PCA revealed four components that had eigenvalues greater than one and which explained 41.9, 56.8, 64.8, and 71.2 percent of the variance, respectively. As such, four components were retained.

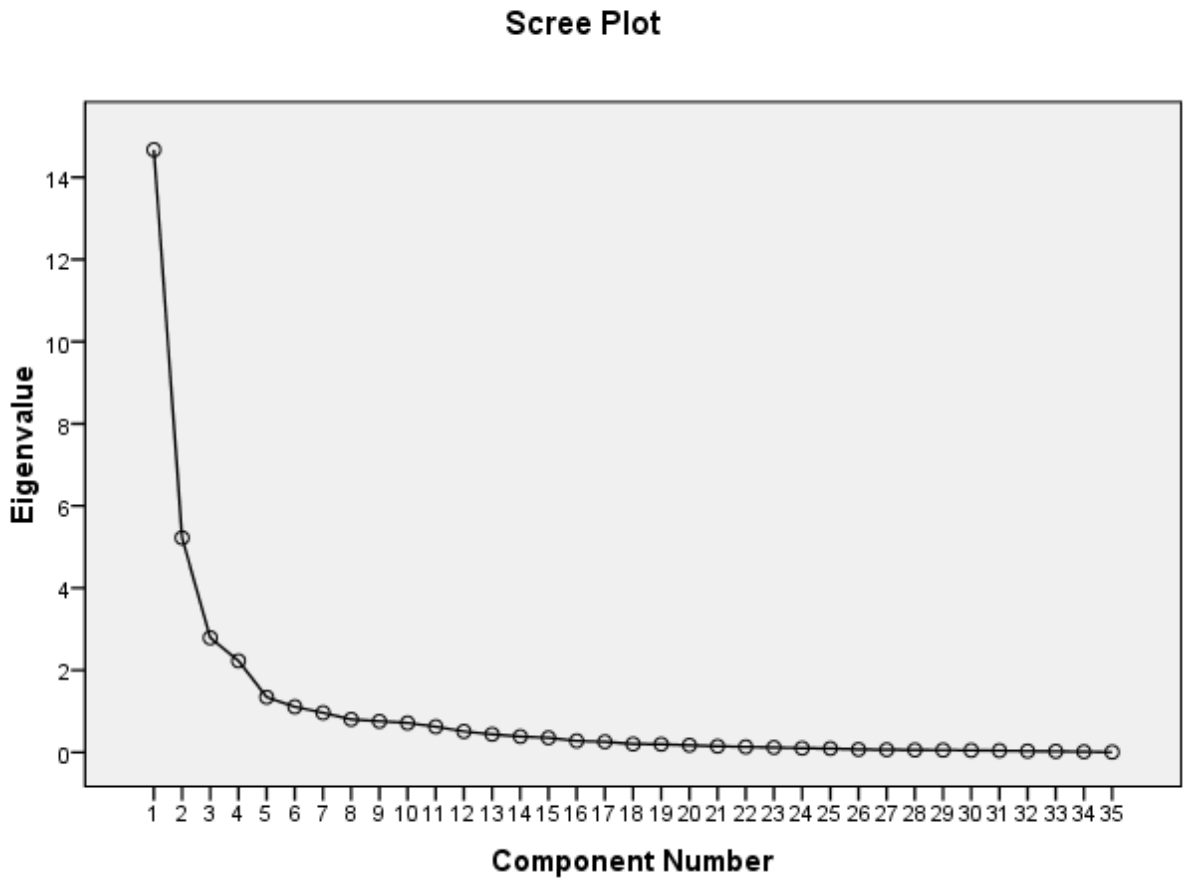

Figure 27. Scree plot for contaminant PCA

A Varimax orthogonal rotation was applied to the four-component solution to aid in interpretability. Component loadings of the rotated solution are shown in

Table 19. The component loadings are summarized below:

- Component 1: 15 analytes, exclusively PAHs.
- Component 2: 12 analytes, including: 8 chlorinated benzenes, Naphthalene, 4,4-DDD, and two of the less chlorinated PCBs (congener28 and 52)
- Component 3: 4 analytes: highly chlorinated PCBs (congener 101, 138, 153 and 180)
- Component 4: two analytes: 2,4-DDT and 4,4-DDT

4,4-DDE is uncorrelated with any of the four components, and 2,4-DDD is almost equally correlated with second and fourth component (scores of 0.643 and 0.638, respectively). Results of the PCA are discussed in Section 8.1.

Table 19. PCA: Rotated structure matrix

	Rotated Component Coefficients			
Parameter	Component 1	Component 2	Component 3	Component 4
1,2,3-Trichlorbenzen	0.301	**0.441**	-0.347	0.309
1,2,4-Trichlorbenzen	0.244	**0.872**	0.147	-0.219
1,2-Dichlorbenzen	0.040	**0.833**	0.040	0.141
1,3-Dichlorbenzen	0.203	**0.784**	0.186	-0.186
1,4-Dichlorbenzen	0.088	**0.472**	0.137	-0.432
Acenaphthen	**0.718**	0.248	0.049	0.087
Acenaphthylen	**0.703**	0.165	0.078	0.216
Anthracen	**0.797**	0.080	0.208	0.170
Benzo(a)anthracen	**0.924**	0.092	0.135	0.078
Benzo(a)pyren	**0.921**	-0.016	0.114	0.133
Benzo(b)fluoranthen	**0.913**	0.046	0.054	0.087
Benzo(g,h,i)perylen	**0.788**	0.293	0.214	-0.098
Benzo(k)fluoranthen	**0.853**	0.034	0.035	0.121
Chlorbenzen	0.173	**0.610**	0.130	-0.288
Chrysen	**0.916**	0.214	0.155	-0.005
Dibenz(a,h)anthracen	**0.626**	0.365	0.115	-0.220
Fluoranthen	**0.871**	0.156	0.185	0.049
Fluoren	**0.638**	0.258	0.161	0.059
Hexachlorbenzen	0.113	**0.793**	0.056	0.021
Indeno(1,2,3-cd)pyren	**0.756**	0.201	0.124	-0.092
Naphthalen	0.367	**0.808**	0.032	0.149
o,p'-DDD (2,4-DDD)	0.219	**0.643**	0.014	**0.638**
o,p'-DDT (2,4-DDT)	0.127	-0.091	0.305	**0.656**
p,p'-DDD (4,4-DDD)	0.214	**0.716**	0.031	**0.527**
p,p'-DDE (4,4-DDE)	0.046	0.018	-0.005	0.181
p,p'-DDT (4,4-DDT)	0.018	-0.137	**0.475**	**0.677**
PCB-101	0.324	0.501	**0.737**	-0.043
PCB-138	0.336	0.126	**0.834**	0.124
PCB-153	0.318	0.208	**0.863**	0.170
PCB-180	0.334	0.210	**0.844**	0.116
PCB-28	0.101	**0.727**	0.179	0.129
PCB-52	0.188	**0.571**	0.320	-0.386
Pentachlorbenzen	0.078	**0.906**	0.024	0.005
Phenanthren	**0.891**	0.114	0.166	0.034
Pyrene	**0.873**	0.198	0.176	0.062

Note: Major loadings are in **bold**

6.5 Model Calibration

The 1D simple, 1D floodplain, and 2DFM models were calibrated by comparing simulation results with available measured and observed data and then adjusting model input parameters, within realistic ranges, to give best agreement. Calibration results for all three models are presented below. Appendix B has the final input values for all modules of the 1D simple, 1D floodplain, and 2DFM models. Once the three models were calibrated, they were validated. The results of model validation are described in Section 6.6. Section 6.8 summarizes the results of the impact analysis, the comparison between the 1D model and the 2DFM model.

Despite the different assumptions between the 1- and 2D models, a comparison between the two models enabled an approximate quantification of the impact of groynes on sediment transport and the ability to ultimately integrate interactions between groyne fields and main channel into the 1D model. Results of the impact analysis are presented in Section 6.8.

6.5.1 Simple Model

The HD and AD modules were calibrated by comparing model output and channel conditions with available measured data and adjusting model parameters to optimize agreement between the two. Calibration statistics for the HD, AD, and Xenobiotics modules are shown in Table 20.

Table 20. Calibration statistics for the 1D 'simple' model

Module	Nash-Sutcliff Efficiency	R^2
HD	0.93	0.94
AD[1]	0.12	0.19
Xenobiotics (HCB)	0.08	0.11

Note:

1: Missing daily data excluded from Nash-Sutcliff and R^2 calculations

6.5.1.1 Hydrodynamic Module

Hydrodynamic model calibration focused on fit between observed and modeled discharge and water height at Barby, the gauging station closest to the downstream boundary of the model (See Table 9). Manning's *M* was the primary parameter adjusted for model calibration. During

the calibration, significant difficulty was encountered with insufficient storage widths of individual cross-sections due to the extreme discharges resulting from the August, 2002 flooding (Section 2.2). Given that a number of dams and dikes were physically damaged and/or overtopped during the flooding, a process which is not simulated in the model, the discharge values at Dresden of the peak two days of August, 2002 flood, 8/16/2002 and 8/17/2002, were manually reduced from 4190 and 4500 m^3/s, respectively, to the HQ50 (3690 m^3/s). This modification allowed for calibration to proceed without additional difficulty.

The ideal condition for the calibration and validation of hydraulic models is when historical flow and, in particular, flood levels can be adequately simulated. The model was manually calibrated by running the model for a span of Manning's resistance values (M^2), between 15 and 45, in increments of five. Daily discharge results were exported to Excel, and the Nash-Sutcliff model efficiency (NSE) coefficient, which is used to calculate the predictive power of hydrodynamic models, was calculated (Nash and Sutcliffe, 1970). The NSE equation is provided in Equation 11 below:

Equation 11: $$NSE = 1 - \frac{\sum_{t=1}^{T}(Q_o^t - Q_m^t)^2}{\sum_{t=1}^{T}(Q_o^t - \overline{Q_o})^2}$$

Where Q_o is observed discharge, and Q_m is modeled discharge, and Q_o^t is observed discharge at time t.

The NSE coefficient ranges between -∞ and 1.0. A value of 1.0 indicates a perfect match between the modeled and observed data, and value of 0.0 indicates that the model is no better

[2] Manning's M is the inverse is the more conventional Manning's *n.* The value of *n* typically ranges between 0.01 (smooth channel) to 0.10 (thickly vegetated channel). The corresponding values for *M* are from 100 to 10. So, the lower the "M" value, the rougher the channel.

at predicting discharge than the mean of observed flows. Values of less than 0.0 denote that the calculated mean is a better predictor than the modeled data.

The final M value of 38 was selected, which has a NSE of 0.93. The NSE value was assumed to be satisfactory for the existing data. An excerpt of the Barby observed and modeled discharge hydrograph for the years 2000 through 2004 (viewing all the data simultaneously is difficult on this scale) is shown in Figure 28. Table 21 shows historical weir openings and closings, compared to modeled weir openings and closings, following calibration.

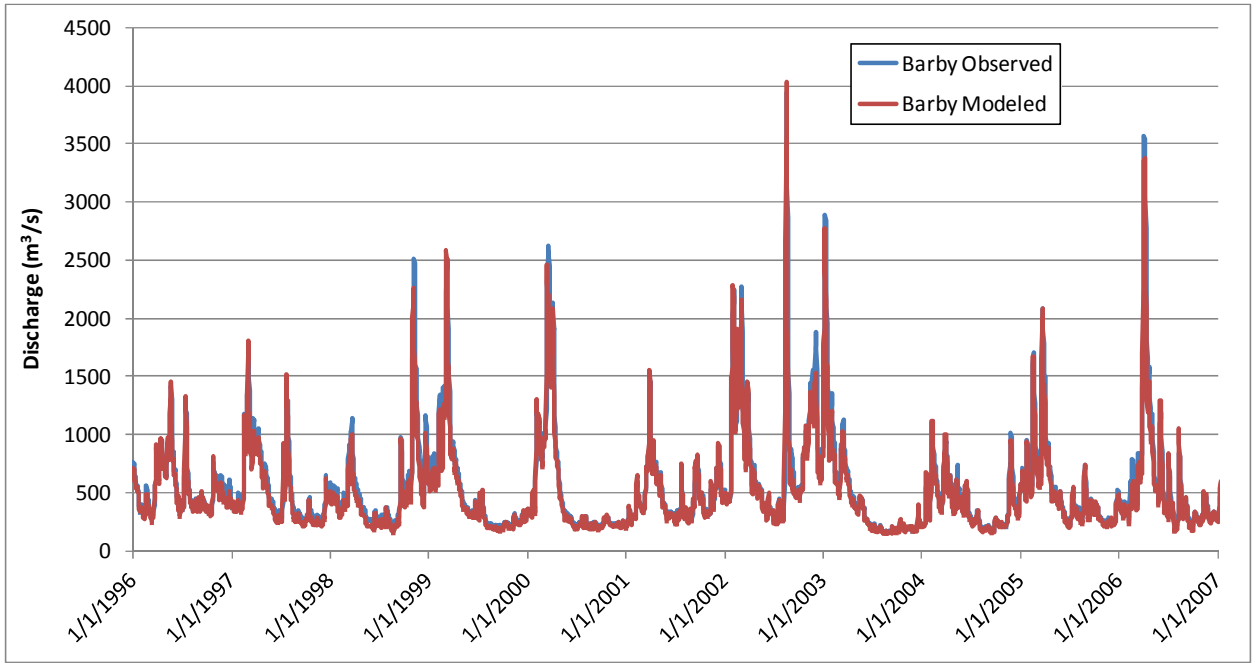

Figure 28. Barby Observed and Modeled Discharge (m^3/s) (1996-2006)

Table 21. Actual and modeled weir openings and closings

Actual Weir Openings			Modeled Weir Openings		
From	To	Number of Days	From	To	Number of Days
3/6/1999	3/15/1999	10	3/5/1999	3/12/1999	8
8/15/2002	8/26/2002	12	8/13/2002	8/22/2002	10
1/4/2003	1/19/2003	16	1/4/2003	1/13/2003	10
3/22/2005	3/27/2005	6	3/22/2005	3/26/2005	5
3/31/2006	4/14/2006	15	3/30/2006	4/12/2006	14

Results shown in Table 20, Table 21, and Figure 28 indicate that the hydrodynamic model is well calibrated, and can thus be assumed to accurately simulate the hydrodynamics of the Middle Elbe. Figure 28 shows that the model is able to simulate both large and small-scale fluctuations in discharge for the calibration period. The largest disparity between modeled and observed discharge occurs during floods events. In particular, while the modeled discharge always reflects the flood event, the magnitude of the modeled peak is sometimes between 5 and 20% smaller than the observed peak. More specifically, the eight flood peaks above MHQ (2071 m^3/s), had a modeled peak discharge that is, on average, 15% smaller than the observed peak[3]. This inaccuracy is likely due to multiple factors, including the numerous small tributaries (e.g. Triebisch, Schwarze Elster, and Weißeritz) to the Elbe which are not including in model setup. Even though these tributaries are small (MHQ between 0.373 m^3/s and 66.1 m^3/s), their exclusion contributes minor uncertainty to the model (Sachsen, 2013; Sachsen-Anhalt, 2012). Additionally uncertainty is likely related to the resolution of model cross-secretions. 1D models are commonly accepted to be accurate within the river channel, but to have significant uncertainty during high water events due to the lack of information about conditions during bank-full or over-bank flow (Bates et al., 1997). The floodplain and banks of the Elbe are highly variable, and the groyne fields are highly incongruous in shape and form. This heterogeneity is simply not captured in the 1D model.

[3] Results from the August, 2002 flood are not included in this calculation. As discussed elsewhere, the August, 2002 flood caused extensive physical damage to hydraulic control structures, and the discharge resulting from these processes cannot be accurately represented in a 1D model.

6.5.1.2 Advection-Dispersion Module

The AD module was calibrated over the same duration as the HD module. The large number of variables in the AD model and the relative scarcity of field measurements for these variables typically complicate model calibration. Unlike the HD model, the AD model was calibrated at Torgau. Attempts were initially made to calibrate the AD model at Barby, but the combined influence of thousands of groynes, and the inputs from the Mulde (which had very sparse suspended sediment data) and Saale proved too strong to allow for an adequate calibration. The primary calibration parameters for the AD module are shear stress, settling velocity and dispersion. However, in 1D, the influence of these variables is minimal. Given the significant spatial and temporal heterogeneity in suspended sediment data, expectations were that the modeled data roughly follows following significant peaks and lows in the measured SSC data, but not necessarily directly corresponding to the data. Figure 29 shows measured and modeled sediment concentration data at Torgau between 1996 and 2006. Missing data are shown below the x-abscissa.

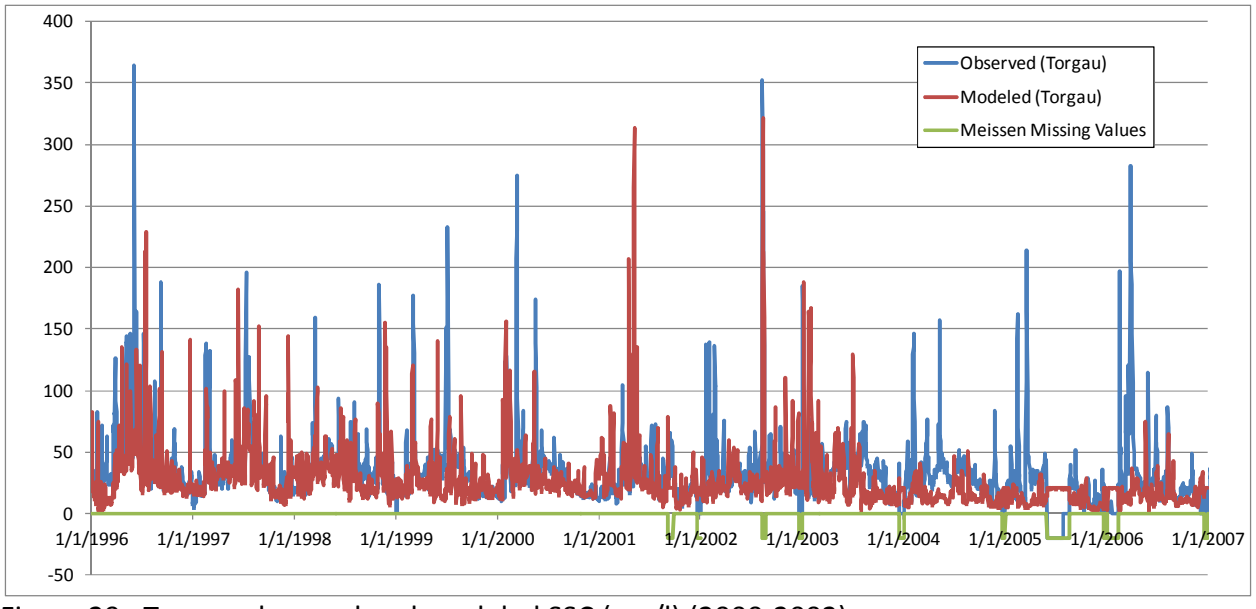

Figure 29. Torgau observed and modeled SSC (mg/l) (2000-2002).
Dates with missing values are shown below the x-abscissa

As was expected, there is a moderate correlation between the modeled and observed data. The magnitude of the concentration is appropriate, and the modeled data sometime follows

measured peaks, but sometimes does not. There are many possible explanations for this. The first reason is the low accuracy of individual suspended sediment values due to sampling methods (i.e. Melitta coffee filter), which is discussed in Section 7.1. A second reason is simply the high heterogeneity of riverine SSC. SSC can vary significantly over small time periods and over short distances. Lastly, the variation may be due to the groyne fields, which alter SSC via processes not replicated in the 1D model.

6.5.1.3 Xenobiotics Module

As discussed in Section 5.3.2, calibration of the xenobiotic module for HCB was conducted using long-term decreases in loads between Zehren, Barby and Magdeburg. The goal of the calibration was to affect a 68.5% decrease in HCB load over ten years, or about 7% per year. Calibration of the HCB module was complicated by several factors. First, an even wider range of input parameters is required, which can both vary greatly in the results research studies and in the natural environment, such as desorption rate in sediment, organic carbon partitioning coefficient (K_{oc}), and the density of dry sediment. Additionally, the monthly, rather than daily, time scale of sediment-sorbed HCB measurements means that the xenobiotics calibration has a significantly lower resolution than for other modules. Lastly, difficulties were encountered with the Ecolab module, where it stalled and required restarting. No reason for these stalls was identified.

Calibration of HCB loads is dependent on the results of the AD module, so again, reasonable expectations were applied to the calibration. The primary calibration parameters of the xenobiotics template were K_{oc} and as the resuspension rate. Settling velocity was assumed to be the same as in the AD module, so K_{oc} was used as the initial calibration value. An extensive summary of literature-based K_{oc} values for HCB, provided by Pohlert, 2009 was used to assign an initial log K_{oc} value of 5.8 (the average of 11 literature-based values) to the model.

Results of model calibration at Dommitzsch are shown in Figure 30, with SSC shown for reference. Only the year 2006 is shown in this figure so that general trends in peaks can be easily discerned. As anticipated, calibration results show a low correlation between measured and modeled HCB loads, due to both the frequency of measurement of HCB concentrations

(monthly) and the very high heterogeneity of HCB concentrations and SSC in the Elbe. Results shown in Figure 30 illustrate a moderate relationship between SSC and HCB loads, which helps to explain the simulated peaks in modeled HCB loads. In particular, the larger of the measured HCB load peaks (August, 2006) are mirrored by modeled results. A baseline load equivalent to approximately 0.005 kg/d is also indicated. As anticipated, HCB loads are highly dependent on peaks in discharge and SSC. Calibration was ultimately assumed to be successful and appropriate for the site, particularly given the low resolution of the input contaminant data.

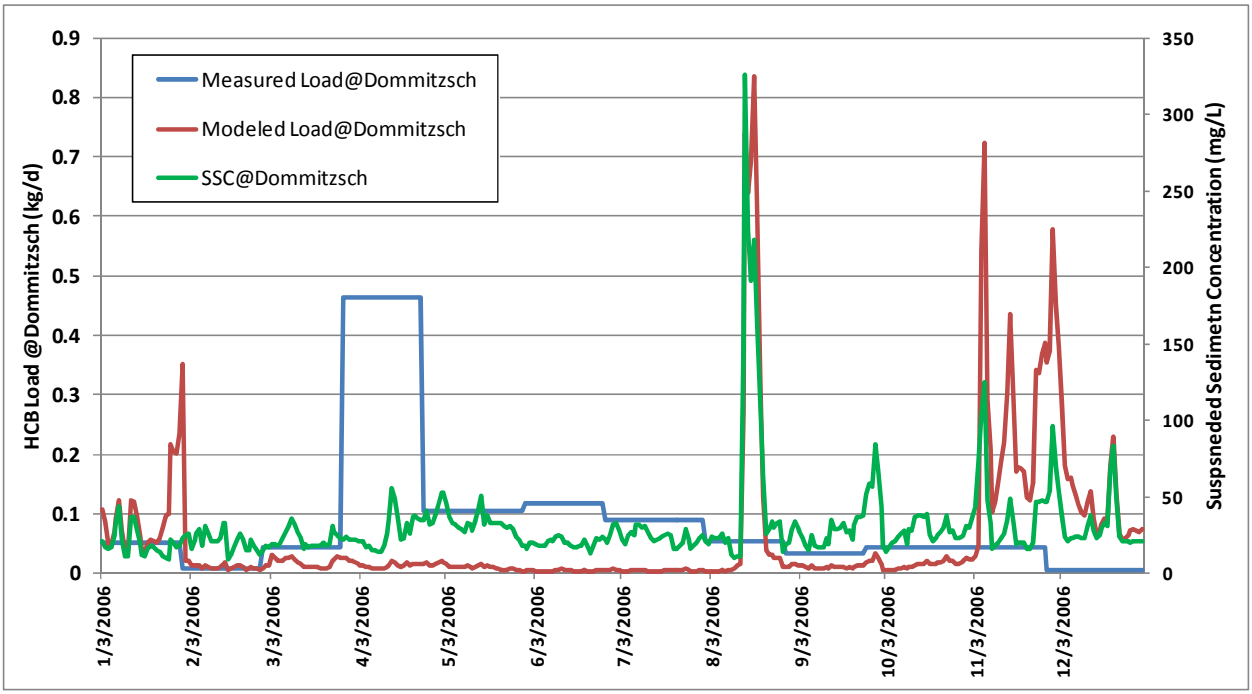

Figure 30. Measured and modeled HCB loads at Dommitzsch in 2006, with SSC for reference

6.5.2 1D Floodplain Model

Calibration of a hydrodynamic model with a large floodplain area requires a thorough calibration process to ensure the hydraulic model accurately reproduces the extent of observed floodplain inundation and flow. This process generally incorporates comparisons between flow data, observed flood levels and areas of inundation, which are unavailable for Elbe floodplains. In addition, validation of the present model was complicated by both the one-dimensionality of the model and the lack of discharge or water depth measurements during flood events. Even though both aerial photos and floodplain inundation maps during high water conditions are

available, it is difficult to correlate quantitative model output from a 1D model with the inundation maps. Thus, validation was accomplished primarily via qualitative techniques; FLYS inundation maps were compared to modeling results to ensure that modeled overbank flooding occurred in appropriate locations, and only during high water conditions (Bundesanstalt für Gewässerkunde, 2009). Calibration statistics for the HD, AD, and Xenobiotics modules are provided in Table 23 below.

To validate the modeled flooding of overbank areas, three reaches of between three and 20km were selected for comparison to FLYS inundation maps. For the purposes of comparison to discharge benchmarks from FLYS, three reaches; Torgau (km 157-160), Wittenberg, (km 206-214) and Aken (260-280) were selected on the basis of (a) having a broad floodplain and (b) close proximity to a gauge. For each of these reaches, FLYS was used to produce inundation maps for four discharge scenarios: MQ, MHQ, HQ50 and HQ100. It should be noted that the difference in inundated area between five, ten and 50 year floods is minimal, so these discharge scenarios were not included.

Next, the discharge corresponding to each scenario was recorded (Bundesanstalt für Gewässerkunde, 2009). Finally, an observed date and discharge was found to correspond to each discharge scenario. If the precise discharge was never observed, then the closest value was used. Notably, several of the observed discharge values for the longer recurrence interval scenarios (i.e. 50 and 100 year floods) occurred during the August, 2002 floods, when extensive damage to flood control structures resulted in discharge irregularities which are not replicated by the model (IKSE, 2004). However, this issue is less problematic given that the most significant change in floodplain inundation occurs between the MQ and MHQ scenarios, and the scale and dimensionality of the modeling precludes detecting the minor differences between the longer recurrence interval scenarios. Values used for floodplain validation are shown in Table 22.

Table 22. Discharge scenarios used for validation of floodplain inundation

Gauge	Scenario	Scenario Discharge (m^3/s)	River km for Floodplain Validation	Observed Discharge Best Matching Benchmark (m^3/s)	Corresponding Date
Torgau (km 154.15)	MQ	337	157-160	336	6/16/1996
	MHQ	1520	157-160	1500	4/4/2000
	HQ50	3680	157-160	*3540*	8/19/2002
	HQ100	4230	157-160	*4290*	8/18/2002
Wittenberg (km 214.1)	MQ	372	206-214	372	1/16/2005
	MHQ	1605	206-214	1606.2	3/22/2005
	HQ50	3685	206-214	*3450*	8/19/2002
	HQ100	4213	206-214	*	*
Aken (km 274.75)	MQ	436	260-280	436	10/5/2007
	MHQ	1851	260-280	1850	1/12/2003
	HQ50	3928	260-280	*3960*	8/19/2002
	HQ100	4431	260-280	*	*

Note:
*No observed discharge close to benchmark
Values in *italic* are from the August, 2002 flood, and therefore may not be reliable due to extensive damage to flood control structures (IKSE, 2004)

Due to the difference between the data available from a 1D model and the floodplain maps, several assumptions were necessary. The flooding that occurred in March and April 2006 was used primarily for the calibration of model floodplains, as the extensive damage to flood control structures during the August, 2002 floods are not replicated in the model.

Table 23. Calibration statistics for the 1D simple and floodplain model

	Nash-Sutcliff Efficiency		R^2	
Module	Simple	Floodplain	Simple	Floodplain
HD	0.93	0.92	0.94	0.91
AD[1]	0.12	0.12	0.19	0.12
Xenobiotics (HCB)	0.08	0.11		

6.5.2.1 Hydrodynamic Module (Main Stem of the Elbe)

As the basic setup of the floodplain model is identical to the setup of the simple model, excepting the addition of the floodplains, the focus of the calibration was to determine the impact of the diversion of water to the floodplains on discharge in the main stem of the Elbe. This issue was particularly important due to the assumption of only positive flow on the floodplains. Thus, flow is diverted from the Elbe to the floodplains during high water conditions, but is not re-routed to the main stem until just upstream of Magdeburg (See Section 5.6 for more details). Thus, it was expected that the NSE would be lower for the floodplain model, and that simulated discharge would diverge from the measured discharge data during high water conditions more strongly than was observed in the simple model. This phenomenon was in fact observed, as seen in Figure 31. While the overall calibration statistics are strong and only slightly lower than the calibration statistics for the simple model (Table 23), it is clear from Figure 31 that the modeled data fail to achieve discharge peaks during high water situation. However, this difference generally occurs for a maximum of 2-3 days. It should be noted that the calibration was at Barby, not far from Magdeburg, where the flow is re-routed to the Elbe, so it represents a worst-case-scenario. Uncertainty and additional implications of this difference between the observed and modeled data for high water periods are discussed in Section 7.2.1.1.

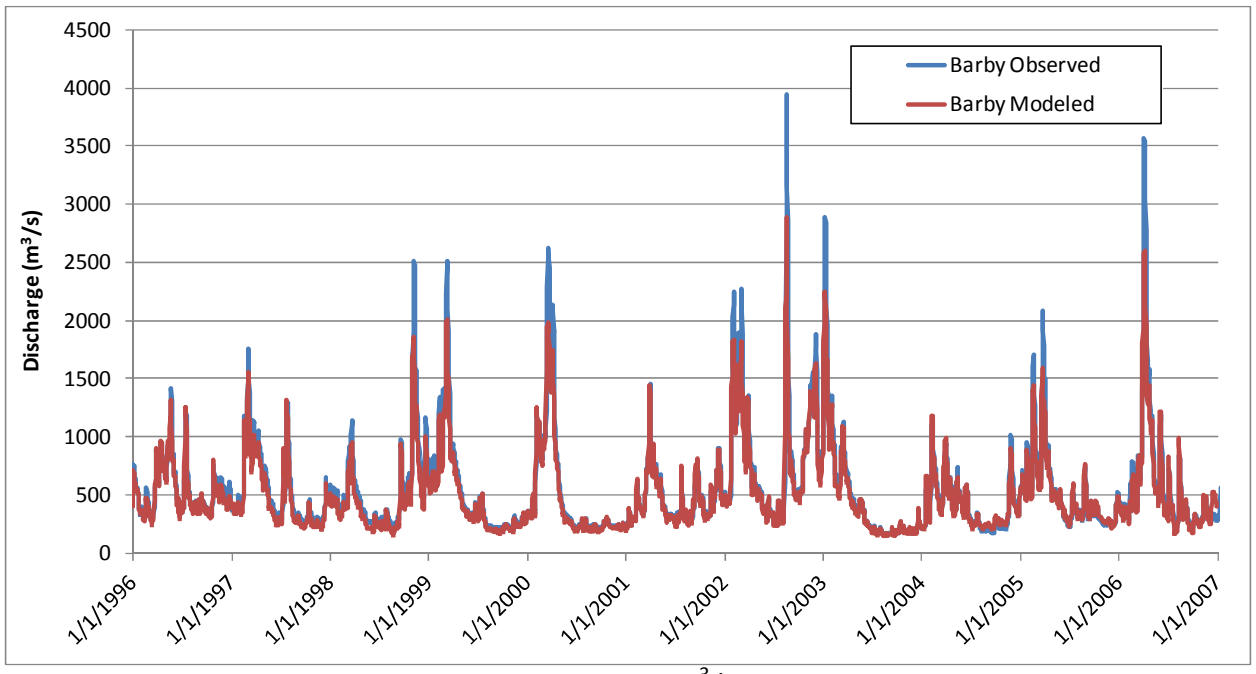

Figure 31. Barby observed and modeled discharge (m^3/s) (1996-2006)

Hydraulic model calibration focused on fit between observed and modeled discharge and water height at Barby, the gauging station closest to the downstream boundary of the model (See Table 9). During the calibration, significant difficulty was encountered with insufficient storage widths of individual cross-sections due to the extreme discharges resulting from the August, 2002 flooding (Section 2.2). Given that a number of dams and dikes were physically damaged and/or overtopped during the flooding, a process which is not simulated in the model, the discharge values at Dresden of the peak two days of August, 2002 flood, 8/16/2002 and 8/17/2002, were manually reduced from 4190 and 4500 m^3/s, respectively, to the HQ50 (3690 m^3/s).

6.5.2.2 Advection-Dispersion and Xenobiotics (HCB) Modules (Main Channel of the Elbe)

Model parameters for the AD and HCB modules were taken directly from the simple model for the main channel of the Elbe. Since Torgau was used for a calibration station for the AD module, and the floodplain channels in the model begin downstream of Torgau, further calibration would not provide additional detail. For this reason, the results are not replicated here. Section 6.5.1.2 describes how the AD module was calibrated for the simple model.

Due to the long run-times of the Xenobiotics (HCB) module once the floodplain channels were included, it was not possible to run the model for simulation periods exceeding two months. Since the primarily calibration occurred in the simple model, HCB-related model parameters were considered calibrated and thus no alternative approach to model calibration had to be developed. Section 6.5.1.3 describes how the Xenobiotics module was calibrated for the simple model.

6.5.3 2DFM Model

6.5.3.1 2DFM Hydrodynamics (HD)

Since there are no gauges between Aken and Barby, calibration of this module was accomplished in a qualitative, rather than quantitative manner. Schwartz (2005) has measured flow velocities in groyne fields and found them to be 5 to 10 cm/s in the center of the groyne field, 15-30 cm/s at the inlet of the groyne field, and 62-103 cm/s during extreme high water. Flow velocities in selected groyne fields were checked, and triangle grid and boundary conditions were modified to ensure realistic values within groyne fields. In addition, three additional qualitative checks were performed on the data. First, Courant, current speed and direction were checked to confirm that values were reasonable. Second, the model was evaluated to make sure that no erroneous values occur at or near the up-and downstream boundaries. Lastly, the interaction between the rectangular and triangular grid was visually inspected for irregularities. Once these objectives were satisfied, the model was considered to be calibrated.

Table 24. Specifications for the flexible mesh calibration simulation

Parameter	Value
Simulation Period(s)	See Table 14
Time Step Interval	60 seconds
Solution Technique	Low order, fast algorithm
	Minimum time step: 0.01 s
	Maximum time step: 120 s
	Critical Courant number: 0.8
Enable Flood and Dry	Drying depth* 0.01 m
	Flooding depth* 0.05 m
	Wetting depth* 0.1 m
Initial Surface Level	45 m
Eddy Viscosity	Smagorinsky formulation, Constant 0.28
Resistance	Manning number. Constant value 18

*Note:
To maintain numeric stability in flooding and drying simulations, the model uses a different water depth for adding and removing a cell from computations:

- Drying depth - minimum water depth allowed in a point before it is taken out of
- Flooding depth - water depth at which the point will be reentered into the
- Wetting depth - When the water depth is more wetting depth, the cell is included in computations

6.5.3.2 2DFM Mud Transport (MT)

As with the 2DFM HD module, there were no sediment sampling stations suitable for use in calibration between Aken and Barby. Therefore, calibration was achieved though qualitative rather than quantitative methods. Measured values of annual accumulation in groyne fields, between 1.5 and 4 cm per year, were used to as a guide to calibrate sediment accumulation (Brügmann, 1995; Schwartz, 2006). Seventeen groyne fields were selected at random from within the modeled area and sediment accumulation was recorded over three simulation periods representing MNW, MQ and MHW at the gauging station Aken. The dates representing these discharge benchmarks are: 7/28/1999-8/10/1999, 10/29/1996-11/11/1996 and 3/15/2000-3/28/2000, respectively. The five locations for used groyne fields are identified in Figure 32.

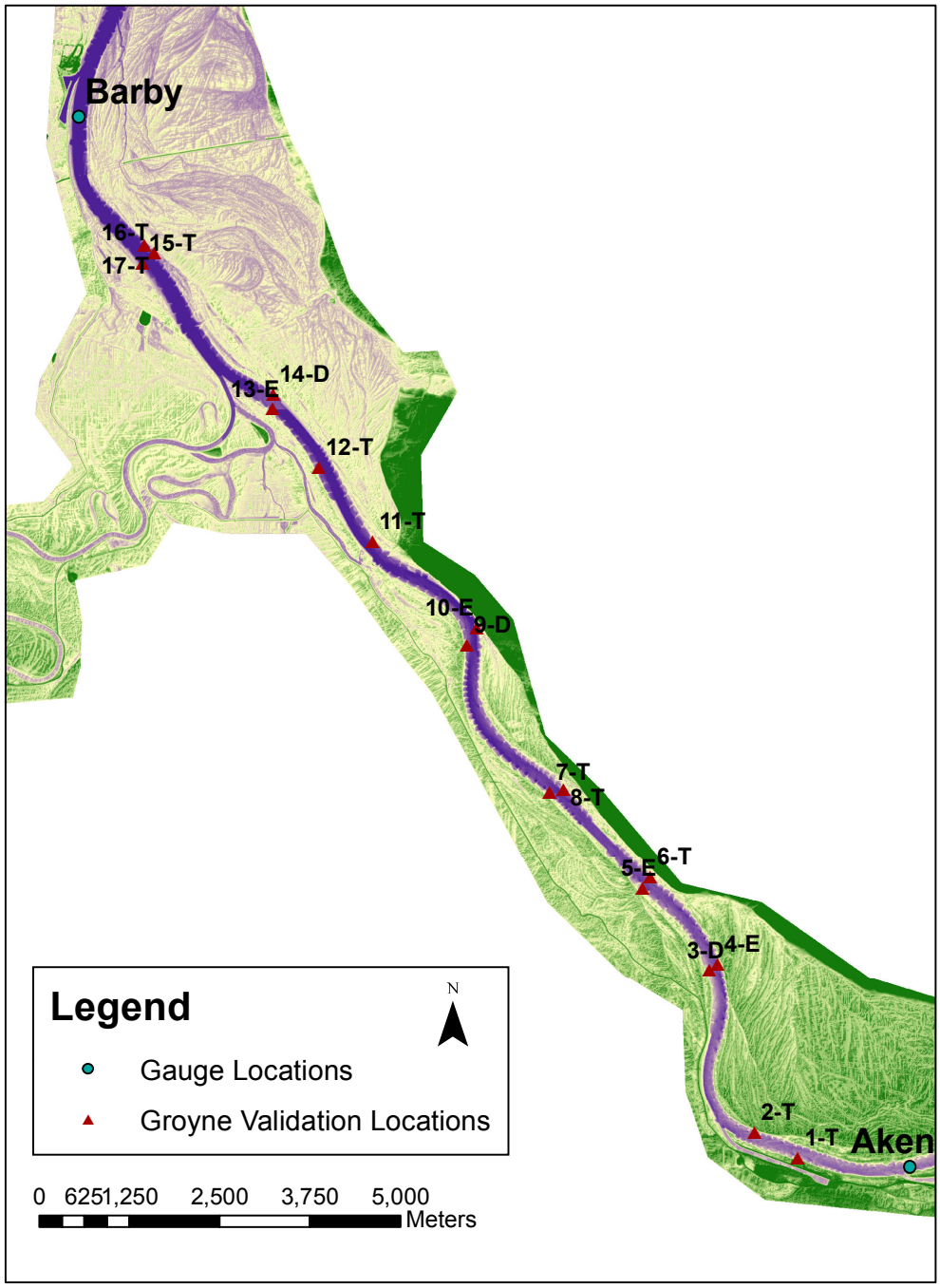

Figure 32. 17 groyne fields used for calibration of the 2DFM MT Module

Using the values from (Brügmann, 1995; Schwartz, 2006) and given that the simulation period is two weeks, net accumulation in groyne fields is expected to be between 0.058 and 0.15 cm. It

is important to keep in mind that these values originate from small studies from a limited number of groyne fields, and do not take into account if the groyne is on the depositional side of the river, where sediment accumulation would be expected, or erosional side of the river, where sediment erosion and/or less accumulation is expected. The MQ scenario was considered most useful for calibration since the values from were taken from a more 'average' time period, but the results of all scenarios are presented (Table 25). The values were within the expected range, but it should be noted that accumulation is may vary highly, depending on exactly where it is measured. Additionally, the model simulation was visually inspected to ensure there were no spatial discontinuities between groynes and main channel.

Table 25. Results of the 2DFM MT calibration

	Fluvial Process[1]	Observed Data: Average Monthly Sediment Accumulation[2] (cm)			Coordinates (GRS 1980 Transverse Mercator)	
Point	Erosional,	MNW	HQ	MHW	Y	X
1-D	Depositional	1.17	0.038	-0.05	3295968.44	5749615.27
2-T	Transport	0.392	0.054	-0.18	3295367.11	5749971.66
3-D	Depositional	0.001	0.026	-0.01	3294741.29	5752217.66
4-E	Erosion	<0.001	0.061	-0.05	3294862.51	5752302.31
5-E	Erosion	<0.001	0.029	0.08	3293821.76	5753355.68
6-T	Transport	<0.001	-0.019	-0.03	3293925.83	5753513.37
7-T	Transport	<0.001	0.002	0.01	3292525.55	5754686.58
8-T	Transport	0.02	-0.026	0.16	3292723.38	5754722.20
9-D	Depositional	<0.001	0.019	-0.09	3291390.18	5756733.39
10-E	Erosion	<0.001	0.035	0.08	3291522.51	5756971.10
11-T	Transport	<0.001	0.004	-0.01	3290081.36	5758162.06
12-T	Transport	0.003	0.004	-0.01	3289335.51	5759191.75
13-E	Erosion	0.003	-0.001	0.00	3288693.69	5760003.87
14-D	Depositional	1.1	0.001	0.02	3288700.00	5760212.02
15-T	Transport	0.16	0.008	0.08	3286892.87	5762034.91
16-T	Transport	0.08	0.042	0.01	3287050.56	5762167.37
17-T	Transport	0.14	0.016	0.00	3286918.25	5762270.19
	Average	0.30	0.038	0.002		

Notes:

1. Assumed, based on the DEM
2. The dates of the MNW, MQ and MHW are as follows: 7/28/1999-8/10/1999, 10/29/1996-11/11/1996 and 3/15/2000-3/28/2000, respectively

6.6 Model Validation

The simple, floodplain, and 2DFM models were validated by comparing model output to measured gauge data between 1/1/2007 and 12/31/2009. Results of the validation for all three models are detailed below.

6.6.1 Simple Model

The 1D HD model was validated between 1/1/2007 through 12/31/2009. The AD, and HCB simple models were validated between 1/1/2007 through 5/01/2009, since that the suspended sediment database. The HD model was calibrated at Barby, the AD model at Torgau (for reasons described in Section 5.5.1). The HCB Model was validated for 6 months (due to long run times) between 1/1/2007 and 6/1/2007 at Dommitzsch. Figure 33 and Figure 34 show the model output and measured values at the validation station for the HD and AD models, respectively. Table 26 presents validation statistics for the AD, HD, and xenobiotics modules.

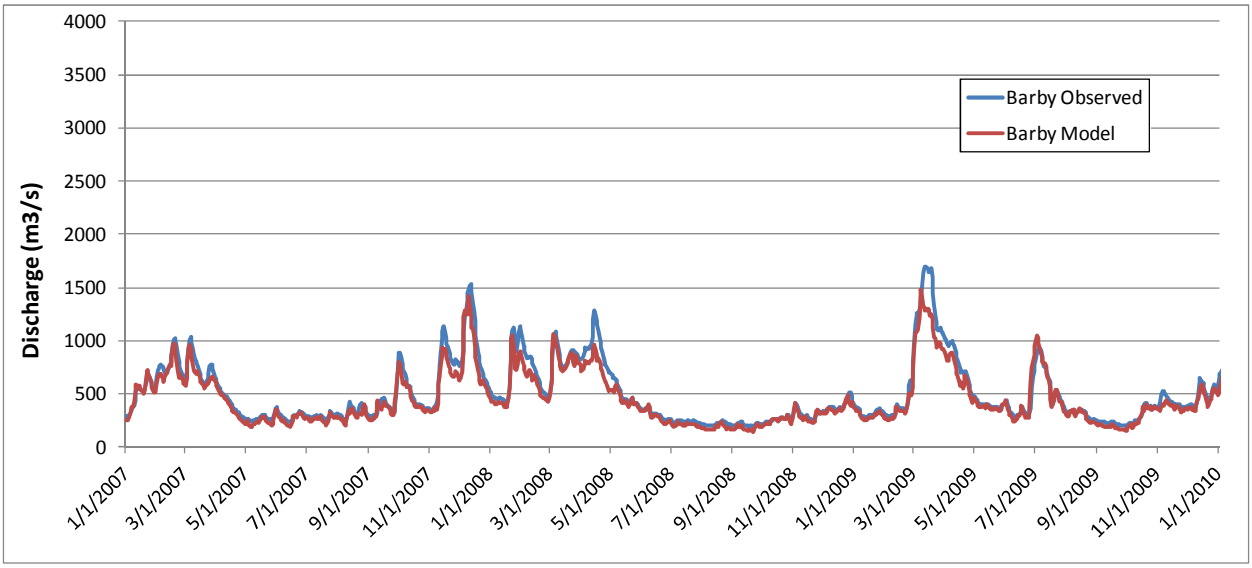

Figure 33. HD simple model validation: 1/1/2007 through 12/31/2009

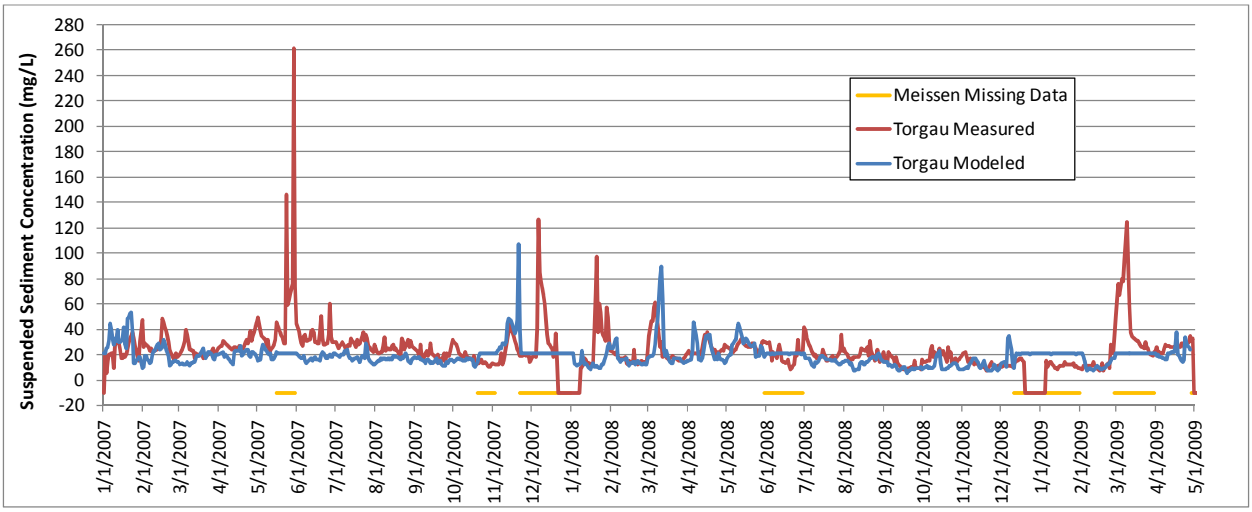

Figure 34. AD simple model validation: 1/1/2007 through 5/01/2009.
Data missing from either the upstream boundary (Meissen) or from the validation station (Torgau) are shown as "-10"

Table 26. Calibration and validation statistics for the 1D 'simple' model

	Nash-Sutcliff Efficiency		R^2	
Module	Calibration	Validation	Calibration	Validation
HD	0.93	0.92	0.94	
AD[1]	0.12	0.09	0.19	0.16
Xenobiotics (HCB)	0.08	0.08		

Note:
1: Missing daily data excluded from Nash-Sutcliff and R^2 calculations

The HD model shows good agreement between simulated and measured results, (Figure 21) particularly during low to moderate flow situations; the validation becomes less accurate in some high water situations since flow can exceed bankfull widths and different actual roughness coefficients are likely, particularly when interactions with groyne fields occur. The largest deviation between modeled and observed flow occurs during a two-week high water period which occurred in March, 2009, but the errors do not persist for an extended period of time. Since NSE for the validation is almost identical to the NSE for the calibration (Table 26), the validation statistics and assessment of graphical results were assumed to be satisfactory.

There is good agreement between the simulated and measured values of suspended sediment for the time period 1/1/2007 through 5/1/2009. A significant issue in the validation is that a combined total of 23% of the data are missing from either the upstream boundary (Meissen) or the validation station (Torgau). In these, the missing data from Meissen or Torgau make a it impossible to directly compare measured and modeled data. Unfortunately, the data gaps occur during many of the peaks in SSC (e.g. 5/30/2007, 12/6/2007, and 3/9/2009). As with the calibration, these missing data somewhat impede model validation. However, the modeled data is frequently of the correct magnitude, and the moderate SSC closely mimic what is seen in the measured data. As shown in Figure 34, some peaks in measured SSC accurately simulated (i.e. 3/11/2008), while some are not (i.e. 1/21/2009). For these data, the NSE for the validation period is somewhat lower than is seen in the calibration period, likely due to the preponderance of missing data. Overall, validation statistics and assessment of graphical results for SSC were found to be satisfactory. .

6.6.2 Floodplain Model

Given the fact that the floodplain and simple models were identical, with the exception of the floodplain branches, no additional validation was performed on the floodplain model. Additionally, since no additional data were available for validation of movement of water, suspended sediment, or HCB on the floodplains, a comparison with simulated data would not provide any additional information. However, as described in Section 6.5.2, the floodplain model was previously calibrated using floodplain inundation maps.

6.7 1D Suspended Sediment Package

In total, four scenarios were used to evaluate suspended sediment transport times downstream of Dresden; MNQ, MQ, MHQ and the March, 2006 flooding. Figure 35 illustrates the results from the MHQ scenario, as an example. As explained in Section 5.6, suspend sediment transport times were calculated as the time for the concentration peak to travel between to various locations (Dreden to Torgau, Dresden to Aken, etc.). Results from this analysis are summarized in Table 27.

Results indicate that suspended sediment velocities range between 0.78 m/s and 2.8 m/s for the MNQ and 2006 discharge scenarios, respectively. Validating these velocities directly is difficult given the lack of comparable field data. However, it is possible to provide context to the simulated values by comparing them to published Elbe flow velocities. For example, at discharges of 1,500 m^3/s and 3,000 m^3/s at Dresden, the average flow velocity is 1.6 m/s and 2.10 m/s, respectively (IKSE, 2004). Results of suspended sediment simulations for discharges of 1,118 m^3/s and 1523 m^3/s in this study yielded average suspended sediment travel velocities of 2.0 m/s and 2.8 m/s. These simulated suspended sediment flow velocities are 25 and 33.5 percent larger than the published flow velocities. Generally, the expectation would be that the velocity of the flood wave exceeds the velocity of the suspended sediment wave (Bull, 1997) and the text that follows provides an discussion of the implications of these results.

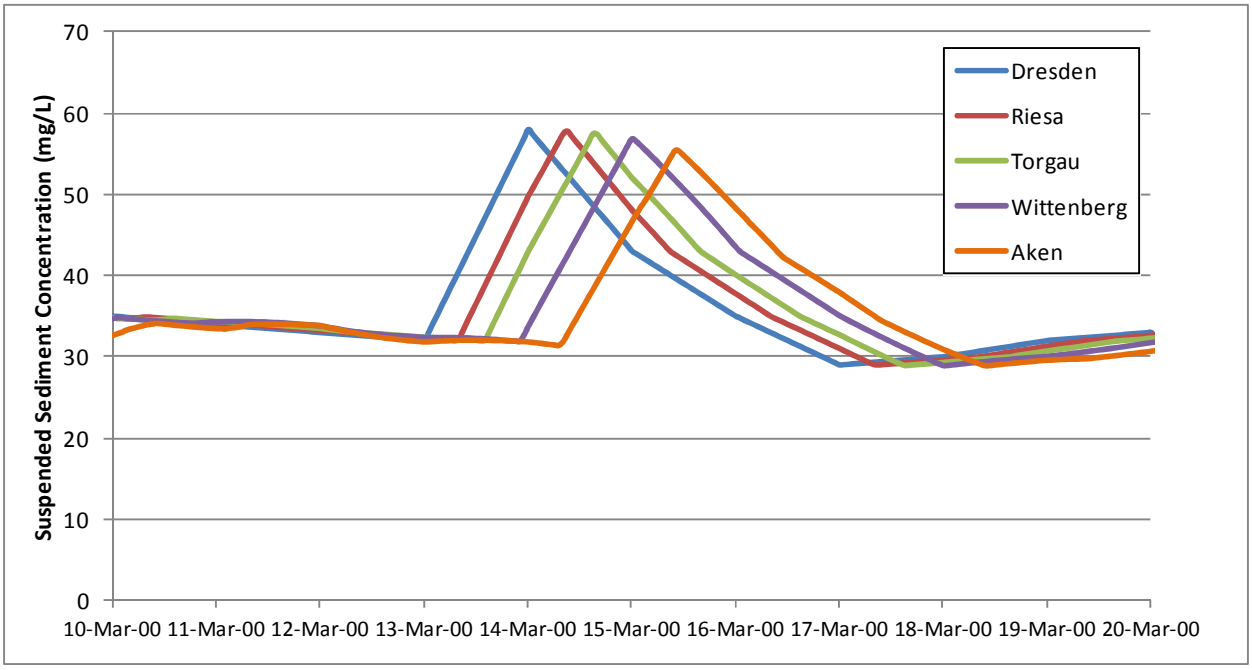

Figure 35. Modeled suspended sediment transport at Dresden during the March, 2006 flood.

A key question from these results is whether the simulated values are representative of actual field conditions or are a result of model variability and/or error. It is important to keep in mind that the published flow velocities reproduced above are not necessarily from the peak of the flood wave. The suspended sediment velocities do, however, represent conditions of peak SSC,

when velocities are likely to be largest, which may partially explain why the SSC velocities are higher. Attempts to compare modeled results to observed field data were unsuccessful due to the daily resolution of the field data; a finer (i.e. hourly) resolution is required to accurately track the suspended sediment wave as it travels downstream. In this 1D model, the primary force driving the transport of suspended sediment transport is discharge. Variables such as sediment sources and bank erosion are not parameterized in the model. Given these factors, and due to the high variability in both measured and modeled SSC, it is difficult to determine the validity of the simulated sediment travel times. In particular, a quantification of the variability of in-river suspended sediment measurements would be particularly useful to help understand the range of expected variability in modeled results. If this variance is, for example, approximately equivalent to 25% of the measured SSC, then the simulated velocity results likely represent an accurate simulation of field conditions.

Table 27. Sediment travel times under varying discharge scenarios

Discharge Scenario (Dresden)	Scenario Average Discharge (m^3/s)	Simulation Period	Sediment Travel Time, Hours from Dresden (River Km)				Average Suspended Sediment Travel Velocity (m/s)
			Riesa (108.4)	Torgau (156.6)	Wittenberg (214.1)	Aken (274.8)	
MNQ (96 m^3/s)	99 +/- 8.3	8/2/2003-8/15/2003	21	35	67	90	0.78
MQ (319 m^3/s)	396 +/- 101.8	7/16/1996-7/29/1996	13	25	36	51	1.4
MHQ (1610 m^3/s)	1118 +/- 330.8	3/6/2000-3/26/2000	9	15	24	36	2.0
High Water: 2006	1523 +/- 741.8	3/26/2006-4/27/2006	6	11	18	26	2.8

6.8 Impact Analysis: Comparison of 2DFM Model and 1D AD Model

The objective of the impact analysis is to compare results of the 2DFM and 1D AD simulations to determine if the groyne fields have a significant effect on the transport time of cohesive sediments. As discussed in Section 5.8, this was accomplished by comparing the results of the two models over two-week time periods representing the MLQ, MQ and MHQ between Aken (km 274.7) and Barby (km 294.8). For clarity, these simulations, used to evaluate the impact of the groynes, are referred to as the "impact analysis".

Two important issues had to be resolved before the impact analysis could be conducted. First the additional dimension in the 2D model, compared to the 1D, required that additional parameters are needed to govern transport of cohesive sediments, thus there are several assumptions that had be made to compare the two models. Appendix B details the input parameters for both models. The obvious difference between the two models is the dimensionality of the models, and the more complete picture of the Elbe River bottom, banks, and groyne fields captured by the 2D model. In addition to the dimension-related differences in input parameters, another issue was determining how to setup boundary conditions for hydrodynamic and suspended sediment in the 2DFM model. The alternatives was to use either observed discharge and SSC measured at the Aken and Barby gauges, or to use the output from the 1D 'simple' model directly as input to the 2DFM model. While the discharge differences between the observed and modeled data were generally minor, differences in SSC between the two data sets were sometimes significant, due primarily to the expected heterogeneity in SSC. Thus, it was decided to use the discharge and SSC output from the 1D simple model at Aken and Barby as boundary conditions for the 2DFM_Impact model. While this dataset had the disadvantage to being simulated rather than actual measured data, it allowed for the most direct comparison possible between the two models, and thus the most accurate assessment of the impact of the groyne fields.

The impact analysis was conducted by selecting two, two-week simulation periods where the average discharge within this two week period was equivalent to the discharge scenario's benchmark. These periods are henceforth referred to as the simulation periods. In both the

1D and 2DFM models, three lateral cross-sections were drawn across the Elbe. These cross-sections are all located upstream of the confluence with the Saale so that viability in the input doesn't affect results of the impact analysis. The models were both run over the simulation periods and the cumulative mass of sediment that passes through the cross-section was recorded. The average percent difference for each of the discharge scenarios was then recorded. The results of this comparison are shown in Table 28.

Results indicate that the average percent difference for the MNW, MQ, and MHW scenarios is 13.71%, 14.94% and 3.23%, respectively. These results suggest that groyne fields have a significant impact on sediment transport during low and average water conditions, but a very low impact during high water conditions. During high water conditions, groynes are commonly over-topped and the high kinetic energy of the discharge precludes the groyne field from trapping sediment in groyne fields. Resuspension and remobilization of cohesive, consolidated bottom sediments within the groyne fields is also more likely to occur during high water events. Deposition and accumulation of fine sediment is most likely during low and average discharge conditions.

The uncertainty in these calculations can be caused by errors in model parameter assumptions, boundary conditions or in model setup. The standard deviation of the average difference between the 1D and 2D models gives the most quantitative representation of uncertainty. The standard deviation for the MNW and MQ simulations represent approximately 40% of the average difference between the two models. The standard deviation for the MHW simulation represents approximately 80% of the average difference between the two models. While the variability in average difference may be due to multiple factors, including discharge fluctuations (rising vs. falling limb of the hydrograph) and sediment loads under each scenario, and the nature of the sediment load (capacity vs. non-capacity flows), the standard deviation from all three scenarios is a significant. This indicates that while these estimates of percent difference are a useful first step in determining the role of groyne fields, additional work is required to accurately predict the impact of groynes under various hydrologic conditions. Additional discussion of model uncertainty and results are provided in Sections 7.2 and 8.3, respectively.

Table 28. Results of the impact analysis: 1D vs 2D sediment transport times

Discharge Scenario	Scenario Discharge (m3/s)	Simulation Period	Cross-Section	14-dayLoad, 1D Simple Model (ton/14d)	14-day load, 2DFM Model (ton/14 day)	Percent Difference	Average	StDev
MNW	168	7/28/1999-8/10/1999	A	5,224	4,599	13.59%		
			B	6,678	5,426	23.08%		
			C	5,207	4,515	15.32%		
MNW	168	6/13/2000-6/26/2000	A	5,209	4,867	7.04%		
			B	6,802	5,884	15.61%	13.71%	
			C	5,169	4,803	7.61%	+/-5.63%	5.63
MQ	436	10/29/1996-11/11/1996	A	11,902	10,016	18.83%		
			B	17,254	15,447	11.70%		
			C	11,880	10,768	10.33%		
MQ	436	3/7/2001-3/20/2001	A	8,451	7,589	11.35%		
			B	11,800	9,270	27.30%	14.94%	
			C	8,453	7,675	10.14%	+/-6.86%	6.86
MHQ	1851	3/15/2000-3/28/2000	A	51,580	49,609	3.97%		
			B	64,740	62,109	4.24%		
			C	51,405	50,802	1.19%		
MHQ	1851	3/24/2006-4/6/2006	A	42,670	41,083	3.86%		
			B	50,024	50,417	-0.78%	3.23%	
			C	42,977	40,213	6.87%	+/-2.66%	2.66

6.9 Transport and Accumulation on Floodplains

Simulations were run for all time periods between 1996 and 2008 when discharge at Dresden or Magdeburg approached or exceeded MHQ (Figure 2 and Figure 3). Simulation periods were selected graphically for each high water event, with the simulation starting well before the peak of the flood wave to ensure for adequate travel time between Dresden and Magdeburg, as for effects such as hysteresis to be appropriately modeled. These nine simulation periods are listed in Table 29. For ease of reference, simulation flood was assigned a 'Reference Date'; equivalent to the month and year when the simulation was started (i.e. a simulation starting in 3/1/1999 has the reference date of '3/1999').

Table 29. Simulaton periods for the floodplain model

Simulation Reference Date	Days above MHQ (Dresden)	Days above MHQ (Magdeburg)	Simulation Start	Simulation End
10/1998	1	5	10/30/1998	11/19/1998
3/1999	4	9	3/1/1999	3/19/1999
3/2000	3	16	3/6/2000	4/13/2000
1/2002	3	11	1/22/2002	3/15/2002
8/2002	8	11	8/9/2002	8/31/2002
12/2002	5	15	12/31/2002	1/25/2003
3/2005	0	6	3/17/2005	4/9/2005
3/2006	12	16	3/26/2006	5/8/2006
1/2011	5	18	1/5/2011	1/27/2011

Simulations were run for the nine high water periods, and the mass of both cohesive sediment and HCB that accumulated and was transported over each floodplain branch saved (in grams). Since each connector channel had three cross-sections, one at the beginning (generally in the Elbe, parallel to flow), one in the middle which acted as a weir, and one at the end adjacent to the floodplain channel, accumulation was measured as model output at this third weir. As described in Section 6.5.2. Since the total area of the modeled floodplain is known (337 km^2), it was then possible to calculate the mass per unit area of cohesive sediment and sediment-bound HCB.

The 2011 flood calculations required a number of assumptions due to significant missing data from the HCB dataset for the Rosenburg and Magdeburg stations. In particular, the suspended sediment-sorbed HCB concentration data from the Saale (Rosenburg station) has ten month gap through much of winter, 2011. The Magdeburg station has a data gap between October, 2010 and March, 2011. To establish model boundary conditions, the Saale and Magdeburg data were interpolated between available data. This method likely underestimates the HCB concentration at these locations, but no other feasible option for substituting the data was found.

Unfortunately, significant difficulty was encountered with the suspended sediment and HCB components of the floodplain model. Results are presented below, but there is considerable uncertainty in the results due to instabilities in the floodplain model output, as identified by negative values, large mass errors, and implausible results near the downstream model boundary. Significant time and effort was expended to try and resolve these issues, but no reasonable solution was found. Results are provided below, but it should be noted that there is significant uncertainty in the results of the floodplain modeling. In order to quantify this uncertainty, a theoretical calculation with the objective of quantifying floodplain accumulation is also presented. These calculations are based on the observation (unpublished) that 20-30% of the annual load of suspended sediment travels downstream during a flood event. Thus, 25% of the measured annual load of suspended sediment and HCB at Zehren (the upstream model boundary) was compared to the modeled values. These calculations are intended to provide context and a potential upper bound to simulated values. In addition, potential reasons for the modeling difficulties are discussed further in Section 8.3.

6.9.1 Transport and Accumulation of Cohesive Sediment on Floodplains

Results of model simulations to estimate the mass of suspended sediment that accumulates on floodplains are shown in Table 30. Results are shown as the total mass of suspended sediment accumulated on the floodplain divided by the total area of the modeled floodplain. Results range between 2.1 g/m^2 for the 3/1999 flood and 1217.5 g/m^2 for the August, 2002 flood. It

should, however, be noted that results from the August, 2002 flood may have accuracy issues due to the physical damage done to flow control structures by the flood.

The cumulative deposition of cohesive material from the nine floods amounts to 2.9 kg/m^2. To place this value in context, if topsoil is assumed to have a density of 1 g/cm^3 and a soil surface layer is 5 to 10 cm deep, then there the average surface density of soil is 50 to 100 kg/m^2. The cumulative deposition from the eight floods then represents 2.9% to 5.6% of the soil that is already *in situ.* It should also be noted that even though the increased roughness of the floodplain is taken into account in floodplain modeling, there are several processes not accounted for in this calculation, including the action of wind and rain during storms, seasonal variability in floodplain roughness, and overbank flooding from tributaries.

Table 30. Torgau-Magdeburg: Accumulated sediment on floodplain branches

Flood Identifier	Days above MHQ: Dresden	Days above MHQ: Magdeburg	Simulation Start	Simulation End	Torgau-Magdeburg: modeled accumulated Sediment on Floodplain (g/m^2)	25% of Annual Suspended Sediment Load at Zehren (g/m^2)
10/1998	1	5	10/30/1998	11/19/1998	14.4	133.5
3/1999	4	9	3/1/1999	3/19/1999	2.1	100.9
3/2000	3	16	3/6/2000	4/13/2000	281.0	66.6
1/2002	3	11	1/22/2002	3/15/2002	204.4	347.2[1]
8/2002	8	11	8/9/2002	8/31/2002	1217.5	
12/2002	5	15	12/31/2002	1/25/2003	303.6	
3/2005	0	6	3/17/2005	4/9/2005	98.5	182.5
3/2006	12	16	3/26/2006	5/8/2006	666.6	362.8[2]
1/2011	5	18	1/5/2011	1/27/2011	160.3	Data N/A
Sum					2948.4	

Note:
1. Suspended sediment loads are estimated on an annual basis, so this calculation could not differentiate between flood events within one year
2. The Zehren sampling station was out of commission for seven months in 2006, resulting in an artificially low load and thus an implausible result.

The results of calculations of 25% of the Zehren load are also summarized in Table 30. In general, model estimates of floodplain accumulation are within one order of magnitude of the load

difference estimates. Modeled suspended sediment loads from the first two floods (10/1998 and 3/1999) are 89 and 98% less than the calculated values, respectively, while the 3/2000 flood is 76% more than calculated values. The simulated loads for the 3/2005 flood are 46% less than calculated values. All other floods (1/2002, 8/2002, 12/2002, 3/2006, and 1/2011) are difficult to compare due to the sample collection periods or incomplete data records.

Published sediment load (SL) values from Kruger et al. (2005) and Baborowski et al. (2007) were used to provide context to the results shown in Table 30. Both authors used artificial lawn mats to measure sediment accumulation following high water events at the Schönberg Deich (km 435 to 440). The Schönberg Deich is located more than 100 km downstream the area focused on in this study, but as these are the only published sediment load values from Elbe floodplains; they are reproduced here for comparison with modeled results. Kruger et al. (2005) measured accumulation of fine sediments over five time periods; spring 1997, autumn and winter 1998/1999, summer 2002, summer and winter 2002/2003 and spring 2003 at four types of locations; groyne edge, flood channel and depressions and plateau areas. Results from Kruger et al. (2005) are reproduced in Table 31. Baborowski et al. (2007) found between 150 and 550 g/m^2 (dw) of sediment accumulated on lawn mats at various locations following the 2005 flooding. Sediment load measurements from both authors range between 70 to 8321 g/m^2 (dw), depending on discharge conditions and sampling location. Generally, the most deposition occurred at groyne edges and the least on high-lying plateau areas, where flood waters are least likely to reach.

Table 31. Sediment load in g/m^2 in the floodplain near Schönberg Deich
Kruger et al. (2005)

High water	Spring 1997	Autumn/ winter 1998/1999	Summer 2002	Summer/ winter** 2002/ 2003	Spring 2003
Maximum water discharge rate (m^3/s)	1800	2360	3800	3260	1300
SL at groyne edge (0.4 m MW)	3810	8321	1485	nsl	127
SL in flood channel (0.4 m MW)	204	242	nsl	405	70
SL in depression (0.7 m MW)	298	397	nsl	502	78
SL on plateau area (1.5 m MW)	nsl	nsl	220	nsl	nsl

Note:
*nsl: no sediment load
** Positions flood channel and depression were permanent flooded from summer 2002 until winter 2002/2003; for this reason separate measurements of sedimentation rates were impossible

A direct comparison between the results from this study and the work of Kruger et al. (2005) and Baborowski et al. (2007) is complicated by the different locations and time periods used for sampling and modeling. However, a broad comparison shows that sediment loads are generally of similar magnitude. For example, results from Kruger et al. (2005) indicate sediment loads of between 220 and 1485 g/m^2 coincident with the August, 2002 flooding. Modeling results for this time period (August, 2002 flood) are 1218 g/m^2, within the range of the values measured by Kruger et al. (2005). This flood is, of course, not ideal for validation purposes due to the physical damage to flood control structures not included in model simulations. Kruger et al. (2005) also reports sediment loads of between 397 and 8321 g/m^2 in autumn/winter 1998/1999. Model simulations for the 10/1998 and 3/1999 floods amount to sediment loads of 16 g/m^2, significantly lower than the measured values. Differences may be due to the location of the flooding (upstream vs. downstream), position of sampling mats, or the duration of flooding. In particular, a review of the data shows that the 2002 flooding appears to have originated more upstream in the basin than the 10/1998 and 3/1999 floods. Namely, the Mulde and Saale peak discharges were higher in 1998 and 1999 than they were during the 2002 flooding. Thus, the location of the flooding may be the main cause for the varying orders of magnitude between study results and published results.

6.9.2 Transport and Accumulation of Sediment-Bound HCB on Floodplains

Results of model simulations to estimate the volume of sediment-bound HCB that accumulates on floodplains are shown in Table 32. Results are shown as the total mass of HCB accumulated on the floodplain divided by the total area of the modeled floodplain. Results range between 0.067 µg/m^2 for the 10/1998 flood and 8.384 µg/m^2 for the August, 2002 flood. It should, however, be noted that results from the August, 2002 flood may have accuracy issues due to the physical damage done to flow control structures by the flood.

The cumulative deposition of sediment-sorbed HCB from the nine flood amounts to 19.38 µg/m^2. To better understand the implications the results, the cumulative HCB load was converted to a concentration; assuming a soil density of 1 g/cm^3 and only the top layer of soil (1cm), there is 10 kg of soil per m^2. This yields 16.827 µg HCB per 10 kg soil, or a HCB concentration 1.6827 µg/kg.

Table 32. Torgau-Magdeburg: Accumulated HCB on floodplain branches (µg/m^2)

Flood Identifier	Days above MHQ: Dresden	Days above MHQ: Magdeburg	Simulation Start	Simulation End	Torgau-Magdeburg: Accumulated HCB on Floodplain (µg/m^2)	25% of Annual HCB Load at Zehren (g/m^2)
10/1998	1	5	10/30/1998	11/19/1998	0.067	29
3/1999	4	9	3/1/1999	3/19/1999	0.0134	12.8
3/2000	3	16	3/6/2000	4/13/2000	2.145	11.0
1/2002	3	11	1/22/2002	3/15/2002	2.096	26.5[1]
8/2002	8	11	8/9/2002	8/31/2002	8.384	
12/2002	5	15	12/31/2002	1/25/2003	0.591	
3/2005	0	6	3/17/2005	4/9/2005	0.513	7.4
3/2006	12	16	3/26/2006	5/8/2006	3.018	4.2[2]
1/2011	5	18	1/5/2011	1/27/2011	2.557	Data N/A
Sum					19.38	

Note:

1. Suspended sediment loads are estimated on an annual basis, so this calculation could not differentiate between flood events within one year

2. The Zehren sampling station was out of commission for seven months in 2006, resulting in an artificially low load and thus an implausible result.

The results of calculations of 25% of the Zehren load are also summarized in Table 32. All modeled simulated estimates of floodplain HCB accumulation are significantly lower than the calculated estimates. This disparity is explained by the difficulties encountered in floodplain simulations. More details on this issue are provided in Section 8.3.

Published values of HCB accumulation on the floodplains are scarce, but a few literature values reproduced in Table 33. From this table, the floodplain soils (generally sampled from 0 to 10cm), had HCB concentrations ranging from 79 to 2400 µg/kg. A direct comparison between these concentrations and modeling is complicated by the fact that the HCB concentrations shown in Table 33 are composited over depth (10 or more cm) and likely contain older, more contaminated material than what is being deposited by current floods. For example, the values measured by Götz et al., (2007) show a HCB peak corresponding to flooding that occurred in 1959. Additionally, the simulated HCB concentration is the sum of only nine high water events, whereas the published values represent the cumulative deposition over more than 60 years. Like with the flood sediment measurements (Section 6.9.1), the floodplain HCB measurements were also taken approximately 100 km downstream of the study area. However, the published values can still be used to provide context to simulated values. Uncertainty in the simulated values is discussed in Section 7.2.

Table 33. HCB concentrations on Elbe floodplains, from various publications

Location	River km	Matrix	Concentration (µg/kg)	Reference
Pevestorf, downstream of Schnackenburg	485.0	Floodplain soils, 0-10 cm	808	Witter et al., 1998
Schönberg Deich (near Wittenberge)	435-440	Floodplain soils, 0-10 cm	79-96	Kiersch et al., 2010
Schönberg Deich (near Wittenberge)	435-440	Floodplain soils, 0-10 cm	100-321	Witter et al., 2003
Pevestorf, downstream of Schnackenburg	485.0	Floodplain soils, up to 45cm	Max: 2400 (1959)	Götz et al., 2007

7 Uncertainty Evaluation

Uncertainties and errors in model results can be described as the difference between true and measured results. In most cases, the difference between these two values is not known, and thus must be estimated. This document summarizes uncertainty related to results of the 1D simple, 1D floodplain and 2DFM models. This information can be used to assess model reliability and to better understand confidence in model output.

Evaluating and characterizing the transport of cohesive sediment and contaminants in an aquatic system as dynamic and large-scale as the Elbe poses technical challenges that underscore the importance of addressing uncertainty. Variability in natural processes, inadequate information about these processes, and incorrect assumptions made in the absence of sufficient data are the primary contributors to model uncertainty (Loucks and Van Beek, 2005). In the present study, four primary sources of uncertainty were identified:

- Sampling, measurement and analysis of field data; missing data
- Model parameter values
- Model structural and computational errors
- Data interpretation

Each of these sources of uncertainty is discussed in detail in the following sections.

7.1 Sampling, Measurement and Analysis of Field Data

The hydrodynamic, suspended sediment and sediment-bound contaminant concentration data that were used both to establish boundary conditions and to calibrate and validate the model come from reliable, long-term historical databases. The potential of measurement uncertainty to contribute to uncertainty is discussed below for these three matrices. In addition, the significance of uncertainty contributed by either the resolution or static nature of the DEM is discussed.

The discharge and water height gauging data are considered highly reliable, with the notable exception of the August, 2002 flood discharge data (see Section 2.2). These data have accuracy issues due to extensive damage to flood control structures caused by the flooding. As discussed in Section 5.4.2, the SSC data have some moderate uncertainty due both to sampling methods, and the naturally high heterogeneity of SSC. Therefore, the measured values are considered meaningful, but not highly reproducible. There is no systematic collection of parallel samples, so it is difficult to determine the extent of variability and/or uncertainty contributed by SSC to model output. There is, however, a documented systematic error associated with the sampling method; it overestimates suspended concentrations below approximately 20 mg/L and underestimation the actual values at concentrations from starting at approximately 25 mg/L. Due to the high dispersion of the values caused by to the non-constant pore diameter of the Melitta filter used to collect samples, this error cannot be further quantified (Hillebrand, 2012).

The primary sources of uncertainty for the chemical concentration data are the laboratory methods used to calculate sediment chemical concentrations. Sensitivity of these methods is particularly important because of the need to reliably discern between sediments with high, moderate, and low contamination concentrations. Due to the fact that most analytical methods for determining chemical concentrations in sediments are very sensitive, the chemical analyses likely contribute very little uncertainty to model results (MacDonald and Ingersoll, 2003). Uncertainty can also result from storage of sediments if oxidation occurs, or the results of freezing altering the sediment's structure. However, these processes also contribute little uncertainty to overall model output.

For the purposes of model development and the reliable simulation of conveyance of water and suspended sediments, topographic representation is critical to model output. The DEM is a model of the elevation, and errors can occur due to digitization, positional inaccuracy, grid cell resolution, interpolation, and re-sampling procedures. The DEM used for floodplain topography and river bottom bathymetry represents a source of uncertainty due to the fact that it is representative of only the time frame in which the data were collected (2004). It can therefore be considered a static description of an extremely dynamic system. Minor changes

have most certainly occurred to the river bottom elevation and to the floodplains during high water events. However, the true nature and extent of these errors is extremely difficult to quantify given the absence of a more recent DEM dataset. For the purpose of this study, it can be assumed that contributions to total uncertainty are relatively minor due to good data consistency, particularly when compared to higher level data when the DEM is visually inspected.

7.1.1 Missing Data Values

7.1.1.1 Missing Data

Data gaps in both discharge and suspended sediment data contribute to uncertainty in model results. Few data gaps exist in the discharge data, with the notable exception of missing discharge from the Priorau (Mulde) gauge between 8/1/2004 and 11/30/2005 (inclusive). Data substitution methods are discussed Section 5.5.2 but given the relatively high R^2 (0.7841) between the Priorau data and the substitution dataset, only minimal uncertainty can be expected from this data gap.

As detailed in Section 5.4.2, suspended sediment data are generally collected Monday through Friday, and interpolated over the weekends. In addition to the weekend interpolation, there are several week to month long data gaps in the data record. Quantifying the uncertainty contributed by the missing weekend data is straightforward; if two of seven days are missing, from the record, and if no relationship between subsequent days is assumed due to the high heterogeneity of suspended sediment data, this alone could contribute a maximum uncertainty of 28.6% (~30 %) to SSC used at model boundaries. A superficial analysis of Monday through Friday data showed the clear existence of trends, so it is likely that the uncertainty is significantly less that 28.6%. However, exact quantification of the contribution to uncertainty is difficult, and likely depends on the magnitude of the Friday and Monday concentrations, as discussed in Section 7.1.

Similar to the weekend data gaps, quantifying the implications of longer data gaps in the suspended sediment record is difficult. Longer data gaps occur regularly in the suspended

sediment record during December-January, and during high water periods. Section 5.4.2.1 describes how data substitution occurred during two of the high-water periods (8/2002 and 12/2002). Substitution of missing data depended on the availability of data at other stations and whether the missing data occurred during high-water periods. Most of the data gaps were substituted with the average of the sampling station's concentration; with the exception of substituting Torgau for Meissen during the August, 2002 high water period due to data availability. This method, however, is a source of uncertainty when the data gaps fall during high water periods. Two of the data gaps occur during high water periods and are discussed in additional detail below.

7.1.2 Data Sampling and/or Measurement Frequency

Discharge, water height, and SSC data were available on a daily basis, contaminant and concentration data were available as a single concentration representing a multi-week collection period. The monthly contaminant data were ultimately interpolated to both daily and five- minute time steps to be consistent with the other datasets at model boundaries. An interpolation of this sort has the potential to cause uncertainty in HCB-related model results due to the fact that using a single concentration to represent a month may disguise the influence of short-term peaks in contaminant loads. For example, if a short period of high discharge and high suspended sediment occurs during the sampling month, a significant fraction of the contaminant load may arrive during a brief period of time. This 'pulse' is essentially ignored when using a single concentration to represent a month. Further, the nature of interpolating monthly data to minutes has inherent conceptual flaws; extrapolation are generally conducted from larger units of measurements to smaller units of measurements, not the reverse.

7.2 Model parameter values

For the purposes of this study, model parameter values are defined as data used to characterize individual contaminants, sediment/contaminant interactions, or sediment properties. A likely source of uncertainty in model output results from uncertain or imprecise estimates of model

parameter values. Parameter estimates within the model vary from those based on well developed datasets (e.g. K_{oc} and contaminant desorption rates) to those based on loose approximation (e.g. sediment porosity and suspended sediment settling velocity). Parameter approximations result in residual model error, which increases with decreasing parameter knowledge. Further, the increased complexity of the 2DFM model requires more parameters than the 1D model, and thus represents additional sources of error in model output. Uncertainty can also result from imprecise specification of parameters, such as boundary conditions. In addition, while seasonal variability in variables such as organic carbon and biological activity are integrated into the model in an intrinsic manner via suspended sediment and sediment-sorbed HCB concentrations, they are not explicitly addressed by means of model input values. The influence of season on SSC is discussed in additional detail in the Section 6.1.1.

7.2.1.1 Model Structural and Computational Errors

Uncertainty in model results may result from errors in model structures relative to the real system, as well as from approximations made by numerical methods used to simulate the system. Sources of structural and computational errors are varied, and may include: model time-step, the frequency and resolution of cross-sections, the location of floodplain channels, branches, and weirs, as well as any errors in the MIKE software program. Even though steps were taken to minimize any computational or structural error, quantifying their effect is exceedingly difficult. Thus, a qualitative, rather than quantitative summary of some of the errors is necessary. First, model time-step was selected carefully, generally starting with a small time-step, and increasing the time-step in increments. Model output was compared between time-steps, and the largest time step that caused no disruptions to model output, instabilities, or mass errors was selected. The frequency and resolution of cross-sections was carefully considered to maximize the frequency of cross-sections (500m) without affecting model run-times. Cross-sections included a high resolution of point spacing along the x-axis (2 m).

The location of floodplain channels, branches, and weirs in the 1D model represents a moderate source of uncertainty to model output, particularly suspended sediment and HCB concentrations. Even though all attempts were made to place floodplain connector channels at locations were water was likely to leave the Elbe (every 500 to 1000 m), and inundate the floodplain, the nature of the 1D model is that only small stretches of the floodplain are represented in the model. It can be safely assumed that having either fewer or additional floodplain channels could potentially alter model output. Additionally, the weirs located on floodplain channels were setup as one-way valves (i.e. water could only flow outwards to the floodplains). Without this step, any flow that occurred in the opposite direction (i.e. from the floodplain into the Elbe) is signified in model output as negative discharge. This negative discharge was caused by the routing of all floodplain branches to one channel. The high cumulative water height of all floodplain branches often caused backwards or negative flow, in the direction of the Elbe. While not explicitly an issue in the HD model, the negative discharge caused large disruptions to the AD model, so it was necessary for the weirs to function as one-way valves. However, the one-way flow of water, suspended sediments and contaminants could lead to uncertainty in model output. First, water that inundates the floodplains is routed away from the Elbe, along the floodplain branches, and returned to the Elbe just upstream of Magdeburg. This varies, of course from the natural system, where water inundates the floodplains, flow velocity decreases, suspended sediment frequently settles, and water either evaporates or returns to the Elbe once flood waters have subsided. The implications to the model from this routing are twofold; first, since floodplain inundation occurs only during high water, and water is artificially routed away from the Elbe, and return downstream from where it may 'naturally' return, flow is essentially removed from the top of flood peaks. The most significant implication of this is that model results for discharge and SSC during high water may not be spatially accurate. For example, flow may be diverted from the Elbe to the floodplains significantly upstream of where the inundation actually occurs. Due to this diversion, estimates of suspended sediment and HCB mass on floodplains are not highly accurate. For this reason, 1D floodplain model results are presented only as a total for the entire floodplain, rather than results for smaller areas.

Additionally, difficulties with the Ecolab module may contribute to uncertainty in modeled results. This module frequently stalled while running, and required multiple restarts of both the module and the computer running the module. While this may be partially due to the large number of module variables and the related high processing times, it does highlight that there may be unknown issues in the module. Lastly, biological and chemical processes, such as the influence of high summer temperatures and low discharge on phytoplankton growth or reductive dechlorination of HCB are not included in the modeling scenarios. The impact of these processes is difficult to estimate because the many of the processes themselves are poorly understood.

7.3 Data Interpretation

Errors in data interpretation may contribute additional uncertainty to model results. In particular, several assumptions were made in model setup, particularly in the Ecolab module, due to incomplete documentation. Every effort was made to contact the model developers to obtain a better explanation of model parameters and input, but this information was also incomplete or difficult to obtain. In addition, human error in data manipulation, calculations and interpreting model output is possible. Given the nature of these errors, their likelihood and magnitude is difficult to assess.

8 Discussion

This study details a novel and exploratory approach to modeling contaminated sediments in large river basins. The research presented in this thesis focuses on an investigation of the fate and transport of cohesive sediment and sediment sorbed-HCB within the reach of the Middle Elbe River located between Dresden (km 55.6) and Magdeburg (km 326.6), including the left and right floodplains north of Torgau. Integral to this assessment is an evaluation of sediment transport within and between groyne fields, and an assessment of the impact of groyne fields on transport of sediments and sediment-bound contaminants. In addition, a thorough analysis of trends in suspended sediment and HCB loads is detailed. The sections below provide a discussion of the implications of model results, as well as detail key factors that may contribute to observed differences between model simulations and measured results. For ease of readability, a discussion of the results of individual modules (HD, AD and Xenobiotic) is provided in the relevant section of Chapter 6. A discussion of the sediment package simulations is provided in Section 6.7, following presentation of results.

8.1 Trends in Suspended Sediment, Discharge, and HCB

The analysis of SSC at Meissen and Magdeburg shows two clear trends; higher SSC in summer relative to winter, and a long-term decrease in SSC over time, beginning approximately contemporaneously with the August, 2002 flooding. As previously discussed, the seasonal difference is likely caused by seasonal phytoplankton blooms (Section 6.1.1). This is also highlighted by the stronger correlation between discharge and SSC observed in winter than summer. Since phytoplankton growth is regulated by temperature, sunlight and nutrient availability, phytoplankton blooms are likely to cause a weakening of the relationship between sediment and discharge in the summer months (Eppley, 1972; Rhee and Gotham, 1981).

The trend of decreasing SSC over time is consistent with field observations that volumes of fine grained sediment in groyne fields were significantly lower following the August, 2002 flood than before the flood, particularly in the upper reaches of the Elbe. While this observed trend has not been published, numerous anecdotal reports from field survey crews indicate that groyne

fields in the Elbe contained significantly less fine material following large flood events. More specifically, the August, 2002 flood, and potentially other subsequent floods (e.g. 2006) have transported large volumes of suspended material, essentially 'washing out' groyne fields, transporting material downstream and to floodplains, and resulting in less cohesive material being available for transport. Thus, the groyne fields in the Upper Elbe have less fine sediment than groyne fields in the middle and lower Elbe. An additional reason for this change is that the volume of fresh sediment and organic material entering the Elbe has declined since German reunification. Numerous sources of pollution, including municipal, pharmaceutical, agricultural, and industrial all contributed to high contaminant loads previous to 1989, but with German reunification came the closure of industrial facilities and the reconstruction and enlargement of sewage treatment plants (Baborowski et al., 2004; Guhr, 2001, 1995; Lehmann and Rode, 2001). The closure of facilities contributing to pollution and the improvement of wastewater facilities had the collective effect of reducing sediment load to the Elbe.

The analysis of HCB loads at Schmilka and between Schmilka and Schnackenburg identified two important trends. First, there is a strong relationship, on an annual basis, between the HCB loads crossing the Czech/German border and the HCB loads measured in Schnackenburg. From a statistical perspective, there is no numerical difference between the loads at the two locations. Particularly given the moderate uncertainty in the load calculations, the finding that the HCB load 'signal' can be observed at both locations has important implications, namely that remediation or source control on HCB-contaminated material in the Czech Republic would likely cause a relatively rapid and proportional decrease downstream. This finding also suggests that, on an annual basis, the majority of HCB-contaminated suspended sediments are transported within the main stem of the Elbe, and a smaller amount is likely stored in bottom sediments or deposited on floodplains. Resuspension of HCB contaminated sediments and/or higher than average contributions from the Mulde and Saale are the probable cause for years when the HCB loads are higher in Schnackenburg than in Schmilka. With the exception of the 2006 data, the Mulde and Saale HCB loads are low in comparison to the Schmilka loads, so they are unlikely to represent a significant contribution to Schnackenburg loads. However, given the

yearly resolution of the load calculations, it is difficult to identify the exact hydrodynamic conditions that cause annual loads to be higher in either Schmilka or Schnackenburg

Interpretation of the second trend depends which of the two assumptions detailed in Section 6.2 is more likely; if one assumes that HCB rates will continue to decrease at rates consistent with available historical data, then an approximately 90% decrease in HCB loads at both Schmilka and Schnackenburg can be expected by 2020 if no management measures are implemented. Alternately, if one assumes that the loads will continue to behave in a manner consistent with the more recent (2003-2009) data, then it will likely take another extreme high water event of approximately the magnitude of the August, 2002 flood to resuspend significant amounts of contaminated material and transport it downstream. When data are grouped by year (1994-2002 and 2003-2009), future loads cannot be predicted because the recent data do not show a statistically significant decreasing trend. It is difficult to determine which of these assumptions is more appropriate, but given the results of the analysis of long term SSC trends and those discussed below, the latter seems more likely. Once they become available, the 2010 through 2012 HCB load data will hopefully shed further light on this issue.

The rating curves developed at Meissen and Magdeburg have generally low correlations between suspended sediment and discharge, but some patterns do emerge from the analysis. First, the correlation between discharge and SSC is generally stronger at Dresden than at Magdeburg. The two most obvious reasons for this difference are the groyne fields and influence of the Mulde and Saale tributaries. Since there are no groyne fields upstream of Dresden, the relationship between SSC and discharge is less complex at Dresden that it is at Magdeburg. When rating curves are calculated, discharge is used as a convenient proxy for the actual forces that transport sediment, shear stress and stream power. In many rivers, the SSC/discharge relationship is strong enough that a statistically significant rating curve can be developed. However, if the assumed dependence of SSC on the force as water (expressed as discharge) is more complicated due to the changes in turbulence structure caused by bedforms such as groyne fields, then the resulting rating curve is less likely to have a strong correlation coefficient. Additionally, this difference between Dresden and Magdeburg may be due to the

SSC gradient that results from delayed mixing between the Saale and Mulde with the Elbe (Weigold and Baborowski, 2009).

Results of the PCA indicate that the modeled contaminant, HCB, is strongly correlated with several other contaminants, including Chlorbenzene, Di- and Tri-Chlorobenzenes, Pentachlorbenzene, PCB 28, PCB 52, Naphthalen, and 4,4-DDD. This correlation suggests that the contaminants may have similar origins and that results for HCB may be applicable to other contaminants of interest in the Elbe Basin. In addition, work by Heise et al. (2008), identified areas of concern for Elbe contaminants in terms of areas where the substances of concern exceed target values, and the areas of concern for PCBs, DDT and HCB are quite similar; primarily upstream or at the Czech-German border, as well as immediately downstream of the border (i.e. Zehren and Dommitzsch) .

The correlation of the chlorinated benzenes is not surprising, since varying amounts of mono-di-, tri- and tetra-chlorobenzenes as well as penta- and HCB are often produced as the unwanted biproducts of the production of chlorobenzenes. In addition, these isomers can be formed during the metabolism of HCB. The primary source of these HCB and some of the lower chlorinated benzenes is the landfills of the Spolek pro chemickou a hutni (Spolek) company in Chabařovice and Vseborice, both located in the district of Usti nad Labem (Czech Republic). HCB contamination also likely originates in the Spolana landfill in the Czech Republic (Heinisch et al., 2007; UNIDO, n.d.). Both of these sites drain to the Elbe River.

8.2 Accumulation of HCB Deposited on Floodplains in Dairy Cows and Cattle

To determine the biological relevance of HCB deposited on the Elbe floodplains, results of sediment-sorbed HCB on Elbe floodplains were used to estimate the concentration of HCB that could accumulate in the milk of dairy cows or the meat of cattle grazing on Elbe floodplain soils and grasses. Even though there is significant uncertainty in the floodplain results, these calculations are included to provide additional perspective to modeled output.

Because milk and dairy products are key components of human diets and are particularly important for bone growth and children's nutrition (Daniels and Greer, 2008), dairy cows and

beef cattle are excellent target organism for this theoretical exercise. The conceptual model for this calculation assumes conditions following a high water event, where cows grazing on an Elbe floodplain consume grass and plants that have cohesive material adhering to them that has been deposited by receding floodwaters. Note that this analysis is intended only to provide an estimate of possible conditions[4]. The following parameters were used:

- Soil adhering to plants: 200 g soil/kg. The published range is 8 to 260 g/kg and since this exercise is intended to mimic the situation immediately following flooding, the higher end of the range is used (Sheppard, 1995).
- Cow consumption of plant material: 50 to 80 kg plants/day (Bützer, 2006). Area density of grass: Grassland contains: 1 kg grass fresh weight/m^2 (Bützer, 2006). If the upper end of grass consumption is assumed (75 kg plants/day), then cows graze approximately 75 m^2/day of plant material.
- HCB deposition on floodplains: 0.003 mg/m^2 in March, 2006 (from Section 6.9.2)
- Transfer coefficients (Tcos) characterize the transfer relationship between contaminant concentration in fresh weight of animal product (in mg/kg, for example) to the daily intake of contaminant by the animal (in mg/day). Tcos for HCB are 0.02 day/kg for cow's milk, and 0.2 day/kg for cattle meat (Anonymous, 2012).

If the assumption is made that all HCB is deposited on the grass during one flood event, such as from the March, 2006 flood, then 0.003 mg/m^2 HCB would be deposited on the floodplains. Multiplying this by 75 m^2/day yields a value of 0.225 mg HCB taken up per day. Applying the Tcos listed above, the resulting concentration values for HCB with a daily intake of 0.225 mg

[4] Assistance in this analysis was provided by Susanne Heise (Heise, 2013a)

would be 4.5 µg/kg in whole milk and 45 µg/kg in whole cattle meat, assuming a steady state. Taking into account a fat content of 4 % in milk, a calculated HCB concentration of 1.125 mg/(kg fat) in milk would result, which exceeds the German legal HCB concentration limit 0.25 mg/kg fat by a factor of more than 4 (BGbl, 1989). Note that the legal limit is based on the assumption of 2% fat. For beef cattle meat, a fat content of 0.19 is assumed (Anonymous, 2012). Converting the above concentration to mg/(kg fat) would result in 2.3 mg/kg and would therefore exceed the regulatory value of 0.2 mg/kg by one order of magnitude (BGbl, 1989).

These calculations are intended to illustrate a worst case scenario. It should be noted that the Tcos assume a steady state which is reached after at least 60 days, and the scenario in these calculations would represent significantly less time than that. Additionally, these calculations assume that all contaminated material will adhere to plants, which is likely to significantly overestimate actual conditions since much of the soil and organic material will ultimately be washed away by rain or wind.

8.3 Model Results

For this study, 1D, 2D, and quasi-2D models were developed to simulate the hydrodynamics, suspended sediment transport, sediment-sorbed HCB transport, and floodplain deposition of the Elbe River between Dresden and Magdeburg. Additionally, the impacts of groyne fields on sediment transport under various hydrodynamic conditions was estimated. Lastly, the volume of sediment and sediment-bound HCB transported to floodplains during high water events was quantified.

The various modeling approaches developed in this study attempted to adequately resolve the large scale and high spatial variability that occurs in the Elbe between Dresden and Magdeburg, including groyne fields and floodplains of varying width and elevation. According to calibration statistics, the calibration of the various modules was successful to varying degrees; the hydrodynamic components were very successfully calibrated, the suspended sediment less so, and the contaminant transport module showed the poorest correlation between modeled and measured results. This outcome can be explained by both the heterogeneity of the Elbe River

system and the resolution of available data. First, discharge data are generally of high quality and flow can be considered uniform. SSC can vary greatly over small units of space and time, as can contaminant concentrations due to the availability of sediment, the proximity of the contaminant source, and sorption kinetics. Second, high-resolution (i.e. daily) discharge data are available at many locations throughout the Elbe, while the suspended sediment data are available for weekdays with some significant data gaps. Contaminant concentration data are the least available; either bi-monthly or monthly at a few locations throughout the Elbe Basin.

The multiple models (i.e. 1D, 2D, quasi-2D) and modules (i.e. HD, AD, Ecolab) utilized were developed to simulate physical processes occurring at a variety of scales and levels of complexity. Our ability to accurately simultaneously simulate the micro-scale processes occurring in individual groyne fields and transport over hundreds of square kilometers of floodplain is limited by the availability of data, computational power, high natural variability, and the many unknowns in the natural system of the Elbe River.

The sediment package analysis investigated the travel times of the sediment peak under various discharge scenarios and found them to be approximately 5.0 km/hr at MQ and 7.2 km/hr at MHQ. Using these velocities, it would take the 'sediment package' almost four days to travel the approximately 475 km between the Czech Republic and Schnackenburg under MQ, and almost three days under MHQ.

This study has shown that groyne fields can slow down sediment (and thus contaminant) transport approximately 15% over the 20 km reach between Aken and Barby during average hydrodynamic conditions. The implications of this result to sediment and contaminant transport is that during average discharge conditions, a significant component of the mobile cohesive sediment and sediment-sorbed contaminants are slowed down by groynes, and that some fraction of this amount is likely to accumulate in groyne fields. Study results also indicate that sediment retention (and related accumulation) does not occur under high water conditions. This finding is consistent with those previously discussed, that most of the material transported during high water events is carried directly downstream. Thus, effective source

control measures will likely have the immediate effect of decreasing downstream HCB concentrations.

However, much about Elbe River groyne fields remain unknown. Unfortunately, little data currently exists about many of the physical properties of groynes, erosion stability, grain size on banks and in groyne fields, and the impact of groyne form on sediment accumulation. A disparity between modeled and observed data is likely due to the ongoing maintenance of Elbe groyne fields by the waterways administration, which may result in the re-suspension of recently suspended fine material separate from any high water event. Additionally, many of the groyne fields on the Elbe have swampy, wooded backwater areas located between the groyne field and floodplain. The impact of these areas as both sources and sinks for cohesive materials is not included in simulations. Lastly, biological and chemical processes, such as the influence of high summer temperatures and low discharge on phytoplankton growth or reductive dechlorination of HCB are not included in the modeling scenarios. The impact of these processes is difficult to estimate because many of the processes themselves are poorly understood.

Difficulties and instabilities with the floodplain model caused issues with the reliability and interpretability of the floodplain sediment and HCB accumulation results. Development of the floodplain model involved exhaustive trial and error, conducted in consultation with DHI, so the likelihood that the model issues derive from user error is low. Thus, the more likely reason for these errors is that the model is unable to accurately replicate the physical processes occurring on floodplains, due to inadequate equations and/or forcings. Additionally, the added floodplain cross sections may be causing mass balance issues due to flow contractions. The weir and channel setup of the floodplain modeling may lead to issues with outflow concentration of suspended sediments and sediment -sorbed HCB. Lastly, floodwave speed may not be accurately represented as the high water propagates over the floodplains.

While the impacts of climate change are not directly addressed in this study, the recent prevalence of flooding events renders the assessment of the impacts of high water events particularly important to the management and understanding of transport processes within the

Elbe Basin. Even though predictions of climate-mediated impacts on discharge vary, it is likely that temperatures will increase and that the warmer, wetter winters predicted for Northern Europe will lead to decreases in summer discharge, increases in winter discharge, and possible increases in the frequency and magnitude of high water events (Hattermann et al., 2011; Huang et al., 2010; Kundzewicz et al., 2005; Lehner et al., 2006; Zebisch et al., 2005). Combined with the knowledge that three large floods (2002, 2006, and 2011) have occurred in the last ten years, further investigation of the fate and transport of historical contaminants under a variety of discharge scenario is vital to both a better understanding of the river system and achieving the goals established by the WFD.

Model results indicate that high water events have a significant and measurable impact on the load of cohesive sediment and HCB transported to Elbe floodplains. As detailed in Section 8.2, following assumptions consistent with a worse-case scenario, the deposited HCB could end up exceeding dietary standards in the milk and beef of cows and cattle for human consumption. Even though HCB loads continue to decrease within the Elbe Basin, the expected increases in the frequency of high water events caused by climate change could result in continued accumulation of HCB in biologically and ecologically sensitive areas. Regular or flood event based monitoring of soil and grasslands of ruminant grazing areas would provide extremely useful information to provide a more thorough assessment of the ecological and human health risk of floodplain deposits of HCB and related contaminants.

In addition to potentially accumulating in floodplain grazing cattle, there is ample evidence from a recent study (unpublished) that HCB accumulates in the tissue of Elbe fish at concentrations exceeding chronic environmental quality standards (EQS). HCB concentrations measured in the muscle, liver and liver fat of nine bream collected from the Tidal Elbe River, upstream of Hamburg, in November, 2011 exceeded the EQS for biota of 10 µg/kg established by the European Commission (European Commission, 2008; Heise, 2013b). Bream liver HCB concentrations ranged between 17 and 33 µg/kg and muscle concentrations ranged between 6.8 and 15 µg/kg. The highest HCB concentration, 62 µg/kg was measured in liver fat. These results demonstrate HCB continues to pose an active risk to aquatic ecosystems in the Elbe.

8.4 Recommendations and Suggestions for Further Work

Even though the role of sediments in the WFD, which mandates holistic river basin planning, is not currently well defined, the importance of sediments to ecological and environmental health is well documented (Crawford et al., 1994; Power and Chapman, 1992; Rhoads and Germano, 1982; Townsend and Riley, 1999). This study provides additional evidence that HCB originating in the upper reaches of the Elbe River basin has a direct relationship to downstream loads and can accumulate in significant quantities on floodplains following high water events. When these contaminated sediments adhere to plant material, the resulting concentrations in dairy cows and beef cattle can exceed dietary limits. Therefore, an obvious recommendation, which has also been published elsewhere, would be the implementation of source control measures to reduce the supply of HCB-contaminated sediments to the Elbe and Elbe tributaries (Netzband et al., 2002). It is highly likely that effective source control measures would reduce long-term concentrations of HCB and related isomers downstream in the Elbe Basin.

With regard to the physical attributes and processes occurring in and on groynes and floodplains, additional field testing (some of which is currently ongoing) will hopefully provide additional valuable information to validate the existing model and/or to inform the development of additional process-based models. As discussed in model setup and the uncertainty section, there are several key parameters that had to be estimated using literature values and/or suggested model-specific values. In particular, information about erosion stability under various discharge and seasonal conditions would be particularly useful to inform any future modeling efforts. Field testing of the contaminant concentrations on floodplain grasses and in soils following a flood event would be tremendously helpful in validating calculations and modeling conducted in this study.

Lastly, the resolution of the suspended sediment and contaminant databases sometimes present an obstacle to a detailed evaluation of fate and transport. The occasional duplicate or replicate suspended sediment sample could provide valuable information about the temporal and spatial heterogeneity of SSC, and enable more robust statistical comparisons between sampling locations. As discussed previously, key data are often missing during high water

events, and the monthly resolution of the contaminant data sometimes precludes a thorough analysis of individual flood events. Additional highly detailed data from a flood event may help to elucidate the nature of flood driven transport processes.

9 Bibliography

Adams, M.S., Kausch, H., Gaumert, T., Krueger, K., 1996. The effect of the reunification of Germany on the water chemistry and ecology of selected rivers. Environmental Conservation 23, 35–43.

Anderson, R.F., Santschi, P.H., Nyffeler, U.P., Schiff, S.L., 1987. Validating the use of radiotracers as analogs of stable metal behaviour in enclosed aquatic ecosystem experiments. Canadian Journal of Fisheries and Aquatic Sciences 44, 251–259.

Anonymous, 2012. Appendix K: Meat, Milk, and Egg Transfer Coefficients. Technical Support Document for Exposure Assessment and Stochastic Analysis, FINAL. Office of Environmental Health Hazard Assessment. California Environmental Protection Agency., California, USA.

Antweiler, R.C., Taylor, H.E., 2008. Evaluation of Statistical Treatments of Left-Censored Environmental Data using Coincident Uncensored Data Sets: I. Summary Statistics. Environ. Sci. Technol. 42, 3732–3738.

Ariathurai, R., Krone, R.B., 1976. Finite element model for cohesive sediment transport. Journal of the Hydraulics Division 102, 323–338.

Asselman, N.E.M., 2000. Fitting and interpretation of sediment rating curves. Journal of Hydrology 234, 228–248.

Baborowski, M., Bozau, E., 2006. Impact of former mining activities on the uranium distribution in the River Saale (Germany). Applied Geochemistry 21, 1073–1082.

Baborowski, M., Büttner, O., Morgenstern, P., Krüger, F., Lobe, I., Rupp, H., Tümpling, W., 2007. Spatial and temporal variability of sediment deposition on artificial-lawn traps in a floodplain of the River Elbe. Environmental Pollution 148, 770–778.

Baborowski, M., Friese, K., 2004. Behaviour of suspended particulate matter (SPM) and selected trace metals during the 2002 summer flood in the River Elbe (Germany) at Magdeburg monitoring station. Hydrology and Earth System Sciences 8, 135–150.

Baborowski, M., von Tümpling Jr, W., Friese, K., 2004. Behaviour of suspended particulate matter (SPM) and selected trace metals during the 2002 summer flood in the River Elbe (Germany) at Magdeburg monitoring station. Hydrology and Earth System Sciences Discussions 8, 135–150.

Bates, P., Horritt, M., Smith, C., Mason, D., 1997. Integrating remote sensing observations of flood hydrology and hydraulic modelling. Hydrological Processes 11, 1777–1795.

Becker, A., Grünewald, U., 2003. Flood risk in central Europe. Science 300, 1099–1099.

Bergemann, M., 2011. Elbe Sedimentfraktion Daten.

Beuge, P., Greif, A., Hoppe, T., Kluge, A., Klemm, W., Martin, M., Mosler, U., Starke, R., Alfaro, J., Anders, B., 1999. Die Schwermetallsituation im Muldesystem, Bd. 1-3 Freiberg, Hamburg. ISBN 3-924330-21-2.

Bever, A.J., Harris, C.K., Sherwood, C.R., Signell, R.P., 2009. Deposition and flux of sediment from the Po River, Italy: An idealized and wintertime numerical modeling study. Marine Geology 260, 69–80.

BfG, 2012. BfG Sediment Data [WWW Document].

BGbl, 1989. Pflanzenschutzmittel-Höchstmengenverordnung - PHmV (1989) Verordnung über Höchstmengen an Pflanzenschutz- und sonstigen Mitteln sowie anderen Schädlingsbekämpfungsmitteln und Tabakerzeugnissen, Bundesgesetzblatt I:1568.

Bohling, B., 2009. Measurements of threshold values for incipient motion of sediment particles with two different erosion devices. Journal of Marine Systems 75, 330–335.

Brack, W., Kind, T., Schrader, S., Möder, M., Schürmann, G., 2003. Polychlorinated naphthalenes in sediments from the industrial region of Bitterfeld. Environmental Pollution 121, 81–85.

Brügmann, L., 1995. Metals in sediments and suspended matter of the river Elbe. Science of the Total Environment, The 159, 53–65.

Bull, L., 1997. Relative velocities of discharge and sediment waves for the River Severn, UK. Hydrological sciences journal 42, 649–660.

Bundesanstalt für Gewässerkunde, 2009. Flusshydrologische Software (FLYS) - Bundesanstalt für Gewässerkunde. Bundesanstalt für Gewässerkunde.

Buttner, O., Otte-Witte, K., Kruger, F., Meon, G., Rode, M., 2006. Numerical modelling of floodplain hydraulics and suspended sediment transport and deposition at the event scale in the middle river Elbe, Germany. Acta hydrochimica et hydrobiologica 34.

Bützer, P., 2006. DDT in der Nahrungskette.

C. R. C. Catchment Hydrology, 2005. Series on Model Choice: 2.

C. R. C. Catchment Hydrology, C.R.C., 2005. Series on Model Choice: 1. General approaches to modelling and practical issues of model choice.

Cattell, R.B., 1966. The scree test for the number of factors. Multivariate behavioral research 1, 245–276.

Chow, V., 1959. Open channel hydraulics. NY etc.: McGraw-Hill.

Cigizoglu, H.K., Alp, M., 2006. Generalized regression neural network in modelling river sediment yield. Advances in Engineering Software 37, 63–68.

COM(2011)876, 2012. Proposal for a DIRECTIVE OF THE EUROPEAN PARLIAMENT AND OF THE COUNCIL amending Directives 2000/60/EC and 2008/105/EC as regards priority substances in the field of water policy.

Cornelisse, 2009. Elbe settling velocity measurements.

Cornelisse, J.M., 1996. The field pipette withdrawal tube (FIPIWITU). Journal of Sea Research 36, 37–39.

Crawford, D., Bonnevie, N., Gillis, C., Wenning, R., 1994. Historical changes in the ecological health of the Newark Bay Estuary, New Jersey. Ecotoxicology and environmental safety 29, 276–303.

D'Eugenio, J., 2005. Environmental Quality Standards (EQS) Substance Data Sheet: Priority Substance No. 16 Hexachlorobenzene.

Daniels, S.R., Greer, F.R., 2008. Lipid screening and cardiovascular health in childhood. Pediatrics 122, 198–208.

DHI, 2010. MIKE 21 FLOW MODEL FM: Hydrodyanmic Module User Guide.

DHI, 2011. MIKE 11: A modelling system for river and channels. User Guide.

DHI Software Group, 2009. Xenobiotics Template: ECO Lab Scientific Description.

Directive 2000/60/EC, 2000. DIRECTIVE 2000/60/EC OF THE EUROPEAN PARLIAMENT AND OF THE COUNCIL of 23 October 2000. Establishing a framework for Community action in the field of water policy.

DVWK, 1986. Schwebstoffmessungen : DK 556.535.6 Schwebstoff, DK 556.08 (083) Messrichtlinie. Kommissionsvertrieb Paul Parey, Hamburg.

Edelvang, K., Lund-Hansen, L.C., Christiansen, C., Petersen, O.S., Uhrenholdt, T., Laima, M., Alvarez Berastegui, D., 2002. Modelling of suspended matter transport from the Oder River. Journal of Coastal Research 18, 62–74.

Egeler, P., Römbke, J., Meller, M., Knacker, T., Franke, C., Studinger, G., Nagel, R., 1997. Bioaccumulation of lindane and hexachlorobenzene by tubificid sludgeworms (Oligochaeta) under standardised laboratory conditions. Chemosphere 35, 835–852.

Engelhardt, C., Krüger, A., Sukhodolov, A., Nicklisch, A., 2004. A study of phytoplankton spatial distributions, flow structure and characteristics of mixing in a river reach with groynes. Journal of Plankton Research 26, 1351.

EPA, 2002. National Primary Drinking Water Regulations: Technical Factsheet on Hexachlorobenzene (HCB). Technical Fact.

Eppley, R.W., 1972. Temperature and phytoplankton growth in the sea. Fish. Bull 70, 1063–1085.

European Commission, 2008. Directive 2008/105/EC of the European Parliament and of the Council of 16 December 2008 on environmental quality standards in the field of water policy, amending and subsequently repealing Council Directives 82/176. EEC 83, 84–97.

Falconer, R.A., Kozerski, H.-P., 2003. Entry and Deposits of Suspended Particulate Matter in Groyne Fields of the Middle Elbe and its Ecological Relevance. Acta hydrochimica et hydrobiologica 31, 391–399.

FGG Elbe, 2009. Hintergrundpapier zur Ableitung der überregionalen Bewirtschaftungsziele für die Oberflächengewässer im deutschen Teil der Flussgebietseinheit Elbe für den Belastungsschwerpunkt Schadstoffe. FGG Elbe, Magdeburg, Germany.

FGG Elbe, 2012. FGG Elbe Suspended Sediment Data [WWW Document]. URL http://www.fgg-elbe.de/ (accessed 2.22.12).

Google Earth, 2012. Google Earth [WWW Document]. https://maps.google.com/.

Götz, R., Bauer, O.-H., Friesel, P., Herrmann, T., Jantzen, E., Kutzke, M., Lauer, R., Paepke, O., Roch, K., Rohweder, U., Schwartz, R., Sievers, S., Stachel, B., 2007a. Vertical profile of PCDD/Fs, dioxin-like PCBs, other PCBs, PAHs, chlorobenzenes, DDX, HCHs, organotin compounds and chlorinated ethers in dated sediment/soil cores from flood-plains of the river Elbe, Germany. Chemosphere 67, 592–603.

Götz, R., Bauer, O.-H., Friesel, P., Herrmann, T., Jantzen, E., Kutzke, M., Lauer, R., Paepke, O., Roch, K., Rohweder, U., Schwartz, R., Sievers, S., Stachel, B., 2007b. Vertical profile of PCDD/Fs, dioxin-like PCBs, other PCBs, PAHs, chlorobenzenes, DDX, HCHs, organotin compounds and chlorinated ethers in dated sediment/soil cores from flood-plains of the river Elbe, Germany. Chemosphere 67, 592–603.

Götz, R., Bauer, O.H., Friesel, P., Roch, K., 1998a. Organic trace compounds in the water of the River Elbe near Hamburg Part I. Chemosphere 36, 2085–2101.

Götz, R., Bauer, O.H., Friesel, P., Roch, K., 1998b. Organic trace compounds in the water of the River Elbe near Hamburg part II. Chemosphere 36, 2103–2118.

Götz, R., Schumacher, E., Kjeller, L.-O., Bergqvist, P.-A., Rappe, C., 1990. Polychlorierte Dibenzo-p-dioxine (PCDDs) und polychlorierte Dibenzofurane (PCDFs) in Sedimenten und Fischen aus dem Hamburger Hafen. Chemosphere 20, 51–73.

Grabowski, R.C., Droppo, I.G., Wharton, G., 2011. Erodibility of cohesive sediment: The importance of sediment properties. Earth-Science Reviews 105, 101–120.

Guan, W.B., Wolanski, E., Dong, L.X., 1998. Cohesive Sediment Transport in the Jiaojiang River Estuary, China. Estuarine, Coastal and Shelf Science 46, 861–871.

Guhr, H., 1995. Sources of heavy metal pollution in the drainage area of the river Elbe in the former GDR. Heavy Metals in the Environment.

Guhr, H., 2001. Entwicklungen in der Fließgewässerbeschaffenheit in den neuen Bundesländern seit 1990-Elbe-Einzugsgebiet. Aktuelle Probleme der Gewässerverschmutzung 77, 20.

Hattermann, F., Weiland, M., Huang, S., Krysanova, V., Kundzewicz, Z., 2011. Model-Supported Impact Assessment for the Water Sector in Central Germany Under Climate Change—A Case Study. Water Resources Management 25, 3113–3134.

Hayter, E.J., Mehta, A.J., 1986. Modelling cohesive sediment transport in estuarial waters. Applied Mathematical Modelling 10, 294–303.

Heinisch, E., Kettrup, A., Bergheim, W., Wenzel, S., 2007. PERSISTENT CHLORINATED HYDROCARBONS(PCHCS), SOURCE-ORIENTED MONITORING IN AQUATIC MEDIA. 6. STRIKINGLY HIGH CONTAMINATED SITES. Fresenius Environmental Bulletin 16, 1248.

Heise, S., 2013a. HCB- accumulation.

Heise, S., 2013b. Fish and HCB.

Heise, S., Krüger, F., Baborowski, M., Stachel, B., Götz, R., Förstner, U., 2008. Assessment of risks from particle bound substances in the Elbe river basin (in German). Commissioned by Hamburg Port Authority and River Basin Community (FGG) Elbe. Hamburg, Mai 2008, p 349.

Helsel, D.R., 2005. Nondetects and data analysis. Wiley-Interscience.

Hillebrand, G., 2012. Variabilität in Schwebstoffdaten.

Hinkel, J., 1999. Die Ermittlung vegetationsfreier Fl¨achen entlang der Elbeufer aus Luftbildern und ihre Korrelation mit der Flußgeometrie und dem Uferverbau. Technical University, Karlsruhe.

Honeyman, B.D., Santschi, P.H., 1988. Metals in aquatic systems. Environ. Sci. Technol.;(United States) 22.

Horowitz, A.J., 2002. The Use of Sediment Rating Curves for Monitoring Suspended Sediment Concentrations and Fluxes: Issues of Temporal Resolution, Estimation Errors, and Sampling Frequency.

HPA, 2013. . Perspektiven für Hamburg Herzlich willkommen bei der Westerweiterung EUROGATE. URL http://www.westerweiterung.de/ (accessed 2.26.13).

Huang, J., Hilldale, R., Greimann, B., 2006. Cohesive sediment transport. Erosion and sedimentation manual 4–1.

Huang, S., Krysanova, V., Österle, H., Hattermann, F.F., Huang, S., Krysanova, V., Österle, H., Hattermann, F.F., 2010. Simulation of spatiotemporal dynamics of water fluxes in Germany under climate change, Simulation of spatiotemporal dynamics of water fluxes in Germany under climate change. Hydrological Processes, Hydrological Processes 24, 24, 3289, 3289–3306, 3306.

Hurst, S., 2002. Remediating 700 years of Mining in Saxony: A Heritage from Ore Mining Stephanie Hurst, Petra Sehneider'and Günther Meinrath. Mine Water and the Environment 21, 3–6.
IKSE, 2004. Dokumentation des Hochwassers vom August 2002 im Einzugsgebiet der Elbe (Documentation of the August 2002 flood events in the Elbe Basin).
IKSE, 2005. Die Elbe und ihr Einzugsgebiet: Ein geografisch-hydrologischer und wasserwirtschaftlicher Überblick. Internationale Kommission zum Schutz der Elbe, Magdeburg, Germany.
Jepsen, R.A., 2006. Uncertainty in experimental techniques for measuring sediment erodability. Integrated environmental assessment and management 2, 39–43.
Kalin, L., Hantush, M.M., 2003. Evaluation of sediment transport models and comparative application of two watershed models. EPA/600/R-03/139, National Risk Management Research Laboratory, US Environmental Protection Agency, Cincinnati, OH 45268.
Karrasch, B., Mehrens, M., Rosenlöcher, Y., Peters, K., 2001. The Dynamics of phytoplankton, bacteria and heterotrophic flagellates at two banks near Magdeburg in the River Elbe (Germany). Limnologica-Ecology and Management of Inland Waters 31, 93–107.
Kiersch, K., Jandl, G., Meissner, R., Leinweber, P., 2010. Small scale variability of chlorinated POPs in the river Elbe floodplain soils (Germany). Chemosphere 79, 745–753.
Kruger, F., Meissner, R., Grongroft, A., Grunewald, K., 2005. Flood induced heavy metal and arsenic contamination of Elbe River floodplain soils. Acta hydrochimica et hydrobiologica 33.
Kundzewicz, Z.W., Ulbrich, U., brücher, T., Graczyk, D., Krüger, A., Leckebusch, G.C., Menzel, L., Pińskwar, I., Radziejewski, M., Szwed, M., 2005. Summer Floods in Central Europe – Climate Change Track? Natural Hazards 36, 165–189.
Lehmann, A., Rode, M., 2001. Long-term behaviour and cross-correlation water quality analysis of the river Elbe, Germany. Water research 35, 2153–2160.
Lehner, B., Döll, P., Alcamo, J., Henrichs, T., Kaspar, F., 2006. Estimating the Impact of Global Change on Flood and Drought Risks in Europe: A Continental, Integrated Analysis. Climatic Change 75, 273–299.
Lichtfuss, R., Brümmer, G., 1981. Gehalte an organischer Substanz, Schwermetallen und Phosphor in Dichtefraktionen von fluvialen Unterwasserböden. Geoderma 25, 245–265.
Lick, W.J., 2008. Sediment and Contaminant Transport in Surface Waters. CRC.
Lin, P., Huan, J., Li, X., 1983. Unsteady transport of suspended load at small concentrations. Journal of Hydraulic Engineering 109, 86–98.
Lindenschmidt, K.E., Huang, S., Baborowski, M., 2008. A quasi-2D flood modeling approach to simulate substance transport in polder systems for environment flood risk assessment. Science of the Total Environment 397, 86–102.
Liu, W.C., Hsu, M.H., Kuo, A.Y., 2002. Modelling of hydrodynamics and cohesive sediment transport in Tanshui River estuarine system, Taiwan. Marine Pollution Bulletin 44, 1076–1088.
Loucks, D.P., Van Beek, E., 2005. Water Resources Systems Planning and Management-Exercises.
Lumborg, U., Windelin, A., 2003. Hydrography and cohesive sediment modelling: application to the Rømø Dyb tidal area. Journal of Marine Systems 38, 287–303.

MacDonald, D.D., Ingersoll, C.G., 2003. A guidance manual to support the assessment of contaminated sediments in freshwater, estuarine and marine ecosystems in British Columbia. Volume III: Interpretation of the Results of Sediment Quality Investigations. Victoria. 63p.
Mehta, A.J., Hayter, E.J., Parker, W.R., Krone, R.B., Teeter, A.M., 1989. Cohesive Sediment Transport Part I: Process Description. Journal of Hydraulic Engineering 115, 1076–1093.
Microsoft, 2007. Microsoft Excel. Microsoft, Redmond, WA.
Murphy, B.L., Morrison, R.D., 2007. Introduction to environmental forensics. Academic Press.
Nash, J.E., Sutcliffe, J.V., 1970. River flow forecasting through conceptual models part I — A discussion of principles. Journal of Hydrology 10, 282–290.
Naumann, S., BÖGEHOLD, M., WIEPRECHT, S., 2003. Wirkungsgrad gravimetrischer Labormethoden zur Schwebstoffbestimmung.
Netzband, A., Reincke, H., Bergemann, M., 2002. The river elbe. J Soils & Sediments 2, 112–116.
Niimi, A.J., Cho, C.Y., 1980. Uptake of hexachlorobenzene (HCB) from feed by rainbow trout (<i>Salmo gairdneri</i>). Bulletin of Environmental Contamination and Toxicology 24, 834–839.
Ockenfeld, K., Guhr, H., Greenfield, P., Ward, S., 2003. Groyne fields- Sink and source functions of“ flow-reduced zones” for water content in the River Elbe(Germany). Water Science and Technology 48, 17–24.
Odd, N.V.M., Owen, M.W., 1972. A two-layer model of mud transport in the Thames Estuary.
Otto, Wilfried, 2012a. Untersuchungsmethodik Schwebstoffmessnetz, Ihre Anfrage AZ: M3/123/3389.
Otto, Wilfried, 2012b. Tageswerte der Schwebstoffkonzentration, Ihre Anfrage, AZ: M3/123/2564.
Overesch, M., Rinklebe, J., Broll, G., Neue, H.U., 2007. Metals and arsenic in soils and corresponding vegetation at Central Elbe river floodplains (Germany). Environmental Pollution 145, 800–812.
Partheniades, E., 2007. Engineering properties and hydraulic behavior of cohesive sediments. CRC Press Boca Raton, Florida.
Peckham, S.D., 2003. Fluvial landscape models and catchment-scale sediment transport. Global and Planetary Change 39, 31–51.
Popp, P., Brüggemann, L., Keil, P., Thuß, U., Weiß, H., 2000. Chlorobenzenes and hexachlorocyclohexanes (HCHs) in the atmosphere of Bitterfeld and Leipzig (Germany). Chemosphere 41, 849–855.
Power, E., Chapman, P., 1992. Assessing sediment quality. IN: Sediment Toxicity Assessment. Lewis Publishers, Boca Raton, Florida. 1992. p 1-18. 3 fig, 1 tab, 42 ref.
Prohaska, S., Jancke, T., Westrich, B., 2008. Model based estimation of sediment erosion in groyne fields along the River Elbe. IOP Conference Series: Earth and Environmental Science 4, 012042 (11pp).
Pye, K., 1994. Properties of sediment particles. Sediment Transport and Depositional Processes 1–24.
Quast, J., Böhme, M., Ehlert, V., Ette, J., Gottschick, M., Jaeckel, A., Knierim, A., Messal, H., Sawicka, M., Sbjeschni, A., Schmidt, W., Szerencsits, M., Tümpling, W.V., 2011. FLOOD RISKS IN CONSEQUENCE OF AGRARIAN LAND-USE MEASURES IN FLOOD FORMATION

AND INUNDATION ZONES AND CONCLUSIONS FOR FLOOD RISK MANAGEMENT PLANS. Irrigation and Drainage 60, 105–112.
Randak, T., Zlabek, V., Pulkrabova, J., Kolarova, J., Kroupova, H., Siroka, Z., Velisek, J., Svobodova, Z., Hajslova, J., 2009. Effects of pollution on chub in the River Elbe, Czech Republic. Ecotoxicology and Environmental Safety 72, 737–746.
Rhee, G.-Y., Gotham, I.J., 1981. The effect of environmental factors on phytoplankton growth: temperature and the interactions of temperature with nutrient limitation. Limnology and Oceanography 635–648.
Rhoads, D.C., Germano, J.D., 1982. Characterization of Organism-Sediment Relations Using Sediment Profile Imaging: An Efficient Method of Remote Ecological Monitoring of the Seafloor(REMOTS super (TM) System). Marine ecology progress series. Oldendorf 8, 115–128.
Sachsen, 2013. http://www.umwelt.sachsen.de/de/wu/umwelt/lfug/lfug-internet/hwz/elbe/index.html [WWW Document]. URL http://www.umwelt.sachsen.de/de/wu/umwelt/lfug/lfug-internet/hwz/elbe/index.html
Sachsen-Anhalt, 2012. Pegel: Löben (Gewässer: Schwarze Elster) [WWW Document]. URL http://www.hochwasservorhersage.sachsen-anhalt.de/wiskiwebpublic/stat_512031368.htm
Saleh, A., Arnold, J.G., Gassman, P.W., Hauck, L.M., Rosenthal, W.D., Williams, J.R., McFarland, A.M.S., 2000. Application of SWAT for the upper North Bosque River watershed. Transactions of the ASAE 43, 1077–1087.
Schneider, P., Reincke, H., 2006. Contaminated Sediments in the Elbe Basin and its Tributary Mulde, in: Merkel, P.D.B.J., Hasche-Berger, D.-G.A. (Eds.), Uranium in the Environment. Springer Berlin Heidelberg, pp. 655–662.
Schwandt, 2012a. Immer mehr Datenfragen....
Schwandt, 2012b. Treffen in Magdeburg?
Schwartz, R., 2006. Geochemical characterisation and erosion stability of fine-grained groyne field sediments of the Middle Elbe River. Acta hydrochimica et hydrobiologica 34.
Schwartz, R., Kozerski, H.P., 2002. Die Bedeutung von Buhnenfeldern für die Retentionsleistung der Elbe. Deutsche Gesellschaft für Limnologie, Tagungsbericht 460–465.
Schwartz, R., Kozerski, H.P., 2003. Entry and deposits of suspended particulate matter in groyne fields of the Middle Elbe and its ecological relevance. Acta hydrochimica et hydrobiologica 31, 391–399.
Schwarzbauer, J., Littke, R., Weigelt, V., 2000. Identification of specific organic contaminants for estimating the contribution of the Elbe river to the pollution of the German Bight. Organic Geochemistry 31, 1713–1731.
Searcy, J.K., Hardison, C.H., 1960. Double-mass curves.
Sheppard, S.C., 1995. Parameter values to model the soil ingestion pathway. Environmental monitoring and assessment 34, 27–44.
Simon, 2005. Die Elbe und ihr Einzugsgebiet - ein geographisch-hydrologischer und wasserwirtschaftlicher Überblick.
Simon, 2010a. PIK Report: Untersuchungen zu anthropogenen Beeinträchtigungen der Wasserstände am Pegel Magdeburg-Strombrücke.

Simon, 2010b. PIK Report: UNTERSUCHUNGEN ZU ANTHROPOGENEN BEEINTRÄCHTIGUNGEN DER WASSERSTÄNDE AM PEGEL MAGDEBURG-STROMBRÜCKE. Potsdam-Institut für Klimafolgenforschung e.V., Potsdam, Germany.

Simon, M., 1994. Hochwasserschutz im Einzugsgebiet der Elbe. Wasserwirtschaft Wassertechnik 7, 25–31.

Singh, V.P., Woolhiser, D.A., 2002. Mathematical modeling of watershed hydrology. Journal of Hydrologic Engineering 7, 270–292.

SPSS Inc., 2007. SPSS for Windows, Version 16.0. Chicago.

Stachel, B., Christoph, E.H., Götz, R., Herrmann, T., Krüger, F., Kühn, T., Lay, J., Löffler, J., Päpke, O., Reincke, H., 2007. Dioxins and dioxin-like PCBs in different fish from the river Elbe and its tributaries, Germany. Journal of Hazardous Materials 148, 199–209.

Stachel, B., Gotz, R., Herrmann, T., Kruger, F., Knoth, W., Papke, O., Rauhut, U., Reincke, H., Schwartz, R., Steeg, E., 2004. The Elbe flood in August 2002-occurrence of polychlorinated dibenzo-p-dioxins, polychlorinated dibenzofurans (PCDD/F) and dioxin-like PCB in suspended particulate matter (SPM), sediment and fish. Water Science and Technology 50, 309–316.

Sukhodolov, A., Uijttewaal, W.S.J., Engelhardt, C., 2002. On the correspondence between morphological and hydrodynamical patterns of groyne fields. Earth Surface Processes and Landforms 27, 289–305.

Taube, V., Gude, K., Bruns-Weller, E., Kamphues, J., Briese, A., Clauss, M., Springorum, A., Hartung, J., 2009. Investigations in order to establish a concept for using dioxin exposed floodplains by beef cattle under food safety aspects. Presented at the Sustainable animal husbandry: prevention is better than cure, Volume 2. Proceedings of the 14th International Congress of the International Society for Animal Hygiene (ISAH), Vechta, Germany, 19th to 23rd July 2009., Tribun EU, pp. 627–630.

Taylor, J.K., Cihon, C., 2004. Statistical techniques for data analysis. Chapman & Hall.

Tolhurst, T.J., Black, K.S., Paterson, D.M., Mitchener, H.J., Termaat, G.R., Shayler, S.A., 2000a. A comparison and measurement standardisation of four in situ devices for determining the erosion shear stress of intertidal sediments. Continental Shelf Research 20, 1397–1418.

Tolhurst, T.J., Riethmüller, R., Paterson, D.M., 2000b. In situ versus laboratory analysis of sediment stability from intertidal mudflats. Continental Shelf Research 20, 1317–1334.

Townsend, C.R., Riley, R.H., 1999. Assessment of river health: accounting for perturbation pathways in physical and ecological space. Freshwater Biology 41, 393–405.

Uijttewaal, W.S.., 2005. Effects of groyne layout on the flow in groyne fields: Laboratory experiments. Journal of Hydraulic Engineering 131, 782.

Undine, 2012. Das Hochwasser der Elbe im Frühjahr 2006 [WWW Document]. Informationsplattform Undine. URL http://undine.bafg.de/servlet/is/12448/ (accessed 6.21.02).

UNEP, 2004. The 12 POPs under the Stockholm Convention [WWW Document]. URL http://www.pops.int/documents/pops/default.htm (accessed 7.12.12).

UNIDO, n.d. Summary of Contaminated Sites.

Van Rijn, Leo C, van Rijn, Leonardus Cornelis, van Rijn, Leonardus Cornelis, 1993. Principles of sediment transport in rivers, estuaries and coastal seas. Aqua publications Amsterdam.

Walling, D., 1977. Limitations of the rating curve technique for estimating suspended sediment loads, with particular reference to British rivers. Erosion and solid matter transport in inland waters 34–48.
Walling, D., Kane, P., 1982. Temporal Variation of Suspended Sediment Properties, in: Catchment Experiments in Fluvial Geomorphology. International Association of Hydrological Sciences, p. 430.
Walling, D., Webb, B., 1988. The reliability of rating curve estimates of suspended sediment yield: some further comments. IN: Sediment Budgets. IAHS Publication.
Weigold, F., Baborowski, M., 2009. Consequences of delayed mixing for quality assessment of river water: Example Mulde-Saale-Elbe. Journal of Hydrology 369, 296–304.
Widdows, J., Friend, P.L., Bale, A.J., Brinsley, M.D., Pope, N.D., Thompson, C.E.L., 2007. Inter-comparison between five devices for determining erodability of intertidal sediments. Continental Shelf Research 27, 1174–1189.
Wigbout, M., 1973. Limitations in the use of double-mass curves. JOURNAL OF HYDROLOGY (NZ) 12.
Wirtz, C., 2004. Hydromorphologische und morphodynamische Analyse von Buhnenfeldern der unteren Mittelelbe im Hinblick auf eine ökologische Gewässerunterhaltung. Doktorarbeit, Fachbereich Geowissenschaften der Freien Universität Berlin.
Witter, B., Francke, W., Franke, S., Knauth, H.D., Miehlich, G., 1998. Distribution and mobility of organic micropollutants in river Elbe floodplains. Chemosphere 37, 63–78.
Witter, B., Winkler, M., Friese, K., 2003. Depth Distribution of Chlorinated and Polycyclic Aromatic Hydrocarbons in Floodplain Soils of the River. Acta hydrochimica et hydrobiologica 31, 411–422.
WSV, 2011. Gauge Data [WWW Document].
WSV, 2012. Pegel Online [WWW Document]. Gewässerkundliches Infosystem. URL http://www.pegelonline.wsv.de/gast/stammdaten?pegelnr=502070 (accessed 2.6.12).
Wu, Y., Falconer, R.A., Uncles, R.J., 1999. Modelling of water flows and cohesive sediment fluxes in the Humber Estuary, UK. Marine Pollution Bulletin 37, 182–189.
Zebisch, M., Grothmann, T., Schröter, D., Hasse, C., Fritsch, U., Cramer, W., 2005. Climate change in Germany. Vulnerability and adaptation of climate sensitive sectors/Klimawandel in Deutschland–Vulnerabilität und Anpassungsstrategien klimasensitiver Systeme. Federal Environmental Agency Germany/Umweltbundesamt, Dessau, Report 201, 41–253.

Appendix A: Ecolab Reference

The following appendix describes the mathematical formulations behind the Ecolab template, and is reproduced from DHI Software Group (2009). The symbols 'S' and 'X' are used to identify soluble and particulate variables, respectively.

- SXE - Xenobiotic concentration in water (dissolved)
- XXE - Xenobiotic concentration in water (adsorbed)
- XSS - Suspended solids concentration in water
- SXES - Xenobiotic concentration in sediment (dissolved)
- XXES - Xenobiotic concentration in sediment (adsorbed)
- XSED - Mass of Sediment

B.1 Dissolved Xenobiotic (SXE)

The concentration of Xenobiotic dissolved in the water column can be described as the sum of the concentrations of desorbed and diffused xenobiotic minus the amount adsorbed to suspended solids (Equation 12).

Equation 12: $\frac{dS_{XE}}{dt} = -\boldsymbol{adss} + \boldsymbol{dess} + \boldsymbol{difv} - \boldsymbol{biodecay} - \boldsymbol{hydrolysis} - \boldsymbol{photolysis} - \boldsymbol{evaporation}$

where:
adss = adsorption
dess = desorption
difv =diffusion

B.1 .1 Adsorption

The partitioning coefficient, K_d, is the ratio of sediment-sorbed xenobiotic to the dissolved xenobiotic concentration at equilibrium. Since xenobiotics bind primarily to organic fraction of sediment, K_d is estimated from the product of the organic carbon partitioning coefficient and the fraction of organic carbon in the sediment (Equation 13). Further, the adsorption and desorption rates are assumed to be related according to K_d (Equation 14). It is therefore possible to estimate the one of the sorption rates (i.e. adsorption) when both the partitioning coefficient and other sorption rate (i.e. desorption) is known. From Equation 13, the adsorption rate, k_a, can then be substituted with k_w and K_d to estimate the sorption rate between the water column and suspended solids (Equation 15).

Equation 13: $K_d = f_{oc} * K_{oc}$
Equation 14: $K_d = k_a / k_w$
Equation 15: *adss* = $k_w * K_d * SXE * XSS$

where:
K_d = Partitioning coefficient for xenobiotic: water to particulate matter
f_{oc} = Fraction of organic carbon in suspended solids

K_{oc} = Organic carbon partitioning coefficient
k_a = Adsorption rate
k_w = Desorption rate in water

B.2 .1 Desorption

Adsorbed xenobiotics can be desorbed from the adsorbed phase to the desorbed phase in the water column (where:
Equation 16).

where:
Equation 16: *dess* = k_w* XXE

k_w = Desorption rate in water
X_{HM}= Xenobiotic concentration in water (adsorbed)

B.3 .1 Diffusion

Fick's first law states that the flux moves from regions of high concentration to regions of low concentration, with a magnitude proportional to the concentration. Accordingly, dissolved xenobiotic can diffuse between sediment porewater and dissolved xenobiotics in the water column (Equation 17).

Equation 17: $\boldsymbol{difv} = \frac{\boldsymbol{fbiot \cdot difw}\left(\frac{\boldsymbol{S_{HMS}}}{\boldsymbol{pors \cdot dzs}} - \boldsymbol{S_{HM}}\right)}{(\boldsymbol{dzwf + dzds}) \cdot \boldsymbol{dz}}$

where:
fbiot =Factor for diffusion due to bioturbation
difv =Diffusion coefficient in water (estimated from xenobiotic's molecular weight)
SXE= Xenobiotic concentration in water (dissolved)
SXE_S= Xenobiotic concentration in porewater (dissolved)
dzwf = Thickness of water film
dzds = Thickness of diffusion layer in sediment
dz = Thickness of actual layer in computational grid

B.4 .1 Xenobioticon Suspended Matter (X_{HM})

The concentration of xenobioticsorbed suspended matter can be described as the amount of adsorbed and resuspended xenobiotic minus the amount lost to desorption and sedimentation (Equation 12).

Equation 18: $\frac{\boldsymbol{dX_{HM}}}{\boldsymbol{dt}} = -\boldsymbol{adss} - \boldsymbol{dess} - \boldsymbol{sev} + \boldsymbol{resv}$
where:
adss = adsorption
dess = desorption

sev = sedimentation
resv = resuspension

B.5 .1 Adsorption

See also the text for SXE.
Equation 19: *adss* = k_w*K_d *SXE*X_{ss}
where:
k_w = Desorption rate in water
K_d = Partitioning coefficient for xenobiotci: water to particulate matter
SXE= Xenobiotic concentration in water (dissolved)
X_{ss}= Suspended solids concentration in water

B.6 .1 Desorption

Adsorbed xenobiotics in the sediment can be desorbed to the water column (where: Equation 16).
Equation 20: *dess* = k_w* X_{HM}
where:
K_w = Desorption rate in water
X_{HM}= Xenobiotic concentration in water (adsorbed)

B.7 .1 Sedimentation

Adsorbed xenobiotics are assumed to be transported with the suspended solids, which undergo sedimentation processes. Settling velocity is the primary control on sedimentation of suspended solids (Equation 21).
Equation 21: $\boldsymbol{sev} = \frac{\boldsymbol{vsm} \cdot \boldsymbol{X_{HM}}}{\boldsymbol{dz}}$
where:
sev = Sedimentation
vsm = Settling velocity of suspended solids
X_{HM} = Xenobiotic concentration in water (adsorbed)
d*z* = Thickness of the layer in the computational grid

B.8 .1 Resuspension

Sediment-sorbed xenobiotics will be resuspended if current speed exceeds a critical value and suspended matter is suspended in the water column (Equation 21). The

Equation 22: $\boldsymbol{resv} = \frac{\frac{\boldsymbol{resrat} \cdot \boldsymbol{X_{HMS}}}{\boldsymbol{X_{SED}}}}{\boldsymbol{dz}}$

where:
resrat = Resuspension rate of suspended solids
X_{HMS}= Xenobiotic concentration in sediment (adsorbed)

X_{SED} = Mass of sediment
dz = Thickness of the layer in the computational grid

B.9 .1 Xenobiotic on Suspended Matter /Solids in water (X_{ss})

The concentration of xenobiotic sorbed suspended matter or solids in water can be described as the sum of produced and resuspended material minus the amount lost to sedimentation (Equation 23).

Equation 23: $\frac{dX_{SS}}{dt} = prss - sessv + ressv$

where:
prss = production
sessv = sedimentation
ressv = resuspension

B.10 .1 Production

Suspender matter can be introduced into the water column by primary production (Equation 24)

Equation 24: $\boldsymbol{prss = \frac{parpro}{dz}}$

where:
parpro = Particle production rate
dz = Thickness of the layer in the computational grid

B.11 .1 Sedimentation

Sedimentation of suspended solids is controlled primarily by the settling velocity of the solids (Equation 25).

Equation 25: $\boldsymbol{ssev = \frac{vsm \cdot X_{SS}}{dz}}$ *where:*
vsm = Settling velocity of suspended solids
X_{SS} = Suspended solids concentration in water
d*z* = Thickness of the layer in the computational grid

B.12 .1 Resuspension

Sediments are resuspended when the current speed exceeds a critical value (Equation 26).

Equation 26: $\boldsymbol{ressv = \frac{resrat}{dz}}$

where:
resrat = Resuspension rate of suspended solids
dz = Thickness of the layer in the computational grid

B.13 .1 Dissolved Xenobioticin the Sediment (SXE_S)

The concentration of dissolved xenobioticin the sediment can be described as the concentration of desorbed xenobioticminus the amount lost to adsorption and diffusion (Equation 27).

Equation 27: $\frac{dS_{XMS}}{dt} = -adsa + desa - difa$

where:

$adsa$ = adsorption

$desa$ = desorption

$difa$ = diffusion

B.14 .1 Adsorption

The adsorption rate, k_a, and the desorption rate, k_d, are assumed to be related via the equilibrium partitioning coefficient k_d (Equation 28). It is therefore possible to estimate the one of the sorption rates (i.e. adsorption) when both the partitioning coefficient and other sorption rate (i.e. desorption) is known. From Equation 28, the adsorption rate, k_a, can then be substituted with k_w and K_{ds} to estimate the sorption rate between the water column and suspended solids (Equation 29).

Equation 28: $K_{ds} = \frac{k_a}{k_s}$

Equation 29: $\boldsymbol{adsa = k_s \cdot K_{ds} \cdot S_{HMS} \cdot \frac{X_{SED}}{dzs \cdot por_s}}$

where:

K_{ds} = Partitioning coefficient for xenobiotic between particulate matter and water

K_a = Adsorption rate in water

K_s = Desorption rate in water

SXE_S = Xenobiotic concentration in water (dissolved)

d*zs* = Sediment layer thickness

X_{SED} = Mass of sediment

por_s = Porosity of the sediment (assumed to be constant)

B.15 .1 Desorption

Adsorbed xenobiotics in the sediment can be desorbed to from the adsorbed phase to the pore water (Equation 30).

Equation 30: *desa*= k_s* X_{HMS}

where:

k_s = Desorption rate in sediment

X_{HMS}= Xenobiotic concentration in sediment (adsorbed)

B.16 .1 Diffusion

Fick's first law states that the flux moves from regions of high concentration to regions of low concentration, with a magnitude proportional to the concentration. Accordingly, dissolved xenobiotic can diffuse between sediment and sediment porewater (Equation 31).

Equation 31: $\boldsymbol{difa} = \frac{\boldsymbol{fbiot \cdot difw}\left(\frac{\boldsymbol{S_{HMS}}}{\boldsymbol{por_S \cdot dzs}} - \boldsymbol{S_{HM}}\right)}{(\boldsymbol{dzwf + dzds})}$

where:

fbiot =Factor for diffusion due to bioturbation

difw =Diffusion coefficient in sediment (estimated from xenobiotic's molecular weight)

SXE= Xenobiotic concentration in water (dissolved)

SXE_S= Xenobiotic concentration in sediment porewater (dissolved)

dzwf = Thickness of water film

dzds = Thickness of diffusion layer in sediment

dz = Thickness of actual layer in computational grid

por_s = Porosity of the sediment (assumed to be constant)

9.1.1.1 Xenobiotic in Sorbed to Sediment (X_{HMS})

The concentration of xenobiotic sorbed to in sediment can be described as the sum of the concentration of adsorbed and sedimented xenobiotic minus the amount lost to desorption and resuspension (Equation 32).

Equation 32: $\frac{dX_{XMS}}{dt} = adsa - desa + sea - resa$

where:

$adsa$ = adsorption

$desa$ = desorption

sea = sedimentation

$resa$ = resuspension

B.17 .1 Adsorption

The adsorption rate, k_a, and the desorption rate, k_s, are assumed to be related via the equilibrium partitioning coefficient k_{ds} (Equation 33). It is therefore possible to estimate the one of the sorption rates (i.e. adsorption) when both the partitioning coefficient and other sorption rate (i.e. desorption) is known. From Equation 28, the adsorption rate, k_a, can then be substituted with k_w and K_{ds} to estimate the sorption rate between the water column and suspended solids (Equation 34).

Equation 33: $K_{ds} = \frac{\boldsymbol{k_a}}{\boldsymbol{k_s}}$

Equation 34: $\boldsymbol{adsa} = \boldsymbol{k_s \cdot K_{ds} \cdot S_{HMS} \cdot \frac{X_{SED}}{dzs \cdot por_s}}$

where:

K_{ds} = Partitioning coefficient for xenobiotic between particulate matter and water

K_a = Adsorption rate in water

K_s = Desorption rate in water

SXE_S = Xenobioticc oncentration in water (dissolved)

d*zs* = Sediment layer thickness

X_{SED} = Mass of sediment

por_s = Porosity of the sediment (assumed to be constant)

B.18 .1 Desorption

Adsorbed xenobiotics in the sediment can be desorbed to from the adsorbed phase to the dissolved phase in the pore water (Equation 30).
Equation 35: *desa*= k_s* X_{HMS}
where:
k_s = Desorption rate in sediment
X_{HMS}= Xenobiotic concentration in sediment (adsorbed)

B.19 .1 Sedimentation

Settling velocity is the primary control on sedimentation of suspended solids (Equation 21).
Equation 36: $\boldsymbol{sea = vsm \cdot X_{HM}}$
where:
vsm = Settling velocity of suspended solids
X_{HM} = Xenobiotic concentration in water (adsorbed)

B.20 .1 Resuspension

Adsorbed xenobiotics in the sediment are resuspended when the current speed exceeds a critical value and sediment is suspended in the water column (Equation 37).
Equation 37: $\boldsymbol{resa = \frac{resrat \cdot X_{XMS}}{X_{SED}}}$
where:
resrat = Resuspension rate of suspended solids
X_{XMS}= Xenobioticin sediment (adsorbed)
X_{SED}= Mass of sediment

B.21 .1 Mass of Sediment (X_{SED})

The mass of sediment can be estimated from the mass of sedimented sediment minus the mass of resuspended sediment (Equation 32).

Equation 38: $\frac{dX_{SED}}{dt} = sessa - ressa$
$sessa$ = sedimentation
$ressa$ = resuspension

B.22 .1 Sedimentation

Settling velocity is the primary control on sedimentation of suspended solids (Equation 39).
Equation 39: $\boldsymbol{sessa = vsm \cdot X_{SS}}$
where:
vsm = Settling velocity of suspended solids
X_{SS}= Suspended solids concentration in the water

B.23 .1 Resuspension

Sediments are resuspended when current speed exceeds a critical value (Equation 37).

Equation 40: $\boldsymbol{ressa = resrat}$

where:

ressa = Resuspension rate of suspended solids

resrat = Resuspension rate of suspended solids

Appendix B: Parameters and Input Values for Hydrodynamic, Cohesive Sediment and HCB Models and Modules

Table B-1. Hydrodynamic Module Parameters

Parameter	Value
Initial Conditions	
Water Depth	2
Discharge	200
Default Values	
Delta	0.85
Delhs	0.01
Delh	0.1
Alpha	1
Theta	1
Eps	0.0001
Dh Node	0.01

Advection-dispersion module parameters are detailed in Table 13

Table B-2. Xenobiotic Module Parameters

Parameter	Default/ Calculated	Value	Units
Dissolved Xenobiotics	Calculated	0.000000070	mg/l
Adsorbed Xenobiotics	Calculated	0.041	mg/l
Dissolved Xenobiotics in sediment pore water	Calculated	0.000000070	g/m^2
Adsorbed Xenobiotics in sediment	Calculated	0.041	g/m^2
Suspended solids	Calculated	30	mg/l
Mass of sediment	Calculated	330,000	g/m^2
Organic-carbon partitioning coefficient	Calculated	630957.34	l/kg
Desorption rate in water (adsorbed to dissolved in water column)	Calculated	0.423	/d
Desorption rate in sediment (sediment to pore water)	Calculated	0.1395	/d
Fraction of organic carbon in suspended solids	Calculated	0.1	

Parameter	Default/ Calculated	Value	Units
Fraction of organic carbon in sediment	Calculated	0.082	
Thickness of water film	Default	0.1	mm
Ratio between thickness of diffusion layer in sediment and sediment thickness	Default	0.2	
Factor for diffusion due to bioturbation	Default	1	
Molweight of Xenobiotic	Calculated	284.78	g/mole
ECO Lab time step			
Density of dry sediment	Calculated	550	kg/m^3 bulk
Porosity of sediment	Default	0.8	m^3 H20/m3 bulk
Settling velocity of SS	Default	540	m/day
Resuspension rate	Default	1000	gDW/m^2/day
Particle production rate	Default	1	gDW/m^2/day
Critical current velocity for sediment resuspension	Default	1	m/s
Biodecay rate water, max	Default	0	/d
Biodecay rate sediment, max	Default	0	/d
Halfsaturation constant biodecay water	Calculated	0	gXe/m^3
Halfsaturation constant biodecay sediment	Default	0	gXe/m^2
Arrhenius temperature coefficient for biodegradation	Default	1.05	
Background concentration air	Default	0	gXe/m^3
Light attenuation water column	Default	0.1	/m
Photolysis rate at surface (/day)	Default	0	/d
Henry's constant (Set Kh 10 1e5---> no evaporation)	Calculated	100	Pa m^3/mol K
Is the compound an acid (0/1)?	Default	0	
Is the compound a base (0/1)?	Default	0	on/off
Dissociation constant acid (pH units)	Default	0	NA
Dissociation constant base (pOH units)	Default	0	NA
Hydrolysis constant, acid	Default	0	l/mol/day
Hydrolysis constant, base	Default	0	/day
Hydrolysis constant, alkaline	Default	0	l/mol/day
Universal gas constant	Default	8.3144	m^3 air Pa/(mol*K)
Temperature	Calculated	11.2	°C
pH, water	Calculated	8	
pH, sediment	Calculated	7.5	
Solar radiation	Default	25	E/m^2/d

Table B-3. 2D FM HD Module

Parameter	Value
Solution technique	
Time Integration	Higher Order
Space discretization	Higher Order
Shallow water: Minimum Time Step	0.01 seconds
Shallow water: Maximum Time Step	5 seconds
Shallow water: Critical CFL number	0.8
Transport equations: Minimum Time Step	0.01 seconds
Transport equations: Maximum Time Step	45 seconds
Transport equations: Critical CFL number	0.8
Flood and dry	
Include?	Yes
Drying depth	0.005 m
Flooding depth	0.05 m
Wetting depth	0.1 m
Eddy Viscosity	
Eddy Type	Smagorinsky formulation
Constant Value	0.28
Minimum eddy viscosity	0.0000018 m2/s
Maximum eddy viscosity	10000000000 m2/s
Bed Resistance	
Resistance Type	Manning Number
Constant Value	38
Ice Coverage	
Type	No ice Coverage
Tidal Potential	
Include Tital Potential?	No
Precipitation-Evaporation	
Precipitation?	No
Evaporation?	No
Sources	
Saale	Yes. Saale discharge data
Structures	
Structures?	No
Initial Conditions	
Type	Constant
Surface elevation	45m
Boundary Conditions	
Aken	Aken discharge data
Barby	Barby discharge data

Parameter	Value
Land	Zero normal velocity

Table B-4. 2D FM MT Module

Parameter	Value
Parameter Selection	
Number of grain size fractions	1
Number of layers	1
Solution technique	
Time Integration	Higher Order
Space discretization	Higher Order
Water Column Parameters	
Include sand fractions?	Yes
Mean Settling velocity?	0.00625
Deposition parameters	Apply Teeter Profile
Critical shear stress for deposition	0.515 N/m2
Bed Parameters	
Erosion description	hard mud
Power of erosion	1
Erosion coefficient	0.00035 kg/m2/s
Critical shear stress (erosion)	0.1 N/m2
Density of bed layer	550 kg/m3
Bed roughness	0.1 m
Forcings	
Waves	No waves
Dredging	No dredging
Dispersion	
Formulation	Scaled eddy viscosity formulation
Constant Value	1.00E+00
Sources	
Saale	Yes. Saale suspended sediment data
Initial Conditions	
Fraction 1	0.01 kg/m3
Layer thickness	0.5m
Fraction distribution	100
Surface elevation	45m
Boundary Conditions	
Aken	Aken suspended sediment data
Barby	Barby suspended sediment data
Morphology calculations included?	Yes